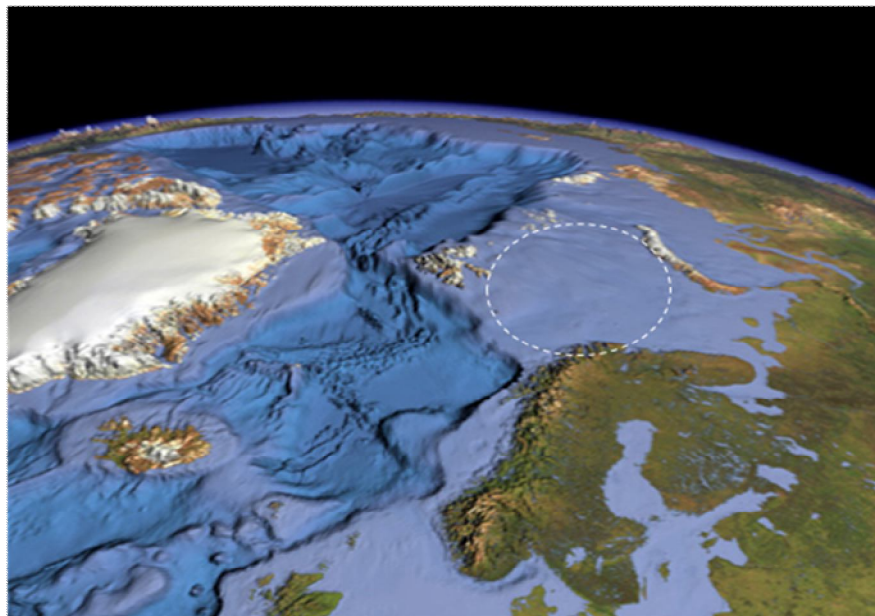


Master Thesis in Geosciences

Oil- prone Carboniferous coals (Tettegras Fm.) from the Finnmark Platform

*Implications for an alternative and new Petroleum
System based on oil generative coals of the Billefjord
Gr. in the Barents Region*

Ronny Moi



UNIVERSITY OF OSLO

FACULTY OF MATHEMATICS AND NATURAL SCIENCES

Oil- prone Carboniferous coals (Tettegras Fm.) from the Finnmark Platform

**Implications for an alternative and new Petroleum System based
on oil generative coals of the Billefjord Gr. in the Barents Region**

Ronny Moi



Master Thesis in Geosciences

Discipline: Petroleum geology and Petroleum geophysics

Department of Geosciences

Faculty of Mathematics and Natural Sciences

UNIVERSITY OF OSLO

July 2008

© **Ronny Moi, 2008**

Tutor(s): Dr. Dag A. Karlsen

This work is published digitally through DUO – Digitale Utgivelser ved UiO

<http://www.duo.uio.no>

It is also catalogued in BIBSYS (<http://www.bibsys.no/english>)

All rights reserved. No part of this publication may be reproduced or transmitted, in any form or by any means, without permission.

Abstract

Generation of commercial quantities of oil is well established for shales and carbonates but remains more disputed for coals. Little direct and irrefutable evidence for coals generating and expelling oil is documented, apart from in the Mahakam delta of Kalimantan, in the Upper Cretaceous Fruitland Formation coals in the USA, the Middle Jurassic coals from the Danish North Sea and New Zealand Tertiary coals. Most of the oil generating coals are “bog-head-coals” i.e. rocks by definition containing more than 50% organic matter, and in case of bog-head coals, with a high proportion of hydrogen rich coal macerals.

Large regions of the Barents Sea have received little exploration, with most of the oil found till date stemming from Upper Jurassic and Triassic shaly source rocks in the Hammerfest and Nordkapp Basins. “Of the 67 wells presently drilled in the Barents Sea nearly all have hydrocarbon shows, and one out of three wells is a discovery, which is a very high success ratio. As Upper Jurassic and Triassic rocks are immature in the huge platform regions, exploration interest focuses on potential deeper source rocks of Palaeozoic age such as Permian and Carboniferous formations”.

In this thesis the aim was to investigate the largely unknown potential of coals of the Tettegras Fm. (Billefjord Gr.) in two wells from the Finnmark Platform and to evaluate the generation and expulsion properties of these coals and to see if evidences suggest that two drill stem test (DST) oils in one of these wells could possibly have some contribution of oil from coals of the Tettegras Fm.

The sample set contains 10 coal samples and two DST oil samples which were collected from wells 7128/4-1 and 7128/6-1 on the Finnmark Platform. In addition, one sample of the North Sea Standard oil (NSO) from the Oseberg Field has been analyzed as a reference sample.

The aim of this study is thus to evaluate the coals themselves in terms of oil generative potential and to also use extracts of the extracted coals for this purpose. These extracts are also used for comparison with the DST oils i.e. to evaluate if the extracts of the coals correlate with the DST oils. Molecular parameters including biomarker finger printing, organic source rock facies parameters and maturity parameters have been used for this purpose.

The maturity figures and diagrams show that the coals plot in the mature zone. The entire sample set, plots within the oil window, spanning the range from early to the late stage of oil generation. The majority of coals are oil prone while the rest plot as gas-prone coals based on different van Krevelen diagrams.

Most of the coal samples plot as type II kerogen and a few as type III kerogen. Since world wide coals in general are classified as containing type III/IV kerogens, it is surprising that the coal samples in this study show more oil prone characteristics.

The oil generative potential of the coals of the Tettegras Fm. is therefore undisputed and documented. Moreover, extracts of the coals and the DST oils seem to correlate to a certain extent with respect to source facies parameters. The DST oils originated from a mixed organic source. The terrigenous input component into the overall mixed marine organic facies deduced for the DST oils, could have been derived from the coals. Alternatively, the DST oils may have a two-source origin, having been partly sourced from the Tettegras coals and partly from marine shale. The GC-FID of the DST oils shows a waxy signature in the C₁₅₊ fraction of the n-alkanes which is similar to that observed for the coals. The high Pr/Ph ratio of the coals is also observed in the DST oils and the value is generally high when compared to the NSO-1 oil. An expanded sample set would clearly be required before more definite conclusions are drawn concerning oil generation, migration and accumulation i.e. a "Petroleum System" based on the Tettegras coals, but this study suggest that such a system may indeed represent an additional exploration potential in the Barents Sea.

Acknowledgements

I would like to thank my supervisor Dr. Dag A. Karlsen for his guidance and support concerning this master thesis. He has always been helpful and given me advice on how to improve my work. I would also give my thanks to Kristian Backer-Owe for his support through laboratory analysis and guidance on the results afterwards. Also, Jan Hendrik van Koeverden has been helpful with respect to the analyzed coal extracts.

In addition, I would like to thank my dearest family for being there for me throughout the work. Especially, I want to express my gratitude to my wife Anne Marit who has supported my work and taken care of our home during the last two years. My children Elisabeth and Jonas André have been my inspiration and given me a lot of laughter and joy when I needed a break from my studies. I would also like to thank my father in law, Ivar Pedersen, for valuable review comments. Also, I would like to thank my friends for encouraging me to take the Master Study after working several years.

Oslo, July 2008

Ronny Moi

1. Introduction	1
2. The sample set	11
3. Analytical methods	13
3.1 Procedure of preparing samples	13
3.2 Iatroscan TLC-FID	13
3.3 GC-FID	15
3.4 GC-MS	17
3.5 Rock-Eval – Hydrous pyrolysis	19
4. Maturity and facies parameters	20
4.1 Data from Iatroscan TLC-FID	20
4.2 Data from GC-FID	21
4.3 Data from GC-MS	24
4.4 Data from Rock-Eval pyrolysis	36
5. Results	40
5.1 Iatroscan TLC-FID	40
5.2 GC-FID	42
5.3 GC-MS	44
5.4 Chromatograms from GC-FID and GC-MS analysis.....	47
5.5 Rock-Eval	54
6. Discussions	57
6.1 Organic facies of coals and oils	57
6.2 Maturity of coals and oils	62
6.3 Petroleum potential, richness and kerogen type	69
6.4 Volumetric contents	77
6.5 Biodegradation of the samples	80
6.6 Summary of source and maturity of the samples	81
6.7 Kerogen type and migration	85
7. Conclusions	86
8. References.....	90

1. Introduction

1.1 Definition of coal

Coal is a readily combustible rock containing more than 50 % by weight, and more than 70 % by volume, of organic material formed from the compaction or indurations of variously altered plant remains. Humic coals are formed from plant cell and wall material deposited under aerobic conditions, whereas sapropelic coals and bog-head coals are formed from spores, pollen and algae deposited under anaerobic conditions (Hunt, 1996).

1.2 Formation of coal

By comparison of coal and petroleum, both originate mainly from organisms of the plant kingdom. Geological processes causing the coalification (figures 1.1a and 1.3) are bacterial action, burial, compaction and geothermal heating, which involve diagenesis and catagenesis. Coal is generally formed at the same place as deposited and consists of a solid and pure massive organic substance (rooted coals). Minor accumulations of eroded or drifted coals may occur if coal beds of rooted coals have been cut by rivers, eroded and re-deposited. The term coal therefore span a large variety of rocks with TOC content exceeding 50% and vary from pure woody type material of terrigenous plants, including even the remains of palaeo-forest fires, to bog-head and channel coals constituted mostly of spores and algal matter with a high hydrogen to carbon ratio (Tissot et al., 1978).

1.3 Macerals

Coals are composed of macerals, which are morphologically recognizable constituents of coals. Macerals are analogous to the minerals of inorganic rocks, but the chemical composition and physical properties are less uniform. In a microscope the macerals can be distinguished based on difference in morphology. Liptinite, vitrinite and inertinite are the dominant coal macerals. Liptinite has the highest hydrogen content, while inertinite has the

lowest values of hydrogen. The macerals show an increase in the carbon content with increasing temperature (Hunt, 1996).

1.4 Main types of coal associated with facies

Nonmarine and paralic conditions are favourable facies with respect to deposition (Tissot et al., 1978). More than 80 % of the world's coals are formed from humic organic matter and under oxic conditions, and vitrinite makes more than 70 % of their macerals. Humic coals consist of plant cell and wall material, mainly composed of lignin, cellulose and aromatic tannins. The generation of humic coals accelerates by the presence of oxygen and heat, like environments of tropical climates (Hunt, 1996).

Sapropelic coals represent less than 10 % of the world's coals and accumulate in swamp environments or in stagnant parts of lakes. This type of coals consists of sapropel, which is a water ooze of spores, pollen, cuticles and resins of plant materials in addition to the organic remains of algae and plankton. Sapropelic coals when buried are termed cannel and bog head coals.

These major coal types display different values concerning the atomic ratio of hydrogen to carbon. The approximate values are; bog head coals- 1.5, cannel coals- 1.2 and humic coals- 0.8 (Hunt, 1996).

1.5 Quality of Organic Matter

The generation of oil and gas is mainly controlled by the hydrogen content of the organic matter (OM). The amount of hydrocarbons which potentially can be generated and expelled will increase as the atomic hydrogen-to-carbon (H/C) ratio of the OM increases. Sapropelic and humic coals are the two major types of coals (chapter 1.4), which nearly all coal types may be classified into (Potonie 1908, also see the table 1.1 from Hunt 1996). According to the table 1.1, sapropelic organic matter such as fats, oils, resins, and waxes displays high atomic (H/C) ratios in the interval 1.3 to two. End-products with respect to maturation of organic-rich sapropelic deposits are bog head coals and oil shales (Hunt, 1996).

Humic coals in terms of peat show an H/C ratio around 0.9 (table 1.1, Hunt 1996). A value below one is just within the borderline for being an important progenitor of oil. The table 1.1

also shows a decrease of the atomic hydrogen-to-carbon (H/C) and oxygen-to-carbon (O/C) ratios of both sapropelic OM and humic OM, as a function of increasing maturation (coalification). One example may be seen for the H/C ratio of vitrinite, which changes from about one to 0.3 between the stages lignite and anthracite. Another example is wax, which van Krevelen (1961) called “cerinite”. It has the highest atomic H/C ratio of all the constituents of coal (Hunt, 1996).

	<i>Sapropelic</i>		<i>Humic</i>	
Coal maceral groups	Liptinite (exinite)		Vitrinite	Inertinite
Coal macerals	Alginite		Telinite	Fusinite
	Cerinite ^a		Telocollinite	Inertodetrinite
	Sporinite		Desmocollinite	Sclerotinite
	Cutinite		Vitrodetrinite	Macrinite
	Resinite			
	Liptodetrinite			
	Fluorescent Amorphous		Nonfluorescent Amorphous	
Kerogen Types	I	II	III	IV
H/C	1.9 to 1.0	1.5 to 0.8	1.0 to 0.5	0.6 to 0.1
O/C	0.1 to 0.02	0.2 to 0.02	0.4 to 0.02	0.3 to 0.01
Source	Marine, Lacustrine, Terrestrial		Terrestrial and Recycled	

^aWax.

Table 1.1. The classification of the Organic Matter in the Coals and Sedimentary Rocks (Hunt, 1996).

According to Petersen and Rosenberg (2000) the abundance of the vitrinite group of macerals, and in particular the abundance of collotelinite, is the major control on the source rock potential of humic coals (see table 1.1).

1.6 Coal as a source rock

Hedberg (1968) claimed that the largest reserves of coal were deposited in the Late Carboniferous and Permian, while smaller amounts were formed in the Jurassic through the Tertiary. By comparison, the largest oil reserves are found in the Jurassic through the Early

Tertiary. Klemme and Ulmishek (1991) estimated that nearly 50% of the world's oil has been formed from Late Jurassic and Cretaceous source rocks, but only 20% of the world's coal can be found in these rocks. Cretaceous and Tertiary reservoirs are represented by 75% of Hedberg's forty worldwide high-wax oils, but only 5% are in reservoirs of the coal-bearing Carboniferous and Permian periods (Hunt, 1996).

In contrast, when looking for the most frequent candidates for source rocks as coals, it is most likely to find them as Jurassic, Cretaceous and Tertiary coals (Isaksen et al., 1998; Fleet and Crawley, 2000).

1.7 Generation of hydrocarbons with coal as a source

The initial H/C ratio, whether the ratio is low or high, gives an indication of the type of coal. If the ratio is low, the generation of oil will be small, while most of their gas will be yielded directly from the coal (Hunt, 1996). The petroleum potential of individual macerals will increase according to the order of increasing H/C ratio (Hunt, 1979).

Hunt (1996) showed that humic coals release mainly methane with increasing maturation (see figure 1.1). The amount of gas liberated may be huge. Lewan 1993 found that heating coals by hydrous pyrolysis (HP) yielded 5 to 20 wt % waxy oils and one to 4 wt % gas. The H/C ratio of the coals gave the amount and quality of the oil yield. Maturation of coal in these HP experiments continues close to the end of the low- volatile bituminous stage.

Calculations have been done to quantify the amount of gas. According to Kartweil (1969), Juntgen and Klein (1975) 150 litres of gas is generated per kilogram of coal, when maturation reaches the semi anthracite stage. Figure 1.1(A) from Smith (1994) shows that in the meta-anthracite stage; even more gas may be generated. Under very high thermal stress, additional 50 litres of gas may be obtained. This figure gives an indication of loss of nitrogen, carbon dioxide and methane during the coalification process. Small amounts of ethane through butanes are also formed during coal maturation. High adsorption makes it difficult to quantify the amount of these heavier gases.

If the analysis above is correct, quantities of oil and gas generated under different stages of coal maturation may be calculated. By the semi-anthracite stage, one-third of the gas has come directly from coal and two-thirds from the cracking of the oil generated by coal. This

assumes no loss of oil. With further maturation into the meta-anthracite stage, the proportion is approximately 50 % from each mechanism (Hunt, 1996).

Humic coals consist of vitrinite. When these particles are distributed in shales, they are classified as type III kerogen. When the process of maturation follows the same conditions of thermal stress, both coals and type III kerogen generates gas. Figure 1.1(B) indicates that peak gas generation generally occurs at maturities greater than 1.3 % Ro. In addition, the curve shows that about 80 % of the maximum quantity of gas available from a type III kerogen is expelled before a maturity of two % Ro. This figure, by Smith (1994), is based on the differences between gases generated by bedded coal and those from dispersed coaly particles. The latter tend to release C₂, C₃ and C₄, which is generation of wet gases. These compounds are absorbed and adsorbed by bedded coal (Hunt, 1996). When coaly particles are dispersed, the potential of generating gas is bigger compared to bedded coal.

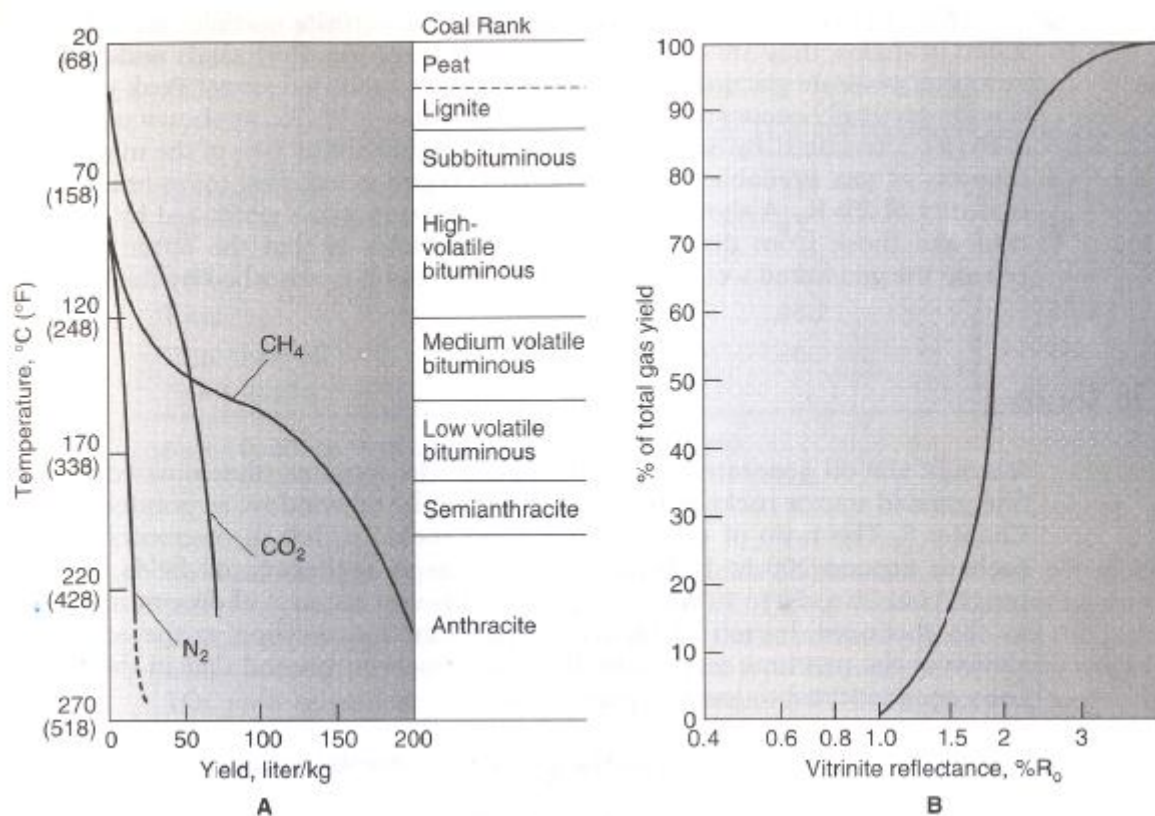


Figure 1.1. A) Calculated curves of gases generated from coal during coalification. [Data from Karweil, 1969]. B) Vitrinite reflectance versus percentage of total gas yield expelled from type III kerogen based on Shell Oil Company data files [Smith 1994].

1.8 Gas from coals

Coals are a major source of gas, mainly consisting of methane and carbon dioxide (pers.com Dag A. Karlsen, 2008). Figure 1.3 shows that coal is matured through the meta-anthracite stage. From a kilogram of coal, 150- 200 litres of methane are generated. Because coals have the ability of adsorption and absorption on its surface and in micropores, some gas “loss” is expelled. Coal acts as both a source and a reservoir (Hunt, 1996).

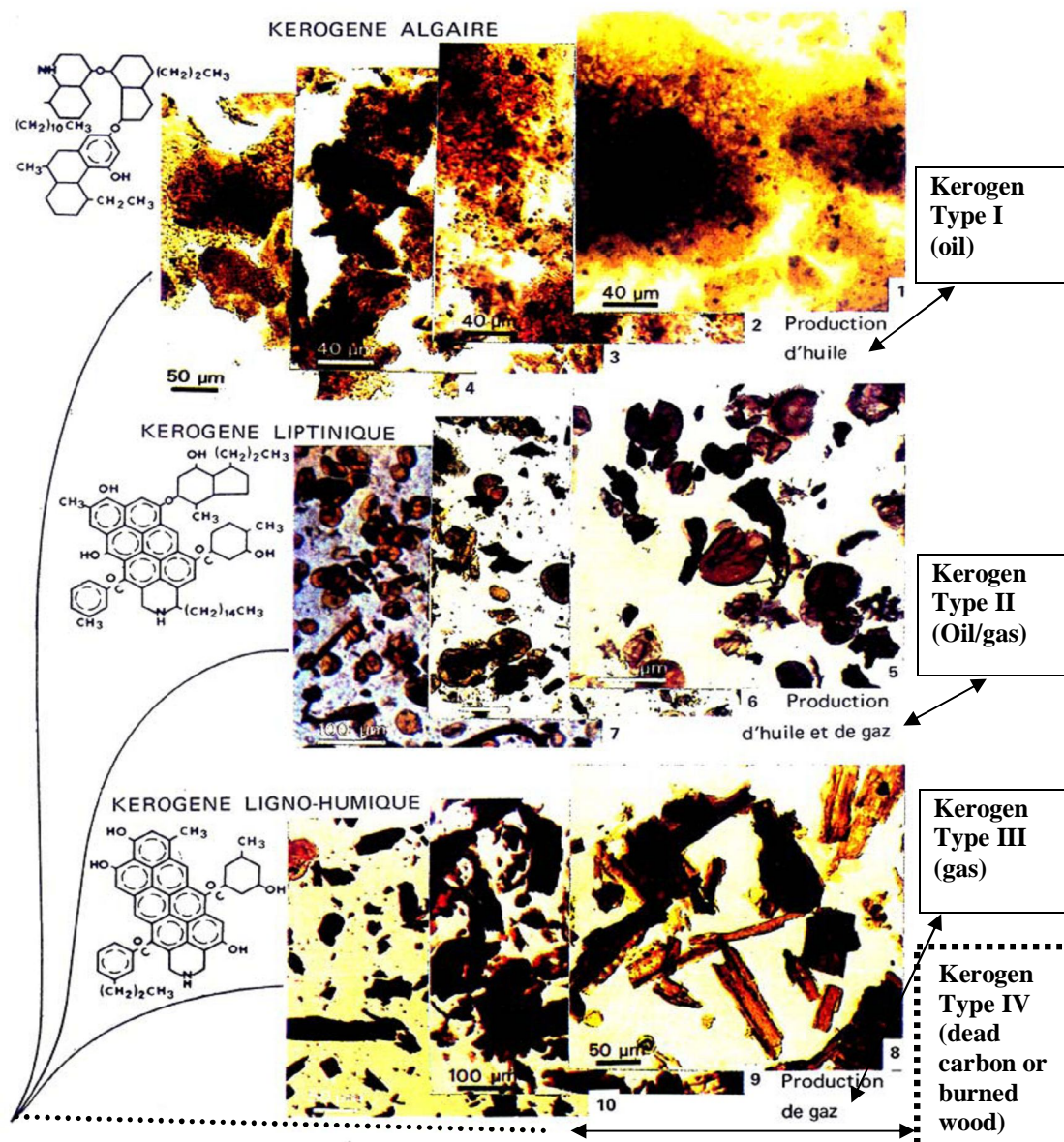


Figure 1.2. Characteristic pictures of the 3 main kerogen types; type I, II and III. Type I consists mainly of algae and generates basically oil in a short interval. Type II, dominating by spores and pollen, generates oil and gas in a broader temperature range than type I. Lignin and Cellulose are main constituents in type III, generating gas. The trends for thermal maturity are also indicated (from Durand, 1980). Kerogen type IV (consists of inertinite) is modified by the author.

The San Juan Basin contains 30 ft³/ft³ of adsorbed gas from coal, which is three times the volume of gas in a cubic foot of an adjacent sand reservoir. Coal has an adsorption capacity which increases with pressure and coal rank. Excess gas is expelled when the capacity is exceeded. One example of expelled gas from Carboniferous coal is the Gröningen field in north Holland (Hunt, 1996).

Gas from coals varies from dry to wet, and the main non-hydrocarbon gases are CO₂ and N₂. Wet gases have high concentrations of C₂+. The C₂+ fraction can be as high as 70% in some Late Carboniferous coal mines, which are found in the western part of Germany (Hunt, 1996). From Rice (1993), the coal-bed production yields methane with 18 % C₂+ in the Piceance Basin and 14% in the San Juan Basin of Colorado. These coals are mainly of humic origin, and have the ability to generate hydrocarbons heavier than methane. In many coal beds, the generation of gas causes over-pressure. The abnormal pressure, like in San Juan Basin, is greater than those of adjacent sand-shale sequences, which consist of waxy oils.

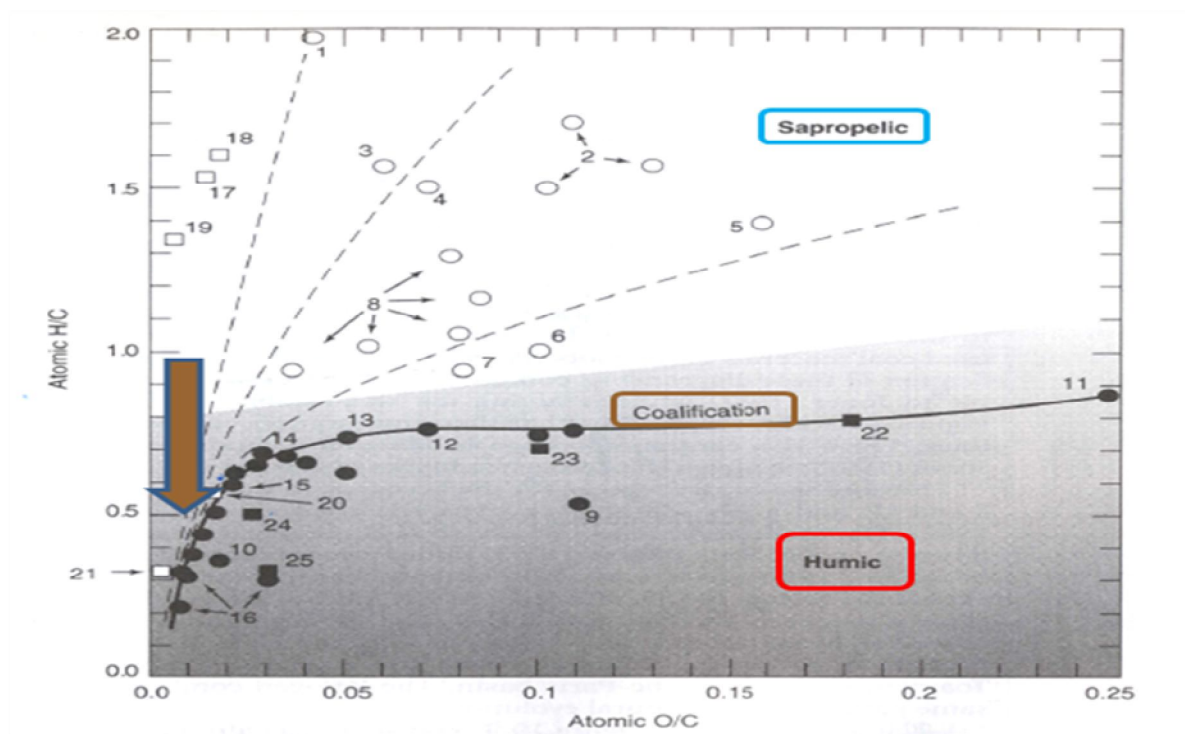


Figure 1.3. The van Krevelen maturation diagram for coals and coal macerals (modified after). The maturity of all samples increases toward the lower left-hand corner of the plot, marked by the dashed and solid curves in addition to the brown arrow. [Data from Hunt 1979; Johnston 1990; Saxby et al. 1986; Stach et al. 1982; Van Krevelen 1961].

1.9 Oil from coals

Coals, normally representing type III or type IV kerogen (figure 1.2), are in general not associated with large accumulations of oil. Still a source rock sequence containing coal and coaly shales may produce oil (Hunt, 1996).

Pyrolysis analysis in the form of experimental simulations has shown that hydrogen-rich coals can generate oil. There have been only a few estimates concerning the expulsion efficiencies from coals, but they are nevertheless in the order of 50% (Wilkins and George, 2002).

Under natural conditions, generation of oil involves adsorption and absorption in primary migration. Generation of oil from bedded coals happens by expulsion through fine pores in the tight structure of coals. Under increasing thermal stress, coal matures even more and may convert oil to gas (Hunt, 1996).

Coals are rocks having a tight internal macrostructure. The initial stages of expulsion may be dominated by activated diffusion of molecular components. Aromatic and in particular polar compounds are adsorbed and absorbed to a large extent. The result is expelled oil, which is enriched in saturated hydrocarbons (Wilkins and George, 2002).

Evidence of coal-derived oils from natural coalification (figures 1.1 and 1.3) is not abundant. Evidence of expulsion from coals is limited since only a few commercial oil discoveries can be confidently correlated to coals. These are Middle Jurassic coals from the Danish North Sea and New Zealand Tertiary coals. The most important source rock producing oil is the Upper Cretaceous Fruitland Formation coals in the USA.

1.10 Scope of thesis

Petroleum geochemistry is the application of chemical principles concerning the origin, accumulation, migration and alteration of petroleum. By the use of this knowledge, a better understanding of petroleum geochemistry in the form of absorption, adsorption, expulsion, migration and accumulation is obtained (Hunt, 1996).

Biomarkers are unchanged or undergo only minor changes to their molecular skeleton from their origin in plants to their preservation in oils, i.e. preserving the carbon skeleton (Tissot and Welte, 1978). The biomarker therefore represents a fingerprint of the geochemical input

and the pH/Eh conditions of the palaeo-depositional environments that resulted in organic matter becoming included into the sediment. These are therefore perfectly suited for correlation problematic. Petroleum contains only a small amount of biomarkers, one % or less. The biomarkers give information about the genetic relationship between petroleum, proof of actual expulsion from coals and other source rocks and the quality and maturity of the source rock from which the petroleum originated.

Thus, the scope of this thesis is to evaluate if Lower Carboniferous coals of the Tettegras Fm. (Viséan time) from the Finnmark Platform to a certain extent may have sourced oils from the same area, with respect to maturity and migration patterns. If the coals turn out to be mature and oil-prone with a high potential for generating petroleum, it must be considered if coals have been acting, or have the potential to act as source rocks for oil, if not in this specific sampled location, but in other parts of the Barents Sea. The results of these investigations may therefore not only pertain to the Finnmark Platform, but to the Bjarmland Platform and other parts of the Barents Region. The Lower Carboniferous could, and I repeat could, represent a new Petroleum System with circumstantial evidence drawn this far only from the Billefjord Gr. at Svalbard, a region where the Russian found oil while drilling for coal. It is therefore of the outmost importance to characterize the geochemical and oil generative potential of these coals.

Therefore, it is the purpose of this study to investigate these coals given the time limits of a master thesis and to try to evaluate if these coals have oil potential and to evaluate if these coals may also have expelled oil and sourced discoveries in well 7128/4-1 on the Finnmark Platform. I will compare the coal extracts with the DST oils concerning similarities and differences concerning maturity, organic facies parameters and overall origin. Determination of terrigenous versus marine origin of oils found on the Finnmark Platform will be important considering the hypothetical but not impossible relationship to coals. It is clear that “absence of proof is not proof of absence concerning correlation, i.e. we are in such a limited study bound by a limited sample set, but attempts must be made.

The core material containing oil is sampled from two places in the same well 7128/4-1. The core depths for DST-1 and DST-2 are 1592-1610m and 1577-1586m, respectively and represent the same reservoir zone. By analyzing the organic material from the cores i.e. the coals, it will be possible to identify the maturity in order to determine the kerogen type.

Biomarkers and sedimentary facies will give information concerning the environment (oxic/anoxic) during deposition. The oils are then geochemically compared to the organic extracts from the coals using GC-FID and GC-MS methods.

The analytical procedures used in this master study are Iatroscan TLC-FID, GC-FID and GC-MS, all based on the extraction process of coals using a Soxtec system. The chromatograms, chemical facies and maturity parameters are used to determine geochemical characteristics of coals. Other methods used to describe the geochemical properties of coals in the form of solid crushed material include the Rock-Eval pyrolysis and the LECO TOC.

Among the samples there are 10 coal samples which are collected from the wells 7128/4-1 and 7128/6-1. In case of Iatroscan TLC-FID characterization it was deemed that it was sufficient for time and cost constraints to analyze only the coal samples 4, 5 and 7 (see table 5.1). Still, due to the importance of molecular characterization for correlation of coals with DST oils, 10 coal extracts have been run through GC-FID and GC-MS and all relevant parameters have been calculated, plus the two oils and the reference NSO oil.

The work was completed within the time-limit of a Master Thesis, which is 20 weeks.

2. The sample set

This chapter is presenting the samples used in this thesis.

The sample set contains 5 coal samples and two DST oil samples from well 7128/4-1. Another 5 coal samples were analyzed from well 7128/6-1. The standard “North Sea Oil” is represented among the samples and is termed the NSO-1 oil sample. It is included as a reference sample and is representative of a medium mature North Sea Oil. As mentioned in the “Introduction”, the main emphasis and focus is on the samples 4, 5 and 7, which represent pure coals according to the table 2.1. Furthermore, the oil samples represented by the DST oils (samples 11-12) are central in this study as these will be geochemically evaluated with respect to the geochemistry of the coal extracts for correlation purposes. More information concerning the samples is found in the table 2.1.

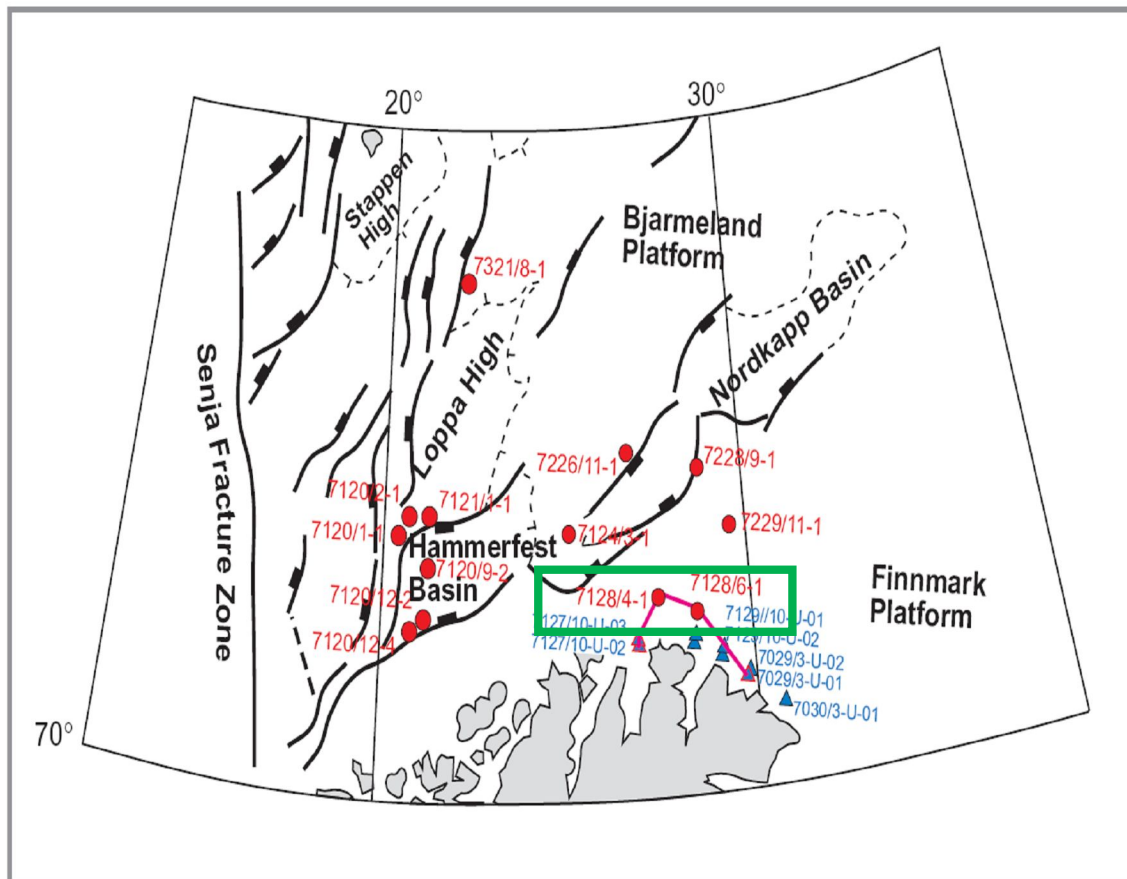


Figure 2.1. The 10 coal samples in addition to the two DST oils were collected from the wells 7128/4-1 and 7128/6-1, marked within the green square on the map. The wells are situated in the western part of the Finnmark Platform, close to the Hammerfest- and Nordkapp basins and may also have relevance for coals on the Bjarmeland Platform.

The 12 samples from the wells 7128/4-1 and 7128/6-1 represent Lower Carboniferous coals of the Tettegras Fm. on the Finnmark Platform, in the Barents Sea. The wells are lying close to each other in the south-western part of the platform, as seen on the map i.e. figure 2.1. The Finnmark Platform is bounded to the west by the Hammerfest Basin, to the north by the Nordkapp Basin and in the NE by the Bjarmland Platform.

Well	Depth from [m]	Depth to [m]	Sample nr	Type	Formation	Lithology	remarks
7128/4-1	2346,00		1	cuttings, unwashed	Tettegras	coal 75 % shale 5%/SS 15 %	washed and sieved (250 μ) at UiO / NOT picked
7128/4-1	2366,50		2	core chips	Tettegras	coal	SS above and below, 1m rooted coal
7128/4-1	2366,80		3	core chips	Tettegras	coal	SS above and below, 1m rooted coal
7128/4-1	2376,10		4	core chips	Tettegras	coal	rooted/near top (10cm), rooted coal 80cm
7128/4-1	2384,70		5	core chips	Tettegras	coal	rooted/below mid-section, 50cm rooted coal
7128/4-1	1592,00	1610,00	11	oil, DST 1			
7128/4-1	1577,00	1586,00	12	oil, DST 2			
7128/6-1	2222,70		6	core chips	Tettegras	coal/shale	
7128/6-1	2226,40		7	core chips	Tettegras	coal	
7128/6-1	2246,20		8	core chips	Tettegras	coal/ rooted	
7128/6-1	2247,70		9	core chips	Tettegras	coal/mudstone (on bag)	
7128/6-1	2349,00		10	Cuttings, washed	Tettegras	coal 90%/SS 10%	NOT picked

Table 2.1. The sample set includes 10 coal samples, 5 samples from well 7128/4-1 and 5 samples from well 7128/6-1. The three oil samples are the two DST oils from well 7128/4-1 in addition to the standard North Sea Oil (NSO) from the Oseberg Field.

3. Analytical methods

The analytical techniques based on geochemical properties can be divided into two main groups; bulk parameters and specific molecular properties. The bulk parameters describe gross composition properties of whole samples, in terms of either whole oil or total extracts. By the use of Iatroscan (TLC-FID) the percentage amount of saturated hydrocarbons, aromatic hydrocarbons and polar compounds can be calculated. The specific properties describe detailed chemical characteristics of either specific sample fractions or whole oils, and can be measured by the use of gas chromatography with flame ionization detector (GC-FID) or gas chromatography – mass spectrometry (GC-MS).

This chapter will describe the analytical methods used in this study.

3.1 Procedure of preparing samples

3.2 Iatroscan TLC-FID

3.3 GC-FID

3.4 GC-MS

3.5 Rock-Eval – Hydrous pyrolysis

3.1 Procedure of preparing samples

30 mg oil (+5 mg) was transferred to a two ml bottle with a Teflon lined plastic cork, and diluted with one ml dichloromethane. For solvent extractions of coals, an instrument called Soxtec was used. The coal samples, weighing around two gram, were finely crushed before extractions. The sample set was analyzed by three different methods.

3.2 Iatroscan–Thin Layer Chromatography – Flame Ionization Detection (TLC-FID)

Iatroscan analysis involves thin layer chromatography and flame ionization detection (TLC-FID) of petroleum fractions (see figure 3.1). It provides a rapid and relative accurate method

for the quantification of saturated hydrocarbons, aromatic hydrocarbons and the polar fraction (resin and asphaltenes) in solvent extracts of petroleum source rocks, reservoir rocks and crude oils (Karlsen and Larter, 1989). The varying proportions of saturated and aromatic hydrocarbons together with polar compounds can be used to characterize the petroleum populations in the reservoir (Bhullar et al., 2000), and differentiate between migrated hydrocarbons, in-situ generated hydrocarbons and also diesel drilling fluids (Karlsen and Larter, 1991). This technique is suitable to screen large sample volumes from petroleum reservoirs to obtain information for selection of samples for high-resolution analysis.

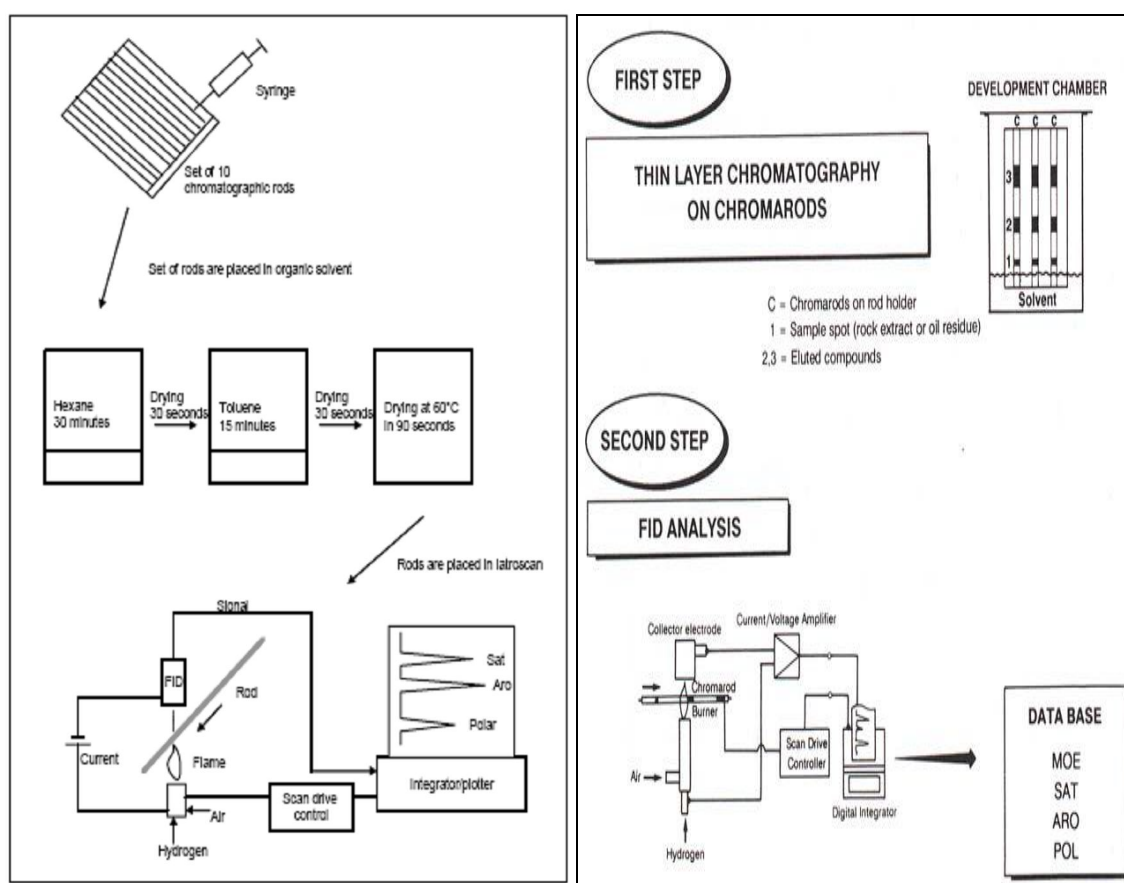


Figure 3.1. The key elements in the TLC-FID analysis for separating and quantifying saturated and aromatic hydrocarbons in addition to polar compounds (resins and asphaltenes) (from Pedersen, 2002 (left) and Bordenave, 1993 (right)).

The coal/ oil samples were analyzed by an Iatroscan TH-10, MK IV (Iatron inc., Tokyo) instrument equipped with a flame ionization detector (FID) and interfaced with an electric integrator (Perkin-Elmer LCI-100) used for rod scanning and quantification. The components were separated using silica rods, type Chromarods-S III (pore diameter 60 Å, particle size 5

micro meters). All of the samples were applied (three micron liters) to a fixed point near the base of the Chromarod. 8 out of 10 rods were used for the samples (two rods pr. sample); the remaining two were used for test runs, one blank and the other one with the NSO-1. To develop the Chromarods, solvents of different polarity were used to separate saturated hydrocarbons, aromatic hydrocarbons and polar compounds. The rods were placed in normal-hexane for 35 minutes, causing the saturated hydrocarbons to rise to the uppermost part of the rods. After air drying the rods were placed in toluene for 6 minutes, causing the aromatic hydrocarbons to move to the middle of the rods. Then the Chromarods were dried at 60 °C (90 sec) and placed in the Iatroscan instrument. The scanning speed was 30 sec/scan, and pure grade hydrogen (180 ml/min) and air (2.1 l/min) supplied by a pump were used for the detector.

3.3 Gas Chromatography-Flame Ionization Detector (GC-FID)

GC-FID methods allow identification and relative or absolute quantification (using internal standards) of individually separable major compounds in petroleum. These are n-alkanes, isoprenoids, toluene, hexane, xylene and more. The whole oil is injected and vaporized before entering a chromatographic column, in which the separation of the different molecules takes place. A film layer on the inside of the column acts as the stationary phase. The short-chained molecules travel quickly through the column, while longer or more branched molecules need a longer period of time to move through the entire column. An inert gas, like Nitrogen (N₂) or helium (He), is used as carrier gas, and this is the mobile phase. The column is heated according to a program from 40 °C to 325 °C in 75 minutes, and is kept on 325 °C for 20 minutes, i.e. one run takes 95 minutes. The reason is to mobilize the compounds that have too low vapor pressure at ambient temperature. When the molecules exit the column, they enter a flame ionization detector as described above. A computer records the signal from the FID, and the final gas chromatogram is edited and plotted using appropriate software. No preparation of the samples is needed.

The GC-FID instrument (see figure 3.2, left) used in this study was a Varian Capillary Gas Chromatograph Model CP 3800 with a 50 m length HP Ultra-one column, which had a 0.2 mm internal diameter and 0.33 micrometer film thickness. Temperature programming was 80

°C for one min, then an increase of 4.5 °C /min to a final temperature of 320 °C held for 25 min (total time 79.33 min). There was a constant column flow of one ml/min, the injector had a temperature of 300 °C and the detector temperature was 330 °C. The analysis was performed with nitrogen carrier gas and split injection.

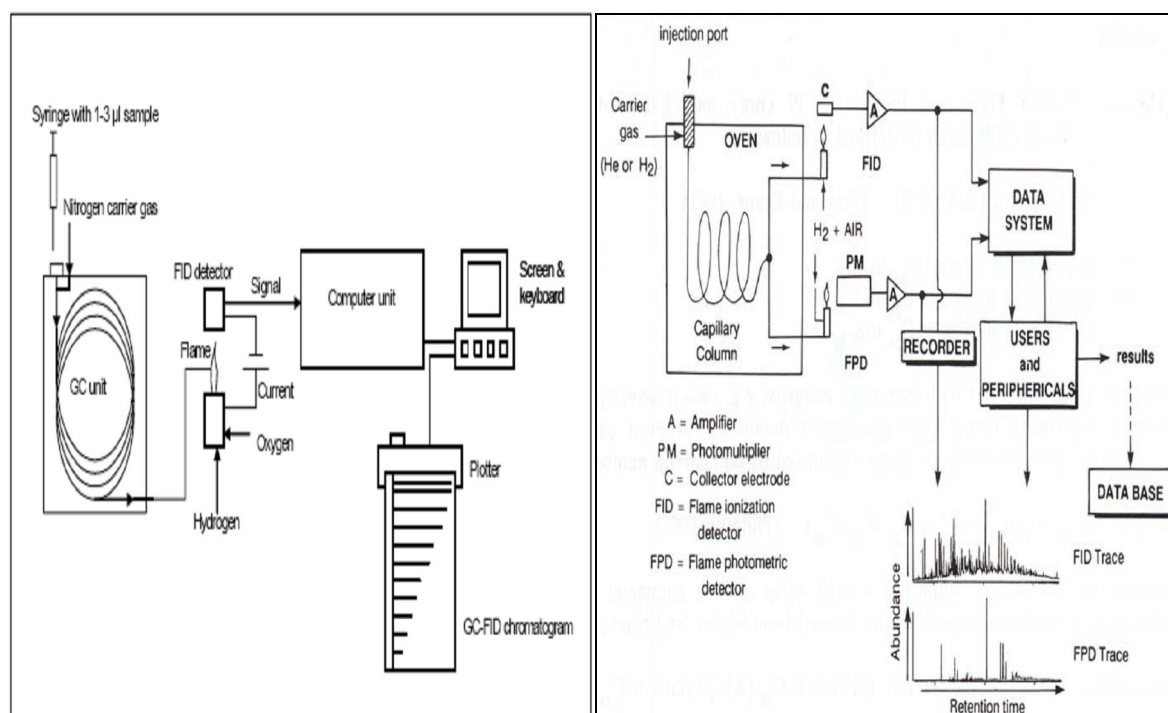


Figure 3.2. Compatible sketches of the GC-FID instrument (from Pedersen, 2002 (left) and Bordenave, 1992 (right)).

Some of the most common parameters in organic petroleum geochemistry studies are based on data collected by the GC-FID. The parameters include:

- Carbon Preference Index (CPI) or Improved Odd Even Preference (OEP)
- Pr/ n-C17
- Ph/ n-C18
- Pr/Ph

These parameters are mainly used as maturity and facies indicators, but GC-FID chromatograms may also be applied for general fingerprinting of the samples.

3.4 Gas Chromatography-Mass Spectrometry (GC-MS)

The GC-MS procedure allows identification and quantification of biomarkers. A GC-MS system forms an instrument capable of separating mixtures into their individual components, identifying and then providing quantitative and qualitative information on the amount and chemical structure of each compound (McMaster and McMaster, 1998).

The GC-MS is a combination of a gas chromatograph (GC) for compound separation and a mass spectrometer (MS) using ionization and mass analysis for detection and identification of the components (see figure 3.3). The ions of interest are selected according to their mass before being detected. The different molecule fragments have different mass (m) and an electric charge (z) equal to unit, and the ratio m/z is specific for many molecules of interest, such as biomarkers. Hopanes and other triterpanes are for example found to have a characteristic fragment with $m/z = 191$. The detector registers the m/z value and the relative abundance of the different ions. A PC program is used in recording and managing the data. The final plot shows the relative abundance of ions with the selected m/z ratio versus time elapsed (retention time).

The GC-MS instrument used in this study was a Fisons MD800 quadrupole -instrument with a 50 m long Chrompage, WCOT, CP-sil 5 CB LOW BLEED/MS column, which had a 0.32 mm internal diameter and 0.40 micron meter film thickness. The injection was done using a CTC A200S auto sampler with a sample volume of 4 micro liters. The starting temperature was 80 °C (one min), then an increase of 10 °C /min to a temperature of 180 °C, and then 1.7 °C/min to a final temperature of 310 °C held for 30 min. The total time of the program was 120 min.

The GC-MS was used in this study to monitor the ions with a mass/charge (m/z) ratio of 178, 191, 192, 198, 217, 218, 231 and 253. Monitoring of these ions will give information about the most common biomarkers and related compounds used to establish the maturity, source and facies of the petroleum and coals in this study.

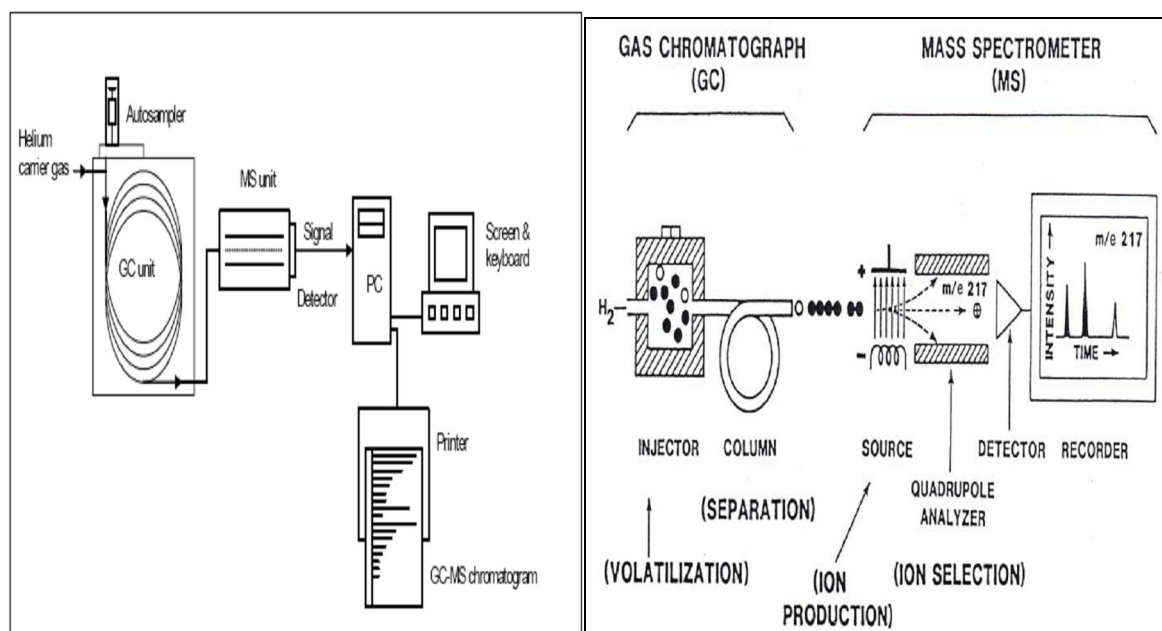


Figure 3.3. Compatible sketches of the GC-MS instrument (from Pedersen, 2002 (left) and from Waples and Machihara, 1991 (right)).

3.4.1 Molecular Sieving

For many years organic geochemists have been using 5Å molecular sieves to separate n-alkanes from other saturated hydrocarbon components of petroleum (Eglinton and Murphy, 1969). The main purpose for carrying out this separation is to remove the n-alkanes (straight chained hydrocarbons) and polar compounds from the sample. The n-alkanes comprise a major proportion of most petroleum and if present in the sample they will interfere with the signals from the biomarkers. By removing the n-alkanes the biomarker signals will be enhanced relative to the interference from n-alkane fragments. The molecular sieve is a special compound with a well-defined molecular structure. The n-alkanes fit into the long-, channel-like pores in the molecules and are trapped inside, while the bigger biomarkers are unaffected by the molecular sieve. When the sieve is separated from the sample, the biomarkers and aromatic compounds remain in the solution. In this way the sample is enriched in biomarkers and depleted in n-alkanes. In this study 5Å silicalite UOP MHS2-420LC (a synthetic zeolitic form of silica) was used.

About 0.18 g of molecular sieve was transferred into a 15 ml glass vial. three drops of sample were then mixed with the powder-like sieve using a pipette. The sample mixture was diluted with two-2.5 ml cyclohexane and stirred thoroughly. Then the vial was centrifuged at 2000 rpm for 3 min in a Heraeus Sepatech Labofuge H, to settle the sieve. Subsequently, the

sample was decanted into a new 15 ml glass vial, and about $\frac{3}{4}$ of the solvent evaporated by a flow of nitrogen. After the sample had been up-concentrated the procedure was repeated. After the final evaporation of cyclohexane, the sample was transferred to two 40 X 6 mm glass vials with a pipette and sealed with a Teflon-lined cap.

3.5 Rock-Eval – Hydrous pyrolysis

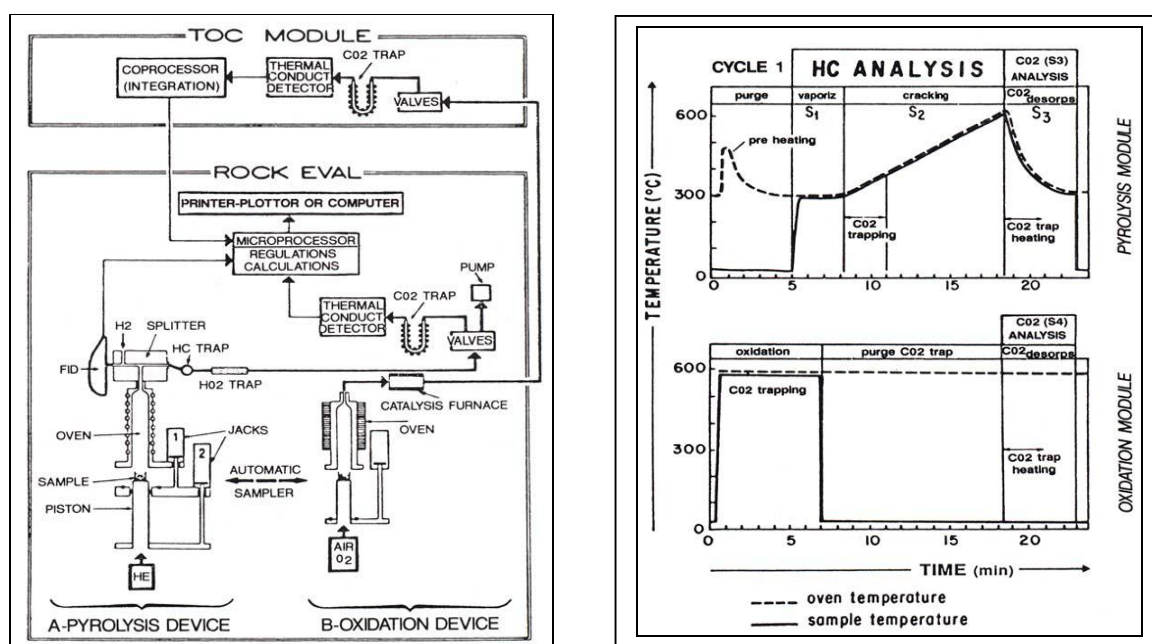


Figure 3.4. Rock-Eval pyrolysis and module of TOC (left), S_1 top is the result of thermal heating while the tops S_2 and S_3 represent the result of the pyrolysis (right) (both pictures taken from Bordenave, 1993).

Pyrolysis is defined as heating of organic matter in the absence of oxygen, to yield organic compounds. In Rock-Eval pyrolysis, pulverized samples are gradually heated in an inert helium atmosphere (see figure 3.4, left). This heating distills the free organic compounds (free hydrocarbons; $C_1 - C_{25}$, Karlson and Larter (1989)). Further cracking of kerogen gives pyrolytic products from the insoluble organic matter (kerogen).

The figure 3.4 illustrates the principle of the Rock-Eval pyrolysis. The S_1 signal from thermal evaporation is measured in mg HC/ g rock, as well as the S_2 peak from pyrolysis. The S_3 top represents the late stage of pyrolysis (figure 3.4, right) and the amount is given in mg CO_2 /g rock.

4. Maturity and facies parameters

The sample set has been run through the various techniques described in chapter three. The parameters which are important for determining maturity and facies will be described in the following:

4.1 Data from Iatroscan TLC-FID

4.2 Data from GC-FID

4.3 Data from GC-MS

4.4 Data from Rock-Eval pyrolysis

4.1 Data from Iatroscan TLC-FID

Saturated hydrocarbons/aromatic hydrocarbons and polar compounds

Thin-layer chromatography and flame ionization detection (Iatroscan TLC-FID) represents an accurate method in terms of quantifying petroleum compounds. These compounds are saturated and aromatic hydrocarbons in addition to polar compounds, divided into resins and asphaltenes. The fractions of petroleum compounds are measured in solvent extracts of petroleum source rocks, reservoir rocks and crude oils (Karlsen and Larter, 1991).

When studying heterogeneities in reservoir zones, the method is used to characterize the horizontal and vertical distributions of gross petroleum composition (Karlsen and Larter, 1989). This technique may also detect or locate oil water contacts (Karlsen and Larter, 1991).

The saturated hydrocarbons/aromatic hydrocarbons (SAT/ARO) mainly reflect source rock quality and maturity (Cornford et al., 1983; Clayton and Bostick, 1986). The ratio increases with increasing thermal maturity. In addition, an increase in the gas-phase of phase-fractionated petroleum during the migration to shallower depths may occur. In oils the polar compound fraction represents either low maturity or biodegradation, eventually a mixture of the two components. The concentration of polar compounds is low in high maturity petroleum and condensates. On the contrary, high values are typical for low maturity coals.

If the Iatroscan TLC-FID is used correctly and knowing its limitations, the instrument represents a major improvement in petroleum geochemical screening (Karlsen and Larter, 1991).

4.2 Data from GC-FID

The GC-FID analyses of various coals and associated oils have been used to analyze n-alkanes, focusing on the C_{15+} compounds for comparison (figure 4.2). The n-alkane distribution together with $Pr/n-C_{17}$ and $Ph/n-C_{18}$ are parameters which may indicate the origin of source, depositional facies, maturity and biodegradation.

n-alkane distribution

The n-alkane patterns can be used to classify chromatograms and give information about the facies and maturity of the samples (Peters and Moldowan, 1993). In normal “North Sea” petroleum the peak height decreases asymptotically with increasing carbon number. This creates a concave curve on the chromatogram. The GC-FID traces may also indicate if there is any biodegradation. The effect of biodegradation will show up as unresolved complex mixture (UCM) of compounds rising above the baseline. The relative concentration of n-alkanes will decrease compared to other compounds like isoprenoids and aromatics (Sutton et al., 2004).

Pr/Ph

Pristane and phytane are isoprenoid isoalkanes derived from phytol, a side chain of the chlorophyll molecule that separates from the porphyrine structure after deposition (Tissot and Welte, 1978). The depositional environment determines whether the phytol transforms into pristane or phytane.

The type of organic facies (kerogen) the sediments contain can then be predicted. If $Pr/Ph < 1$, it may indicate hyper saline, anoxic or carbonate setting. When $Pr/Ph > three$, the hydrocarbons likely comes from organic matter from deltaic facies or humic dominated environment, deposited under dysoxic conditions. Sediments deposited under normal marine

conditions display intermediate values ranging from one to three. Peters and Moldowan (1993) suggested that pristane and in particular phytane also may have a bacterial origin.

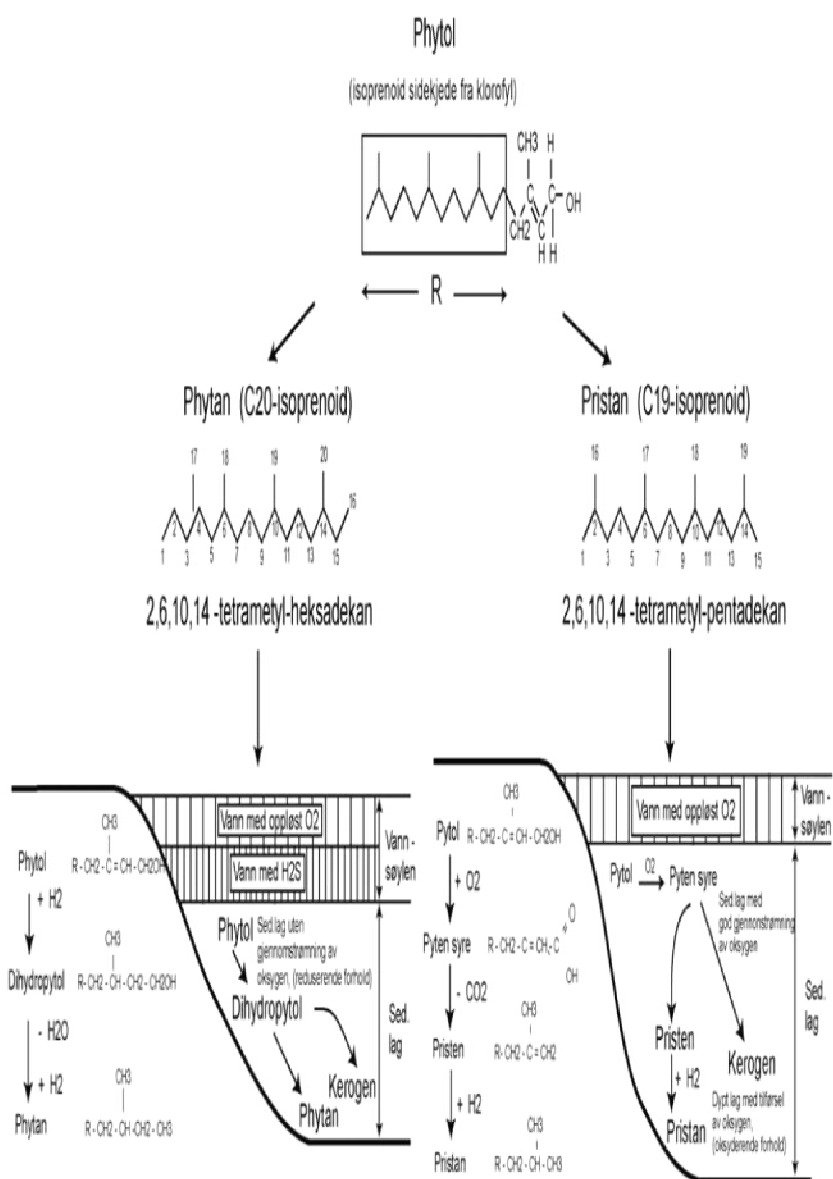


Figure 4.1. Pristane and phytane derived from phytol- the principle (taken from Grønseth, 2004. Modified from Tissot and Welte, 1984).

It is important to be aware that pristane and phytane during diagenesis can be derived from other sources than phytol e.g. bacterial membranes (ten Haven et al., 1987). The ratio should therefore be used together with other parameters for certainty.

Pr/n-C₁₇ and Ph/n-C₁₈

Pr/n-C₁₇ and Ph/n-C₁₈ ratios are used together with other parameters to determine source rock facies, maturity and the degree of biodegradation of hydrocarbons (see table 4.1). Samples having low ratios will be mature since the isoprenoids breaks down more readily than n-alkanes during maturation. Together with other parameters the ratios can be used to rank related, non- biodegraded oils and bitumens based on thermal maturity. Since organic input and biodegradation may affect the ratio, carefulness must be taken into account (Peters and Moldowan, 1993).

Parameters	Marine OM	Terrestrial OM	Lacustrine OM
Pr/Ph	≤2	≥3	1≤Pr/Ph≤3
Pr/n-C ₁₇	<0.5	>0.6	-
Ph/n-C ₁₈	<0.5	>0.6	-

Table 4.1. Parameters used to determine facies for source rocks (Peters and Moldowan, 1993).

Carbon Preference Index (CPI) and Odd/Even predominance (OEP)

The predominance of molecules with an odd number of carbon atoms can be measured by the Carbon Preference Index (CPI). The ratio of odd to even molecules is measured by weight, (Tissot and Welte, 1978). Bray and Evans (1961) introduced CPI, which can be used to indicate the thermal maturity of an oil or extract. CPI values significantly above or below one indicate thermally immature oil or extract. Peters and Moldowan (1993) suggest that values close to one represent thermally mature oil or extract, though it is not proven.

CPI can also give information about facies and deposition of environments. Values below one indicate carbonate facies, while values higher than one indicate lacustrine environment or siliciclastic source rock. Definitions are given by:

$$CPI = 2(C_{23} + C_{25} + C_{27} + C_{29}) / [C_{22} + 2(C_{24} + C_{26} + C_{28}) + C_{30}]$$

$$OEP = (C_{21} + 6C_{23} + C_{25}) / (4C_{22} + 4C_{24})$$

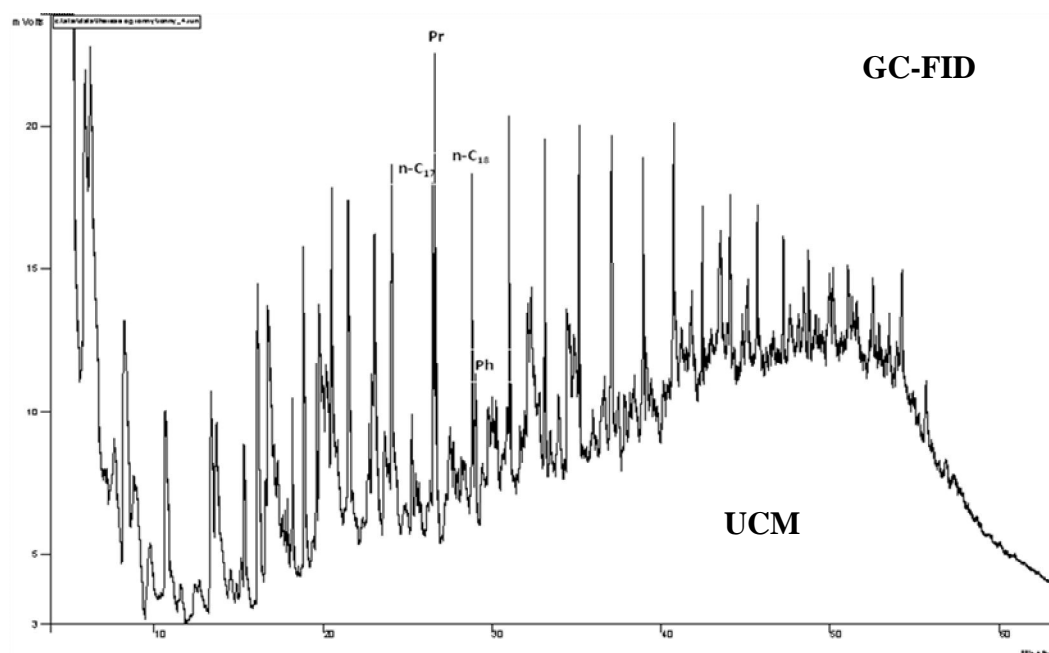


Figure 4.2. The GC-FID chromatogram of the coal extract at 2376.1 m from well 7128/4-1. The peaks n-C₁₇, n-C₁₈, pristane (Pr) and phytane (Ph) are identified (Weiss et al., 2000, Waples et al., 1991).

Vitrinite

Optical reflectance of vitrinite can be measured in a microscope and is frequently used as a maturity indicator. Vitrinite reflectance, which often is presented as (R_o), increases during thermal maturation due to complex, irreversible aromatization reactions. Table 4.2 presents approximate (R_o) values, which have been assigned for the beginning and end of oil generation.

$R_o < 0.5$ to 0.7%	diagenesis stage	source rock is immature
0.5 to $0.7\% < R_o < 0.7$ to 1.3%	catagenesis stage	main zone of oil generation
$ca. 1.3\% < R_o < 2\%$	catagenesis stage	zone of wet gas and condensate
$R_o > 2\%$	metagenesis stage	dry gas zone

Table 4.2. Vitrinite values, generally accepted diagenesis stages and maturity levels (Dow, 1977).

4.3 Data from GC-MC

The GC-MS method was used for the sample set to monitor ions with different mass/charge (m/z) ratio. The following figures display the peaks from the chromatograms for the ratios

$m/z = 178, 191, 192, 198, 217, 218, 231$ and 253 . A table describing every peak and component carefully follows beneath the corresponding figure.

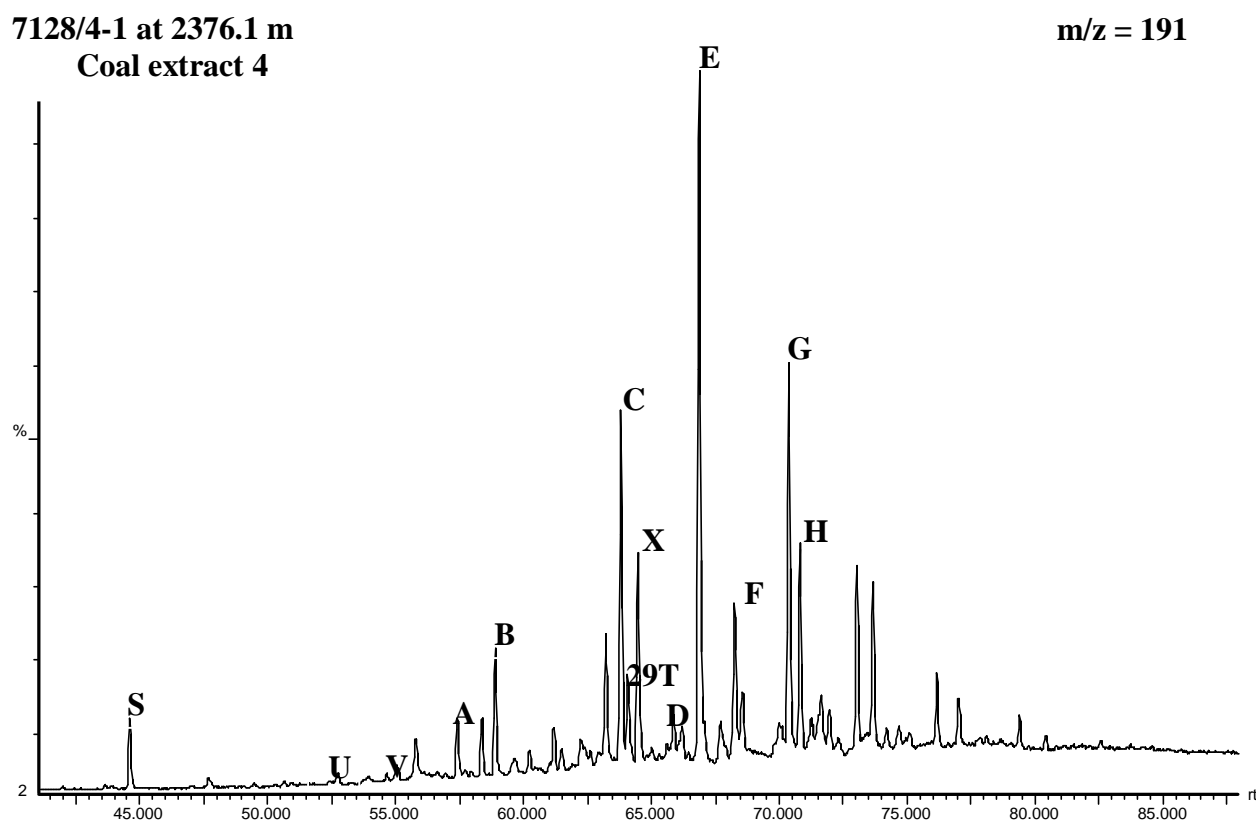


Figure 4.3. The GC-FID chromatogram of the coal extract at 2376.1 m from well 7128/4-1; displaying the triterpanes peaks, see table 4.3 (Weiss et al., 2000, Waples et al., 1991).

Peak	Stereochemistry	Identity	Composition
P		Tricyclic terpane	$C_{23}H_{42}$
Q		Tricyclic terpane	$C_{24}H_{44}$
R	(17R+17S)	Tricyclic terpane	$C_{25}H_{46}$
S		Tetracyclic terpane	$C_{24}H_{42}$
U		Tricyclic terpane	$C_{28}H_{48}$
V		Tricyclic terpane	$C_{29}H_{50}$
A		$18\alpha(H)$ -trisnorhopane	C_{27}
B		$17\alpha(H)$ -trisnorhopane	C_{27}
Z		28,30-bisnorhopane	$C_{28}H_{48}$
C		$17\alpha(H), 21\beta(H)$ -norhopane	$C_{29}H_{50}$
29Ts		$18\alpha(H)$ -30-norhopane	C_{29}
X		$17\alpha(H)$ -diahopane	$C_{30}H_{52}$
D		$17\alpha(H), 21\beta(H)$ -normoretane	$C_{29}H_{50}$
E		$17\alpha(H), 21\beta(H)$ -hopane	$C_{30}H_{52}$
F		$17\alpha(H), 21\beta(H)$ -moretane	$C_{30}H_{52}$
G	22S	$17\alpha(H), 21\beta(H)$ -homohopane	$C_{31}H_{54}$
H	22R	$17\alpha(H), 21\beta(H)$ -homohopane	$C_{31}H_{54}$

Table 4.3. Triterpanes identified from the $m/z = 191$ chromatograms (see the figure 4.3). Some of the peaks or compounds in the table are absent for the coal sample in the figure 4.3, but exist for the oil samples (Weiss et al., 2000, Waples et al., 1991).

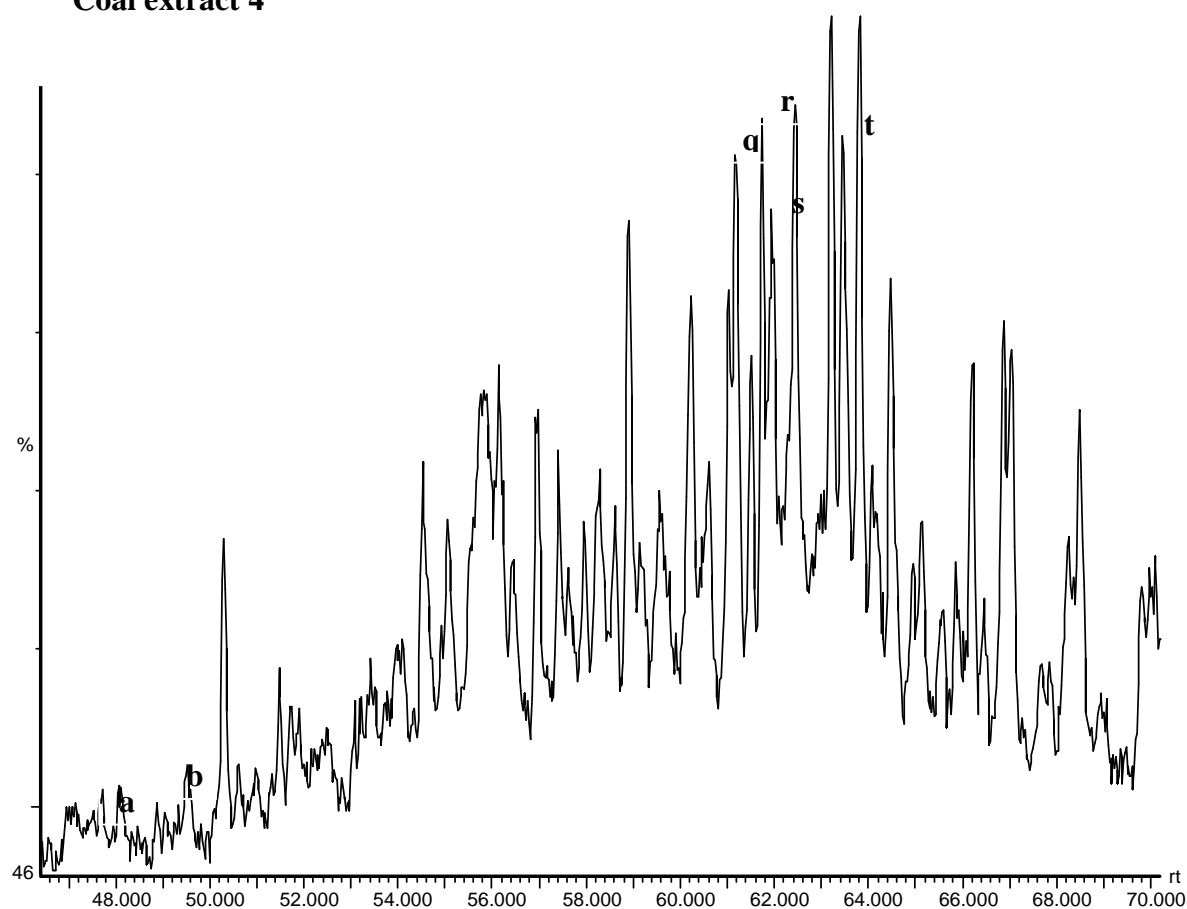


Figure 4.4 The GC-FID chromatogram of the coal extract at 2376.1 m from well 7128/4-1; displaying the steranes peaks, see table 4.4 (Weiss et al., 2000, Waples et al., 1991).

Peak	Stereochemistry	Identity	Composition
a	20S	13 β (H),17 α (H)-dicholestane	C ₂₇ H ₄₂
b	20R	13 β (H),17 α (H)-dicholestane	C ₂₇ H ₄₈
q	20S	14 α (H),17 α (H)-24-ethyl-cholestane	C ₂₉ H ₅₂
r	20R	14 β (H),17 β (H)-24-ethyl-cholestane	C ₂₉ H ₅₂
s	20S	14 β (H),17 β (H)-24-ethyl-cholestane	C ₂₉ H ₅₂
t	20R	14 α (H),17 α (H)-24-ethyl-cholestane	C ₂₉ H ₅₂

Table 4.4. Steranes identified from the m/z = 217 chromatograms, see figure 4.4 (Weiss et al., 2000, Waples et al., 1991).

7128/4-1 at 2376.1m
Coal extract 4

m/z = 218

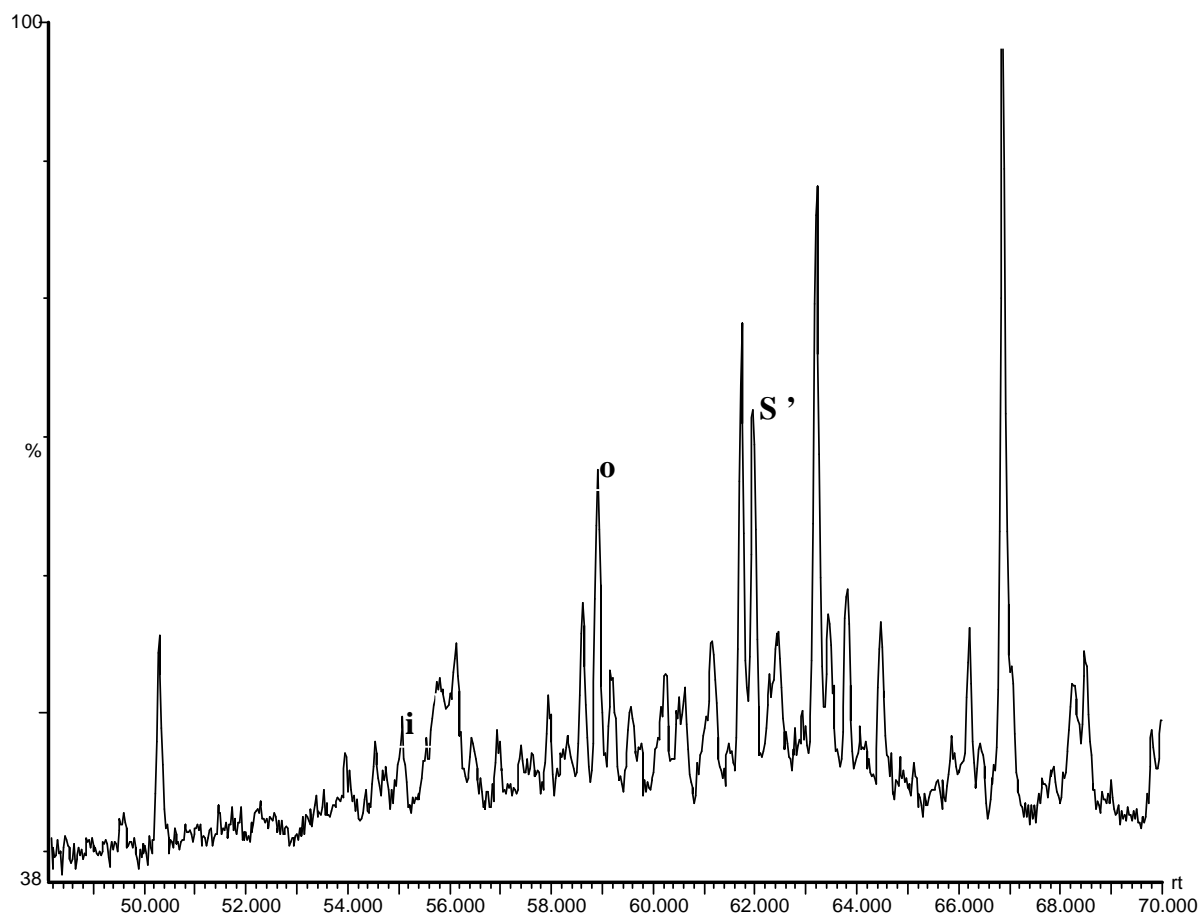


Figure 4.5. The GC-FID chromatogram of the coal extract at 2376.1 m from well 7128/4-1; displaying the steranes peaks, see table 4.5 (Weiss et al., 2000, Waples et al., 1991).

Peak	Identity
i	C ₂₇ regular sterane
o	C ₂₈ regular sterane
s'	C ₂₉ regular sterane

Table 4.5. Steranes identified from the m/z = 218 chromatograms, see figure 4.5 (Weiss et al., 2000, Waples et al., 1991).

7128/6-1 at 2226.4 m
Coal extract 7

m/z = 231

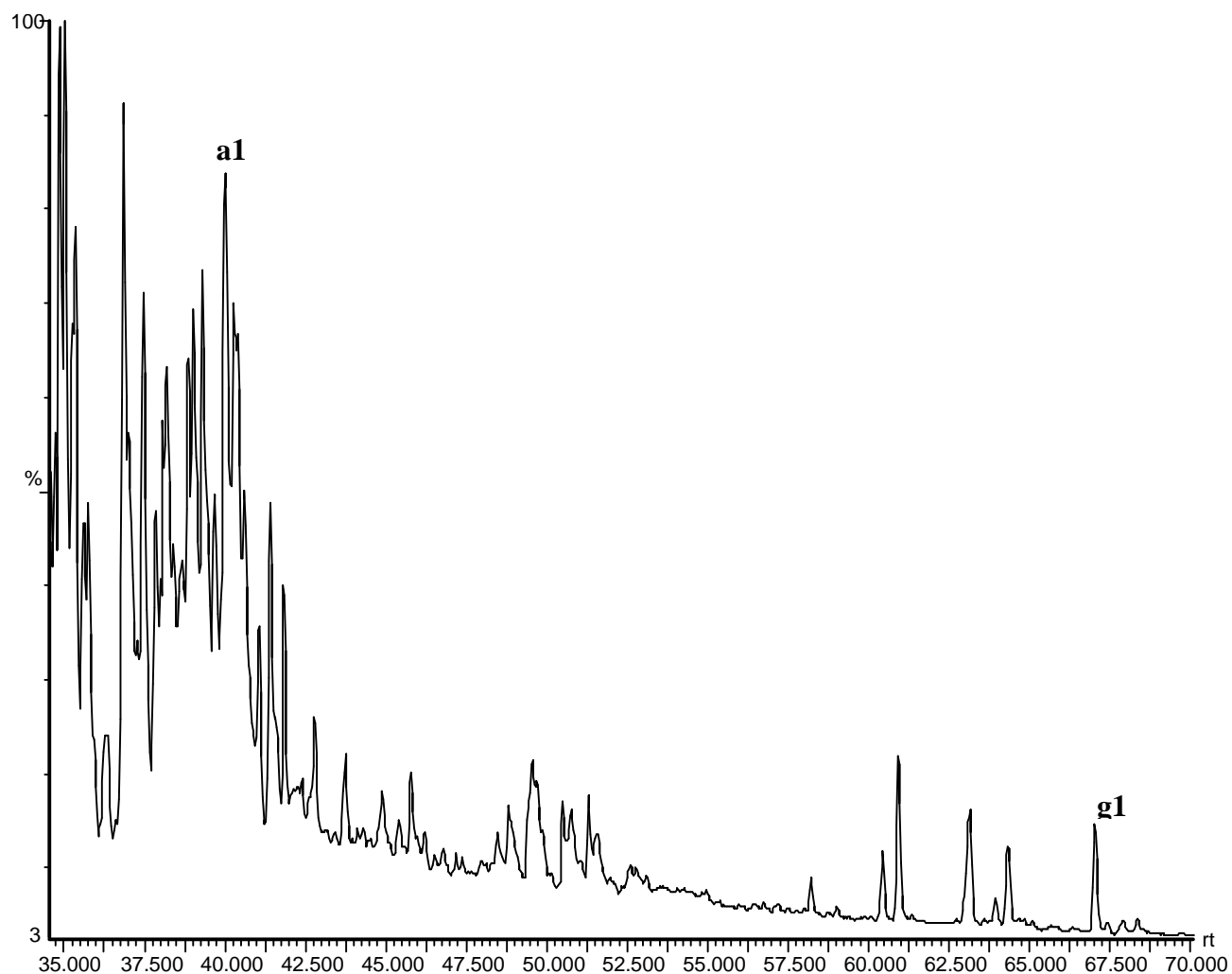


Figure 4.6. The GC-FID chromatogram of the coal extract at 2226.4 m from well 7128/6-1, displaying peaks of the triaromatic steroids, see table 4.6 (Weiss et al., 2000, Waples et al., 1991).

Peak	Identity
a1	C ₂₀ triaromatic steroid (TA)
g1	C ₂₈ triaromatic steroid (TA)

Table 4.6. Triaromatic steroids identified from the m/z = 231 Chromatograms, see figure 4.6 (Weiss et al., 2000, Waples et al., 1991).

7128/6-1 at 2226.4 m
Coal extract 7

$m/z = 253$

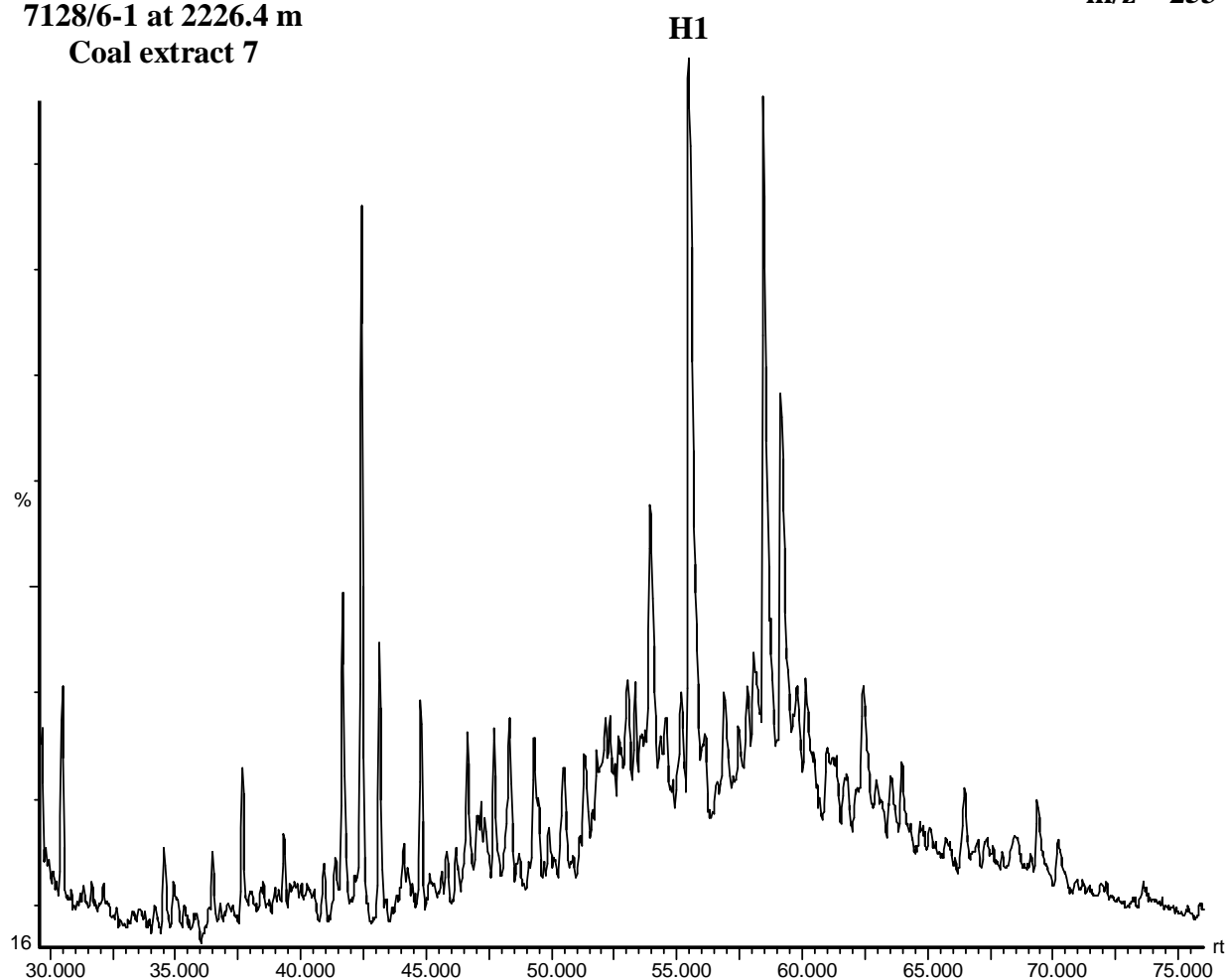


Figure 4.7. The GC-FID chromatogram of the coal extract at 2226.4 m from well 7128/6-1 are displaying peaks of monoaromatic steroid, see table 4.7 (Weiss et al., 2000, Waples et al., 1991).

Peak	Identity
H1	C ₂₉ monoaromatic steroid (MA)

Table 4.7. Monoaromatic steroid identified from the $m/z = 253$ chromatograms, see figure 4.7 (Weiss et al., 2000, Waples et al., 1991).

7128/4-1 at 2376.1 m
Coal extract 4

$m/z = 178 + 192$

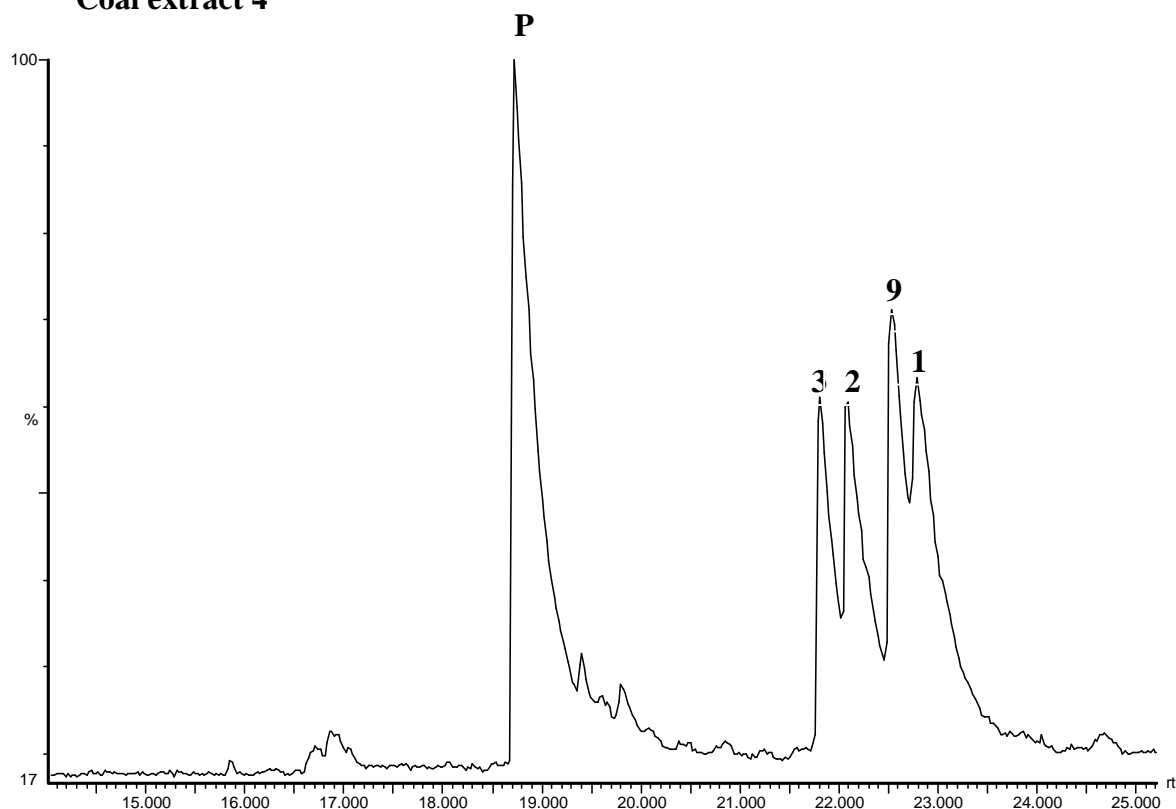


Figure 4.8. The GC-FID chromatogram of the coal extract at 2376.1 m from well 7128/4-1, displaying the peaks of phenanthrene and methylphenanthrene, respectively, see table 4.8. (Weiss et al., 2000, Waples et al., 1991).

Peak	Identity
P	Phenanthrene
3	3-methylphenanthrene
2	2-methylphenanthrene
9	9-methylphenanthrene
1	1-methylphenanthrene

Table 4.8. Phenanthrene and methylphenanthrene identified from $m/z = 178$ and $m/z = 192$ chromatograms, see figure 4.8 (Weiss et al., 2000, Waples et al., 1991).

7128/4-1 at 2376.1 m
Coal extract 4

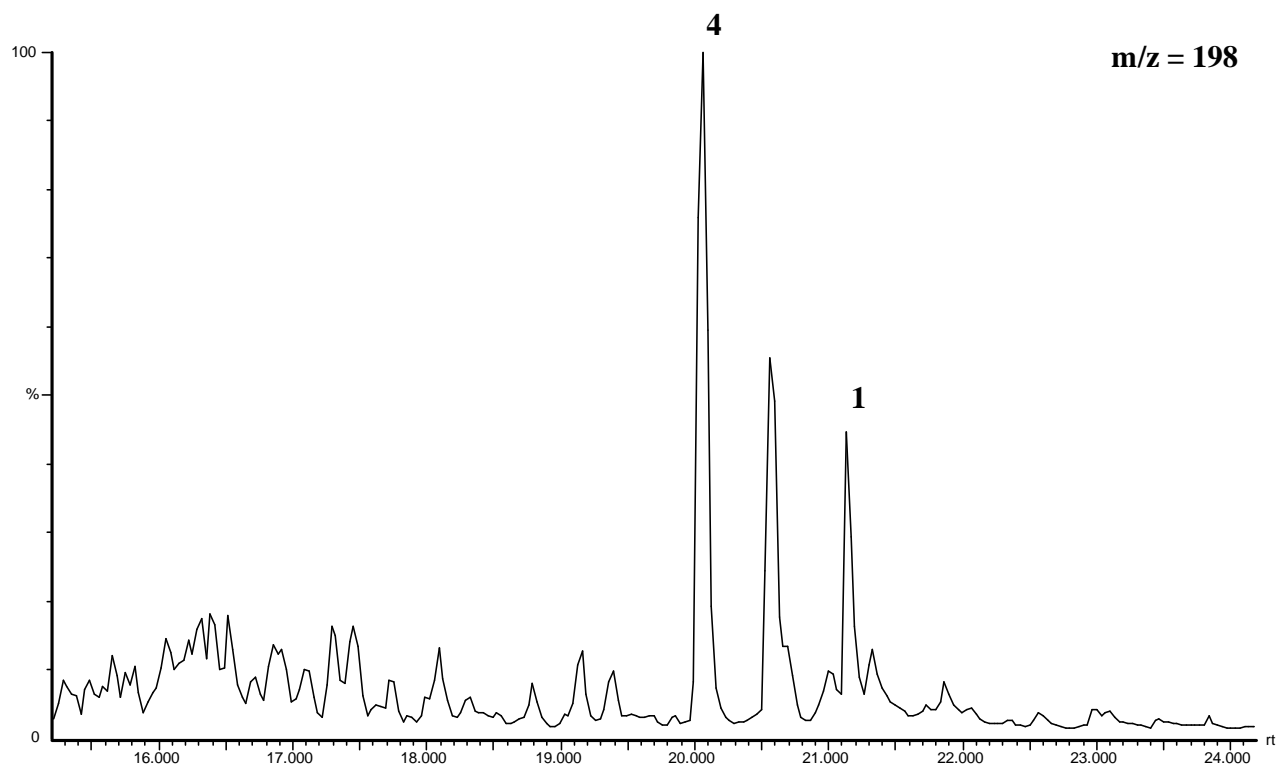


Figure 4.9. The GC-FID chromatogram of the coal extract at 2376.1 m from well 7128/4-1, displaying the peaks of dibenzothiophene, see table 4.9. (Weiss et al., 2000, Waples et al., 1991).

Peak	Identity
4	4-methyldibenzothiophene
1	1- methyldibenzothiophene

Table 4.9. Dibenzothiophene identified from the $m/z = 198$ chromatogram, see figure 4.9. (Weiss et al., 2000, Waples et al., 1991).

Different combinations of the peaks shown above are calculated to get parameters 1-27, which are presented shortly below:

1. 18α (H)-trisorneohopane/ (18α (H)-trisorneohopane+ 17α (H)-trisnorhopane) = Ts/ (Ts+Tm). (Seifert and Moldowan, 1978; Mackenzie, 1984).
2. Diahopane/ (diahopane+normoretane) (Cornford et al., 1986). Diahopane = hopane x (Moldowan et al., 1991).
3. $22S/(22S+22R)$ of C_{31} 17α (H), 21β (H)-hopanes
4. C_{30} -hopane/(C_{30} -hopane + C_{30} -moretane) (Mackenzie et al., 1985).
5. $29Ts/(29Ts + \text{norhopane})$ (Moldowan et al., 1991).
6. Bisnorhopane/(bisnorhopane + norhopane) (Wilhelms and Larter, 1994).
7. C_{23} - C_{29} tricyclic terpanes/ C_{30} $\alpha\beta$ -hopane (modified from Mello et al., 1988).
8. C_{24} tetra cyclic terpanes/ C_{30} $\alpha\beta$ -hopane (Mello et al., 1988).
9. Hopane/sterane from the C_{30} $\alpha\beta$ -hopane and regular C_{29} sterane (Mackenzie et al., 1984).
10. $\beta\beta/(\beta\beta + \alpha\alpha)$ of C_{29} (20R + 20S) sterane isomer (Mackenzie et al., 1980).
11. $20S/(20S+20R)$ of C_{29} 5α (H), 14α (H), 17α (H) steranes (Mackenzie et al., 1980).
12. Diasterane/(diasterane + regular sterane) (Mackenzie et al., 1985).
13. % C_{27} of $C_{27} + C_{28} + C_{29}$ $\beta\beta$ -steranes (Mackenzie et al., 1985).

14. % C_{28} of $C_{27} + C_{28} + C_{29}$ $\beta\beta$ -steranes (Mackenzie et al., 1985).
15. % C_{29} of $C_{27} + C_{28} + C_{29}$ $\beta\beta$ -steranes (Mackenzie et al., 1985).
16. $C_{20} / (C_{20} + C_{28})$ triaromatic steroids (TA) (Mackenzie et al., 1985).
17. $C_{28} \text{ TA} / (C_{28} \text{ TA} + C_{29} \text{ MA})$ (Peters and Moldowan, 1993).
18. Methylphenanthrene ratio, MPR (Radke et al., 1982b).
19. Methylphenanthrene index 1, MPI 1 (Radke et al., 1982a).
20. Methylphenanthrene distribution factor (F1 or MPDF) (Kvalheim et al., 1987).
21. Methyldibenzothiophene ratio, MDR (Radke, 1988).
22. Calculated vitrinite reflectivity, $R_{m(1)} = 1.1 * \log_{10} \text{MPR} + 0.95$ (Radke, 1988).
23. Calculated vitrinite reflectivity, $\%R_c = 0.6 * \text{MPI 1} + 0.4$ (Radke and Welte, 1983).
24. Calculated vitrinite reflectivity, $\%R_o = 2.242 * \text{MPDF} - 0.166$ (Kvalheim et al., 1987).
25. Calculated vitrinite reflectivity, $R_{m(2)} = 0.073 * \text{MDR} + 0.51$ (Radke, 1988).
26. 3-methylphenanthrene/ 4-methyldibenzothiophene (Radke et al., 2001).
27. MDBTs/MPs (Radke et al., 2001).

From chromatogram $m/z = 191$, the most relevant parameters for this purpose follow:

Parameter one:

Ts/ (Ts+Tm) is a maturity parameter, given by the peaks A and B. During maturation, the amount of Ts (C_{27} 18 α (H)-trisorneohopane) will increase compared to Tm (C_{27} 17 α (H)-trisorhopane). Tm is believed to represent the biologically produced structure. The Ts/Tm ratio begins to decrease quite late during maturation ($>0.9\%$ R_o) (Waples and Machihara, 1991), but nevertheless it may be used through the entire oil window. Parameter one may be influenced by the depositional environment, but it is a useful non-quantitative indicator of relative maturity when used on oils of uniform or common organic facies. The maximum ratio is one (Peters and Moldowan, 1993).

Parameter 5:

29Ts/ (29Ts+norhopane) is another maturity parameter given by the peaks; 29Ts and C. The stability of the 29Ts compound is higher relative to norhopane. This means that the ratio will increase with elevated temperature and maturity (Hughes et al., 1985).

Parameter 6:

The bisnorhopane/ (bisnorhopane+norhopane) ratio represents facies parameter (peaks Z and C). Bisnorhopane is believed to indicate anoxic conditions (Peters and Moldowan, 1993), but the maturity will have an impact as well. The amount of bisnorhopane is reduced through the oil window. On the contrary, the norhopane peak will rise relative to bisnorhopane by maturation. Based on this, immature samples may give a more anoxic impression compared to mature samples.

From chromatogram $m/z = 191$ and $m/z = 217$, the parameter 9 is used:

Parameter 9:

Hopane/sterane is a facies parameter. In chromatogram $m/z = 191$ we use peak E, while in ion-chromatogram $m/z = 217$ we use the peaks; q, r, s and t. Hopanes are derived mainly from bacteria, while steranes are mainly derived from algae. If the hopane/sterane ratio is high, it indicates bacteria rich facies, bacterially reworked organic matter or a special terrestrial input.

On the contrary, marine facies represented by algae dominated organic matter, will tend to have a low ratio (Peters and Moldowan, 1993).

Hopanes are less thermally stable than steranes. In a sample set with uniform organic facies, the hopane/sterane parameter will also be affected by maturity in addition to the effect of facies.

From chromatogram $m/z = 217$, the calculated parameters from identification of six isomers of diacholestanes and ethyl-cholestanes follow:

Parameter 10:

$\beta\beta/(\beta\beta+\alpha\alpha)$ of the C_{29} (20R+20S) sterane isomers is a maturity parameter (peaks q, r, s and t).

The $\beta\beta$ -isomer will increase with maturity compared to the $\alpha\alpha$ -isomer. The parameter is valid up till peak oil generation, but it may be affected by the mineralogy in the rock. Maximum equilibrium ratio is 0.7 (Peters and Moldowan, 1993).

Parameter 12:

The diasterane/ (diasterane + regular sterane) ratio works both as facies- and as a maturity parameter (peaks a, b, q, r, s and t). The amount of diasteranes will increase with thermal maturity relative to the regular steranes. The parameter is valid through the entire oil window, and the value one represents the maximum ratio. Oils from carbonate source rocks may have lower ratios than oils from clastic source rocks (Peters and Moldowan, 1993). Presence of diasteranes indicates a siliciclastic source rock.

Tricyclic aromatic hydrocarbons are identified from the $m/z = 178+192$ and $m/z = 198 \& 192$ chromatograms, and utilized in the following parameters. They are calculated from the amount of phenanthrene and the four isomers of methylphenanthrene (peaks one, two, three and 9). The number assigns the location of the methyl group ($-CH_3$). 3-MP and 2-MP are the most thermally stable isomers and the 1-MP and 9-MP isomers will be more rapidly depleted during maturation (Radke et al., 1982b).

Parameter 20:

The methyl phenanthrene distribution factor (F1 or MPDF) represents a maturity parameter (peaks one, two, three and 9). The ratio is given as

$$\text{MPDF} = (3\text{-MP} + 2\text{-MP}) / (3\text{-MP} + 2\text{-MP} + 1\text{-MP} + 9\text{-MP})$$

The vitrinite reflectance has been calculated based on measurements of phenanthrene, methyl phenanthrenes and methyl dibenzothiophene (Radke, 1988).

Parameter 26:

The ratio 3-methyl phenanthrene/ 4-methyl dibenzothiophene works as a facies parameter (peaks three and 4). Parameter 26 can be used together with a parameter like Pr/Ph to indicate different types of organic facies and the relative amount of sulfur in the source rock.

4.4. Data from Rock-Eval pyrolysis

TOC

TOC (wt. %), describes the quantity of organic carbon in a rock sample and includes both kerogen and bitumen. Measuring TOC gives an indication of petroleum potential, even though it is not always a clear indicator. Graphite contains essentially 100% carbon, but will not generate petroleum. For this reason the hydrogen index (HI) is used in conjunction with TOC (Tissot and Welte, 1984).

Rock-Eval

From chapter 3.4, the pyrolysis is described as the heating of organic matter when oxygen is lacking in order to generate organic compounds. The S₁ signal represents the thermal

evaporation, while the S_2 and S_3 describe the intensities in the early and late stage of the Rock-Eval pyrolysis, respectively.

The petroleum potential of source rocks is determined by TOC, S_1 and S_2 . Table 4.10 presents the numbers of each parameter from poor to excellent generative potential (from Peters and Cassa, 1994). S_1 and S_2 are described in the following:

- S_1 measures at 300 °C the free hydrocarbons that can be volatilized out of the rock without cracking the kerogen (mg HC/g rock). The S_1 signal comes from the thermal heating and increases at the expense of S_2 with maturity.
- S_2 measures the petroleum yield from cracking (Rock-Eval pyrolysis) of kerogen (mg HC/g rock) and heavy hydrocarbons. S_2 represents the existing potential of a rock to generate petroleum. S_2 gives the most realistic measure of source rock potential compared to TOC. The reason is that TOC includes "dead carbon" incapable of generating petroleum.
- $S_1 + S_2$ are a measure of genetic potential or the total amount of petroleum that might be generated from a rock.

Petroleum potential	TOC (wt. %)	S_1 (mg HC/g rock)	S_2 (mg HC/g rock)
Poor	0-0.5	0-0.5	0-2.5
Fair	0.5-1	0.5 -1	2.5-5
Good	1-2	1-2	5-10
Very good	2-4	2-4	10-20
Excellent	>4	>4	>20

Table 4.10. Geochemical parameters present the source-rock generative potential. The values are taken from Peters and Cassa (1994).

Production index

$[PI = S_1 / (S_1 + S_2)]$ gradually increases with depth for fine-grained rocks, as thermally labile components in the kerogen (S_2) are converted to free hydrocarbons (S_1). Reservoir rocks

show anomalously high PI values compared to adjacent fine-grained rocks. For Tmax values of < 435 °C and Tmax in the range 435 - 445° C, PI values exceeding 0.4, respectively, are considered anomalous (Tissot and Welte, 1984).

Hydrogen index

[HI = (S₂/TOC) x 100, mg HC/g TOC] is proportional to the amount of hydrogen in the kerogen and represents the potential of a rock to generate oil. A high hydrogen index means greater potential for generation of oil. HI values are readily convertible to geologically useful figures. For instance, HI=700 means that 70% of the TOC can be converted to oil and gas. In general, HI versus OI plots is reliable indicators of kerogen type. Nevertheless, gas prone coals and coaly rocks may give anomalously high HI values that must be confirmed by elemental analysis (Peters, 1986). The average HI in a rock interval is best determined from the slope of a regression line on a graph of S₂ versus TOC (Langford and Blanc-Valleron, 1990).

Oxygen index

[OI = (S₃/TOC) x 100, mg CO₂/g TOC] is related to the amount of oxygen in the kerogen. The S₃ measurement is generally not as reliable as other Rock-Eval parameters. This is due to interference of carbonate minerals or kerogen oxidation resulting from pulverizing the sample. When S₃ results are suspected to be unreliable, one alternative method to determine OI is to plot HI against Tmax (Espitalie et al., 1984). By substituting the OI with Tmax, a more modified van Krevelen diagram is produced (see figure 4.10b).

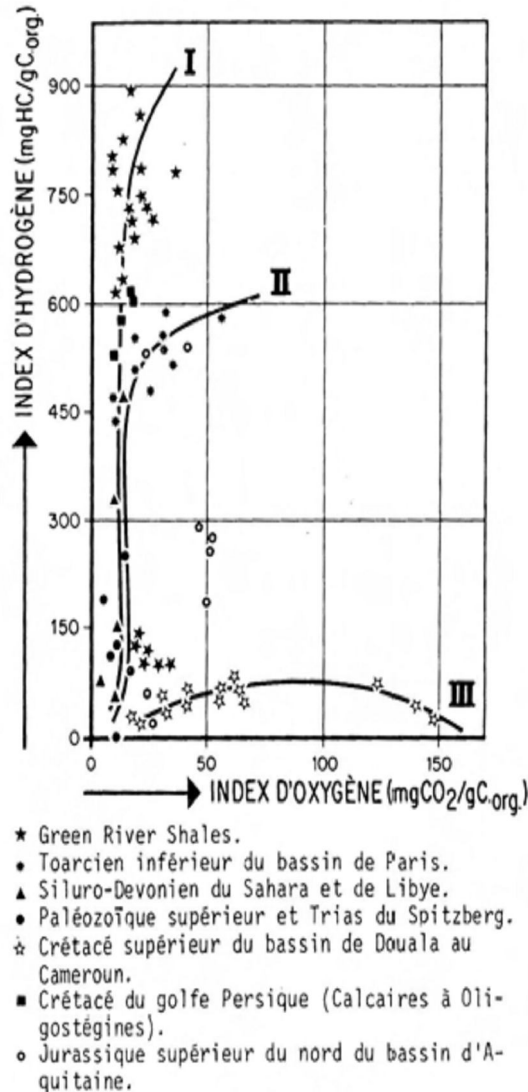
T _{max} < 425°C	immature
T _{max} < 435°C	just mature
T _{max} 435° – 465° C	mature
T _{max} > 465°C	over mature

Table 4.11. The values of Tmax associated with generally accepted maturity levels (from Peters, 1986).

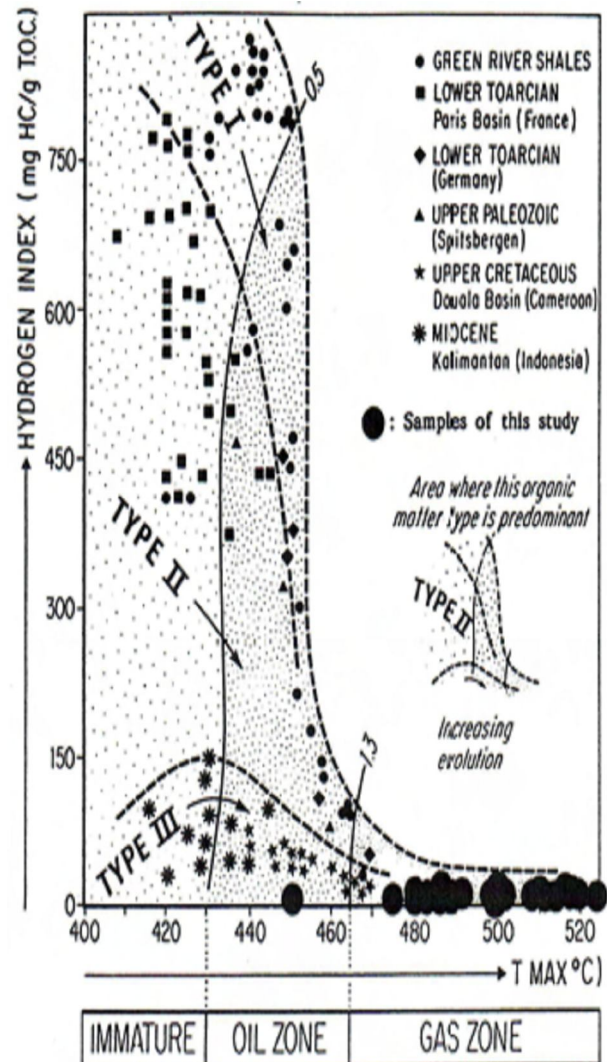
Tmax

Tmax measures thermal maturity and corresponds to the Rock-Eval pyrolysis oven temperature (°C) at maximum S₂ generation. Tmax should not be confused with geologic

temperatures. Tmax, is partly useless for type I kerogens due to their narrow activation energy distribution (Peters, 1986). The table 4.11 gives an overview of the Tmax values and generally accepted maturity levels.



a) The “modified” Van Krevelen diagram.



(b) The “modified modified” Van Krevelen diagram.

Figure 4.10 a) The modified van Krevelen diagrams. Espitalie et al. (1977) described the first diagram in an article dealing with use of Rock-Eval instruments (see also the figure 3.4).

Figure 4.10b) The more modified diagram, was described in Espitalie et al. (1984) as a substitute plot for the 4.10a) in situations where the S₃ results are suspected unreliable because of interference from thermally labile carbonate minerals or kerogen oxidation resulting from pulverizing the sample (taken from Karlsen, 1987).

5. Results

The results from the laboratory analysis will systematically be presented in this chapter. Interpretations and discussions of the results will in the same manner be discussed in the next chapter. All scaled-down chromatograms from GC-MS and GC-FID will be presented for each sample (figures 5.2-5.7). See chapter three for details concerning the methods used for the results.

5.1 Iatroscan TLC-FID

5.2 GC-FID

5.3 GC-MS

5.4 Chromatograms from GC-FID and GC-MS analysis

5.5 Rock-Eval

5.1 Iatroscan TLC-FID

The analysis and results from Iatroscan based on the coals, the DST oils and the NSO-1 oil will be presented in the following. The numbers in the table 5.1 represent the average of two Iatroscan runs in general, except for the coal extract 5 from well 7128/4-1 (2384.7 m), which includes the average of four runs.

The table 5.1 contains the percentages of the saturated- and aromatic hydrocarbons in addition to polar compounds for the coal- and oil samples. Concerning the coals, the SAT-ARO-POLAR fractions are also given in mg/g rock or yield. The yield of the total Extractable Organic Matter (EOM) represents the summation of the SAT-ARO-POLAR fractions. The ratio of the saturated hydrocarbons to the aromatic hydrocarbons is presented in the figure 6.20 A).

Parameters and values from table 5.1:

Saturated hydrocarbon fraction

The studied coal samples have a range in yield from 2.1 mg/g rock (7128/6-1, 2226.4 m, sample 7) to 4.2 mg/g rock (7128/4-1, 2384.7 m, sample 5) of the saturated hydrocarbons. The ranges of relative percentages vary from 2.8% (sample 5) to 5.0 % (sample 7). The oils span from 48.5 % (NSO-1, sample 13) to 79.3 % (7128/4-1 DST-1, 1592-1610, sample 11).

Well	Core depth	Sample	Sample nr	SATURATES		AROMATIC		POLAR		total EOM		SAT/ARO
				mg/g rock	%	mg/g rock	%	mg/g rock	%	mg/g rock	%	
7128/4-1	2376,1	Coal	4	3,5	3,0	61,2	52,4	52,1	44,6	116,7	100	0,06
7128/4-1	2384,7	Coal	5	4,2	2,8	90,3	59,6	56,9	37,6	151,4	100	0,05
7128/6-1	2226,4	Coal	7	2,1	5,0	11,5	27,3	28,5	67,7	42,1	100	0,18
7128/4-1 DST-1	1592 - 1610	Oil	11	ND	79,3	ND	19,1	ND	1,6	ND	100	4,15
7128/4-1 DST-2	1577 - 1586	Oil	12	ND	77,2	ND	21,4	ND	1,4	ND	100	3,60
NSO-1		NPD oil standard	13	ND	48,5	ND	37,7	ND	13,8	ND	100	1,29

Table 5.1. The percentages of the gross composition of the coal extracts and the oils alongside yield. SATURATES = saturated hydrocarbons, AROMATIC = aromatic hydrocarbons, POLAR = polar compounds, EOM = Extractable Organic Matter. ND means no data.

Aromatic hydrocarbon fraction

The coal samples have a range in yield from 11.5 mg/g rock (7128/6-1, 2226.4 m, sample 7) to 90.3 mg/g rock (7128/4-1, 2384.7 m, sample 5) for the aromatic hydrocarbons. The values of relative percentages range from 27.3 % (sample 7) to 59.6 % (sample 5). The oils vary between 19.1 % (DST-1, 1592-1610, sample 11) to 37.7 % (NSO-1, sample 13).

Polar compound fraction

The coal samples have a range in yield from 28.5 mg/g rock (sample 7) to 56.9 mg/g rock (sample 5) for the polar compounds. However, when measuring in relative percentages the lowest and highest values for the corresponding samples 5 and 7 are switched, meaning that the sample 5 represents the lowest percentage with 37.6 % and the sample 7 represents the highest percentage with 67.7 %. This is illustrated in the figure 6.19.

The values for the three oils vary from 1.4 % (DST-2, 1577-1586, sample 12) to 13.8 % (NSO-1).

Total Extractable Organic Matter (EOM)

The total EOM is given in yield and ranges from 42.1 mg/g rock (7128/6-1, 2226.4 m, sample 7) to 151.4 mg/ g rock (7128/4-1, 2384.7 m, sample 5).

Saturated/ Aromatic hydrocarbon fraction

The ratio SAT/ARO is ranging from 0.05 (sample 5) to 0.18 (sample 7) for the studied coal samples. The oils show higher ratios, from 1.29 (NSO-1) to 4.15 (DST-1, 1592-1610, sample 11).

Saturated hydrocarbon fraction/ Total EOM

The ratio SAT/ Total EOM for the coals is 0.03 for both the sample 4 (7128/4-1, 2376.1 m) and the sample 5, while the sample 7 represents the highest value of 0.05.

5.2 GC-FID

The analysis of the coal samples and associated oils by the GC-FID instrument was presented and described systematically in chapter three. Peters and Moldowan (1993) showed that maturity and source rock facies can be determined by the n-alkane and isoprenoid distribution, which is shown by the fingerprints of the GC-FID traces in each chromatogram. Heavy degree of biodegradation, for instance, will give a characteristic chromatogram of unresolved complex mixture (UCM). The relative concentration of n-alkanes will be small compared to aromatics and isoprenoids. In general, the concentration of n-alkanes will decrease compared to aromatics and isoprenoids, as a function of increasing biodegradation.

Typical for the NSO-1 oil is an asymptotically decrease in the n-alkane concentration with increasing carbon number. The chromatogram thus will have a concave shape (figure 5.7). This oil is incipiently biodegraded as shown by reduced n-alkane peak heights in the C₈-C₁₂ range.

In what follows are the presented data from the GC-FID analysis, given in the table 5.2. The overview of all relevant chromatograms for each sample is presented in the figures 5.2-5.7. The sample depths of the coal extracts 4, 5 and 7 from the table 5.1 will be discussed in the following. In addition, 7 of the coal samples in the table 5.2 belong to Jan Hendrik van Koeverden (Department of Geosciences, PhD). These 7 samples will only be used for the plots in chapter 6. As mentioned in the introduction, it was deemed sufficient for time and cost constraints to analyze only the coal samples 4, 5 and 7.

Well	Depth	Sample	Sample nr	Pr/Ph	Pr/n-C ₁₇	Ph/n-C ₁₈
7128/4-1	2346.0	Coal	1	3,06	0,63	0,21
7128/4-1	2366.5	Coal	2	1,69	0,48	0,24
7128/4-1	2366.8	Coal	3	5,06	0,61	0,12
7128/4-1	2376.1	Coal	4	3,24	1,09	0,34
7128/4-1	2384.7	Coal	5	3,12	0,94	0,26
7128/6-1	2222.7	Coal	6	ND	ND	ND
7128/6-1	2226.4	Coal	7	4,56	4,11	0,89
7128/6-1	2246.2	Coal	8	6,20	2,25	0,38
7128/6-1	2247.7	Coal	9	ND	ND	ND
7128/6-1	2349.0	Coal	10	ND	ND	ND
7128/4-1 DST-1	1592 - 1610	Oil	11	2,27	0,51	0,21
7128/4-1 DST-2	1577 - 1586	Oil	12	2,38	0,55	0,22
NSO-1		NPD oil standard	13	1,59	0,74	0,55

Table 5.2. The data set from the GC-FID Chromatograms, given as the ratios Pr/Ph, Pr/n-C₁₇ and Ph/n-C₁₈. ND = no data.

The coals (samples 1-10)

According to the table 5.2, the Pr/Ph ratio vary from 1.69 (7128/4-1, 2366.5 m, sample two) to 6.20 (7128/6-1, 2246.2 m, sample 8). The ratio Pr/n-C₁₇ vary from 0.48 (sample two) to 4.11, represented by the studied sample 7 from well 7128/6-1 (2226.4 m). The ratio Ph/n-C₁₈ vary from 0.12 (7128/4-1, 2366.8 m, sample three) to 0.89 (sample 7). Typical for the coal samples is high proportions of long-chained n-alkanes (waxes) (figures 5.2-5.7).

From the studied coals, the sample 4 (7128/4-1, 2376.1 m) has a broad asymmetric hump (UCM), starting from n-C₁₇. The deeper sample in the same well, sample 5 (2384.7 m), shows a more symmetric hump of unresolved complex mixture (UCM). The sample 7 has an

asymmetric shape of the hump similar to the sample 4, though it is narrower, starting from n-C₁₈.

The peak heights of pristane versus phytane differ in magnitude for the sample 4 (7128/4-1 (2376.1 m) versus the sample 7 (7128/6-1, 2226.4 m). Concerning the sample 7, the isoprenoids pristane (Pr) is among the major peaks.

7128/4-1 DST 1&2 oils (samples 11-12)

The Pr/Ph ratio ranges from 2.27 (DST-1, 1592-1610, sample 11) to 2.38 (DST-2, 1577-1586, sample 12). The values of the ratio with respect to Pr/n-C₁₇ are 0.51 (DST-1) and 0.55 (DST-2). Concerning the ratio Ph/n-C₁₈, the DST- 1 and the DST-2 have the values 0.21 and 0.22, respectively.

None of the DST oils have a marked hump of UCM like the coal samples 4 and 7 (figures 5.5-5.6). There is no depletion concerning the n-alkane distribution. The magnitude of pristane and phytane shows small peaks compared to their associated n-C₁₇ and n-C₁₈, respectively. The chromatogram shows that peak heights decrease abruptly with increasing carbon number compared to the NSO-1 oil, but the curve will still have a concave shape. The DST oils are enriched in long-chain n-alkanes compared to the NSO-1 oil and can be classified as waxy oils.

The NSO-1 oil (sample 13)

According to the table 5.2, the Pr/Ph ratio of the NSO-1 oil (sample 13) is 1.59, while the ratios Pr/n-C₁₇ and Ph/n-C₁₈ are 0.74 and 0.55, respectively.

The peak heights for the NSO-1 sample shows an asymptotic decrease with increasing carbon number, and a concave pattern for the curves is displayed in the chromatogram (figure 5.7).

5.3 GC-MS

The samples were run through the GC-MS instrument. The GC-MS data of the sample set are presented in chapter 3.4. The favorable aspect with the GC-MS method is the possibility of studying compounds present in small concentrations in the complex matrix of petroleum. By

referring to compounds, which are of importance in this study, we in general mean “biomarkers” (Waples and Machihara, 1991).

Selection and combinations of the peaks, which have been measured and calculated, makes the maturity and facies parameters. In chapter three the description of each parameter as well as the peaks is presented. The most important parameters in this study will be presented in the following in the form of numbers. The table 5.3 gives an overview of the values corresponding to each parameter for the sample set. The chromatograms for each sample have been collected, scaled down and presented (figures 5.2-5.7).

The results from the GC-MS analysis are presented in the table 5.3. The three mentioned coal samples 4, 5 and 7 will be discussed in the following. In addition, 7 other coal samples in the table 5.3 belong to Jan Hendrik van Koeverden (Department of Geosciences, PhD) and will only be used for the plots in chapter 6 to determine facies and maturity for the sample set. As mentioned in the introduction, it was deemed sufficient for time and cost constraints to analyze only the coal samples 4, 5 and 7.

Well	Depth	Sample	Sample nr	1	2	3	4	5	6	7	8	9
7128/4-1	2310,0	Coal	1	0,26	0,79	0,62	0,86	0,12	0,03	0,26	0,20	8,32
7128/4-1	2366,5	Coal	2	0,25	0,87	0,66	0,80	0,11	0,08	0,07	0,06	14,60
7128/4-1	2366,8	Coal	3	0,60	0,91	0,64	0,70	0,40	0,14	0,26	0,21	2,11
7128/4-1	2376,1	Coal	4	0,32	0,92	0,65	0,81	0,2	0	0,17	0,1	14,29
7128/4-1	2384,7	Coal	5	0,34	0,79	0,61	0,84	0,19	0,05	0,44	0,3	8,32
7128/6-1	2222,7	Coal	6	0,01	0,08	0,59	0,75	0,01	0,01	0,08	0,06	5,24
7128/6-1	2226,4	Coal	7	0,02	0,11	0,6	0,74	0	0	0,51	0,12	13,57
7128/6-1	2232,7	Coal	8	0,03	0,12	0,61	0,73	0,02	0,01	0,07	0,04	12,86
7128/6-1	2247,7	Coal	9	0,03	0,10	0,60	0,76	0,02	0,01	0,08	0,05	9,18
7128/6-1	2349,0	Coal	10	0,02	0,35	0,61	0,81	0,03	0,03	0,08	0,07	12,72
7128/4-1 DST-2	1592 - 1610	Oil	11	0,58	0,75	0,63	0,83	0,29	0,11	2,2	0,31	2,67
7128/4-1 DST-1	1577 - 1586	Oil	12	0,61	0,77	0,6	0,83	0,28	0,13	1,98	0,28	2,58
NSO-1		NPD oil standard	13	0,55	0,65	0,62	0,9	0,27	0,38	0,44	0,08	2,13

Table 5.3. Parameters calculated from the GC-MS chromatograms for the data set. See chapter 4 for explanation of the parameters.

Well	Depth	Sample	Sample nr	10	11	12	13	14	15	16	17	18	19
7128/4-1	2310,0	Coal	1	0,48	0,66	0,36	24,85	37,57	37,57	ND	ND	1,26	0,58
7128/4-1	2366,5	Coal	2	0,50	0,43	0,07	14,08	42,25	43,66	ND	ND	ND	ND
7128/4-1	2366,8	Coal	3	0,50	0,49	0,11	17,04	30,04	52,91	ND	ND	ND	ND
7128/4-1	2376,1	Coal	4	0,49	0,49	0,07	12,24	40,82	46,94	ND	ND	0,95	0,71
7128/4-1	2384,7	Coal	5	0,44	0,63	0,16	14,39	45,02	40,59	ND	ND	0,93	0,62
7128/6-1	2222,7	Coal	6	0,29	0,49	0,10	9,09	55,56	35,35	ND	ND	1,04	0,76
7128/6-1	2226,4	Coal	7	0,33	0,53	0,34	12,09	56,04	31,87	0,87	0,45	1,13	0,80
7128/6-1	2232,7	Coal	8	0,26	0,54	0,31	27,27	46,67	26,06	ND	ND	1,23	0,56
7128/6-1	2247,7	Coal	9	0,27	0,47	0,12	12,78	56,83	30,40	ND	ND	1,62	0,85
7128/6-1	2349,0	Coal	10	0,41	0,51	0,09	7,88	48,48	43,64	ND	ND	1,13	0,61
7128/4-1 DST-2	1592 - 1610	Oil	11	0,5	0,42	0,65	41,45	24,36	34,18	0,72	0,60	0,96	0,77
7128/4-1 DST-1	1577 - 1586	Oil	12	0,5	0,43	0,62	40,79	24,34	34,87	0,71	0,62	1,03	0,78
NSO-1		NPD oil standard	13	0,51	0,49	0,56	39,88	31,50	28,61	0,50	0,58	0,98	0,60

Table 5.3 (continues). Parameters calculated from the GC-MS chromatograms for the data set. See chapter 4 for explanation of the parameters. ND = no data.

Well	Depth	Sample	Sample nr	20	21	22	23	24	25	26	27
7128/4-1	2310,0	Coal	1	0,48	0,40	1,06	0,75	0,92	0,54	15,88	0,14
7128/4-1	2366,5	Coal	2	ND	ND	ND	ND	ND	ND	ND	ND
7128/4-1	2366,8	Coal	3	ND	ND	ND	ND	ND	ND	ND	ND
7128/4-1	2376,1	Coal	4	0,46	2,30	0,93	0,82	0,87	0,68	0,02	43,97
7128/4-1	2384,7	Coal	5	0,44	2,81	0,92	0,77	0,82	0,72	0,02	37,52
7128/6-1	2222,7	Coal	6	0,49	0,17	0,97	0,85	0,94	0,52	13,15	0,37
7128/6-1	2226,4	Coal	7	0,51	1,65	1,01	0,88	0,97	0,63	34,07	0,03
7128/6-1	2232,7	Coal	8	0,50	0,23	1,05	0,73	0,96	0,53	41,48	0,16
7128/6-1	2247,7	Coal	9	0,57	0,46	1,18	0,91	1,12	0,54	ND	0,02
7128/6-1	2349,0	Coal	10	0,48	1,43	1,01	0,76	0,91	0,61	19,55	0,09
7128/4-1 DST-2	1592 - 1610	Oil	11	0,49	4,00	0,93	0,86	0,94	0,80	0,10	6,97
7128/4-1 DST-1	1577 - 1586	Oil	12	0,50	7,50	0,96	0,87	0,97	1,06	0,12	5,79
NSO-1		NPD oil standard	13	0,44	2,81	0,94	0,76	0,82	0,72	2,46	0,25

Table 5.3 (continues). Parameters calculated from the GC-MS chromatograms for the data set. See chapter 4 for explanation of the parameters. ND = no data.

The coal samples 4, 5 and 7

According to the three studied coal samples, the coals varies from 0.02 (7128/6-1, 2226.4 m, sample 7) to 0.34 (7128/4-1, 2384.7 m, sample 5) for the parameter one, which represents the ratio $Ts/(Ts+Tm)$. The parameter 5, which is the $29Ts/(29Ts+norhopane)$ ratio ranges from 0 (sample 7) to 0.20 (7128/4-1, 2376.1 m, sample 4).

The parameter 6 given by the $bisnorhopane/(bisnorhopane+norhopane)$ ratio has a zero value for the samples 4 and 7, while the sample 5 represents the value of 0.05.

The 7128/4-1 DST 1 & 2 oils (sample 11-12)

The parameter one, which represents the ratio $Ts/(Ts+Tm)$, have values 0.61 and 0.58 for the DST-1 oil (1592-1610, sample 11) and the DST-2 oil (1577-1586, sample 12), respectively. The parameter 5, which is the ratio of $29Ts/(29Ts+norhopane)$, range from 0.28 (DST-1) to 0.29 (DST-2). The $bisnorhopane/(bisnorhopane+norhopane)$ ratio have values 0.13 and 0.11 for the DST-1 and DST-2, respectively.

The NSO-1 oil (sample 13)

The parameter one, representing the ratio $Ts/(Ts+Tm)$, has a value of 0.55 for the NSO-1 oil (sample 13). The $29Ts/(29Ts+norhopane)$ ratio, parameter 5, has the value 0.27. The value of the $bisnorhopane/(bisnorhopane+norhopane)$ ratio is 0.38, representing a high value for the parameter 6 compared to the sample set.

5.4. Chromatograms from GC-FID and GC-MS analysis

Each sample is in the following presented by chromatograms from the GC-FID analysis as well as the GC-MS analysis. All chromatograms are minimized for fit purpose and for better presentation when comparing the various samples.

The chromatogram from the GC-FID analysis gives information about the general isoprenoid and n-alkane distributions, which helps to understand the degree of biodegradation and origin of source. The chromatograms from the GC-MS analysis indicate the level of maturity in addition to depositional environment and organic facies.

7128/4-1, 2376.1 m, coal sample 4

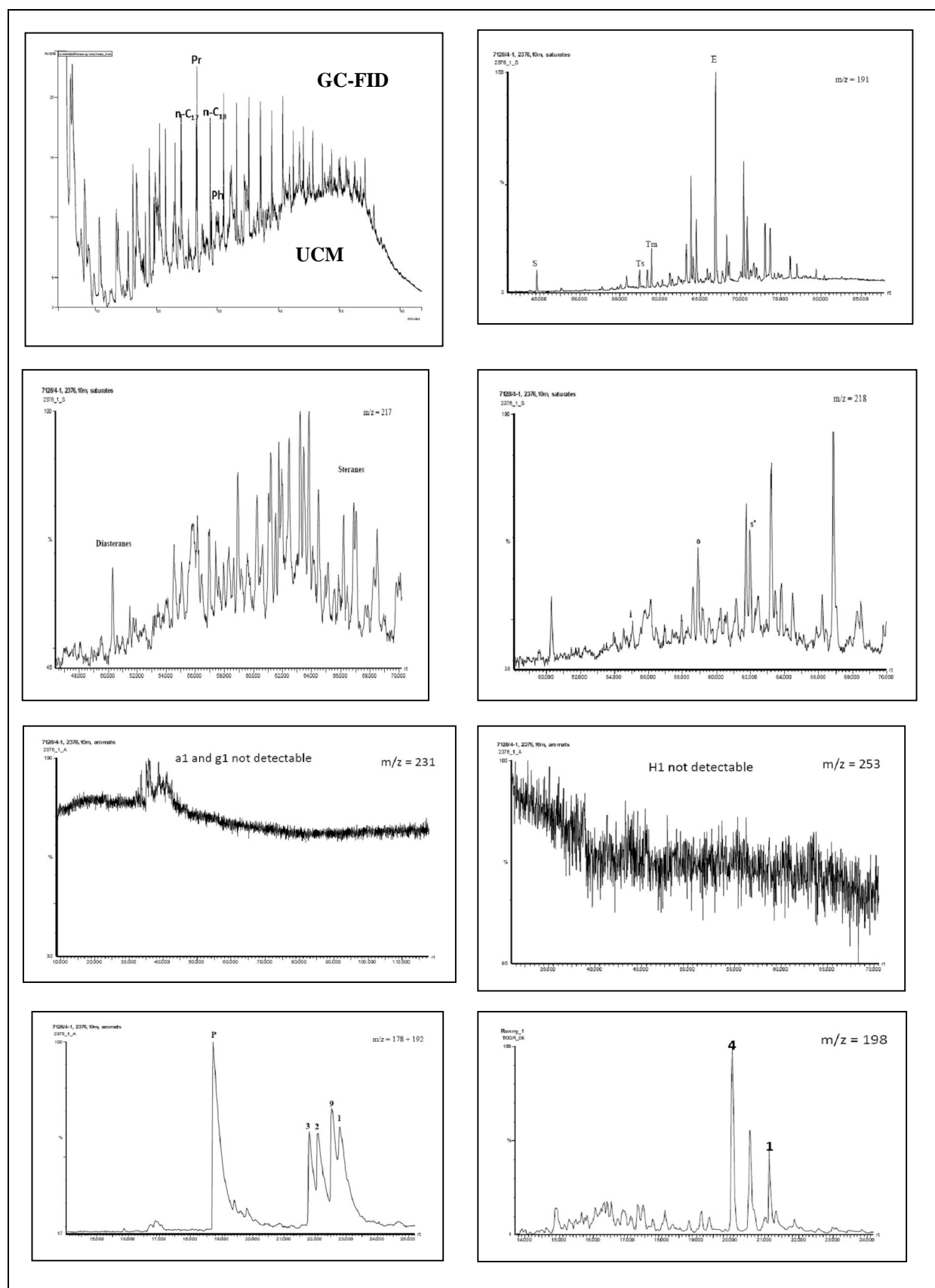


Figure 5.2 the chromatogram of 7128/4-1, taken at the sample depth of 2376.1 m and represents the coal sample 4 (Weiss et al., 2000, Waples et al., 1991).

7128/4-1, 2384.7 m, coal sample 5

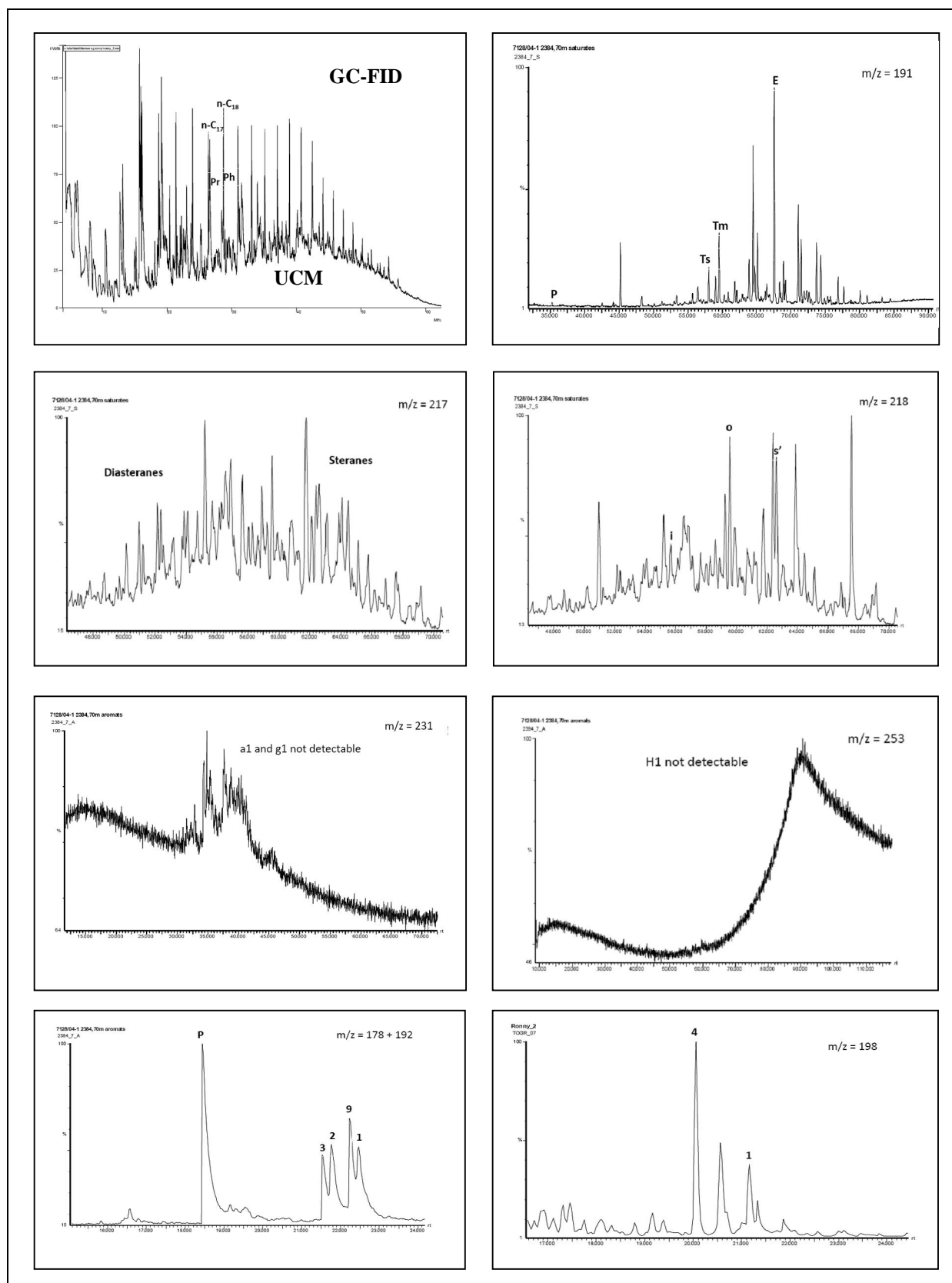


Figure 5.3 the chromatogram of 7128/4-1, taken at the sample depth of 2384.7 m and represents the coal sample 5. (Weiss et al., 2000, Waples et al., 1991).

7128/6-1, 2226.4 m, coal sample 7

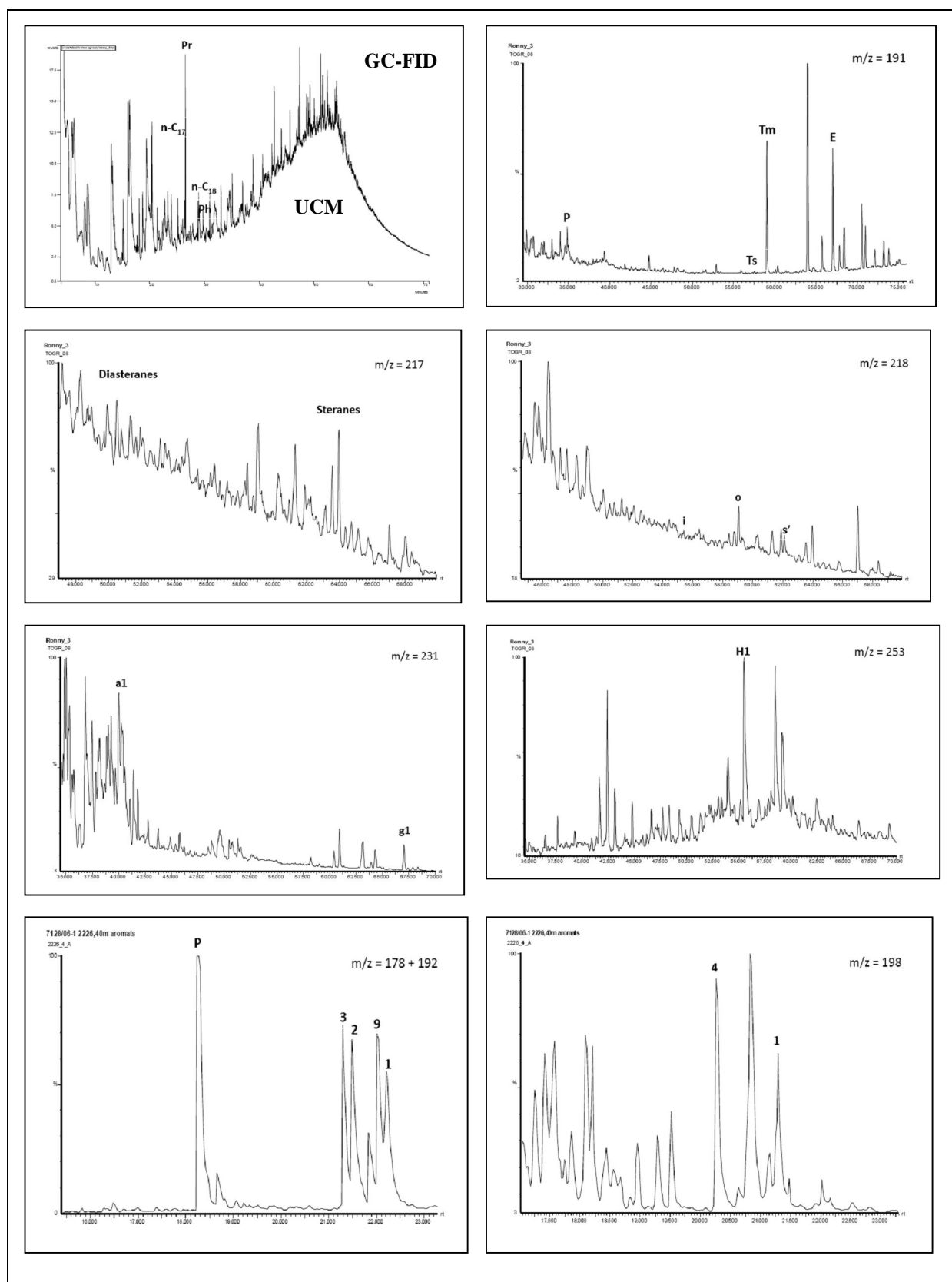


Figure 5.4. The chromatogram of 7128/6-1, taken at the sample depth of 2226.4 m and represents the coal sample 7(Weiss et al., 2000, Waples et al., 1991).

7128/4-1 DST-1 Oil, 1592-1610 m, sample 11

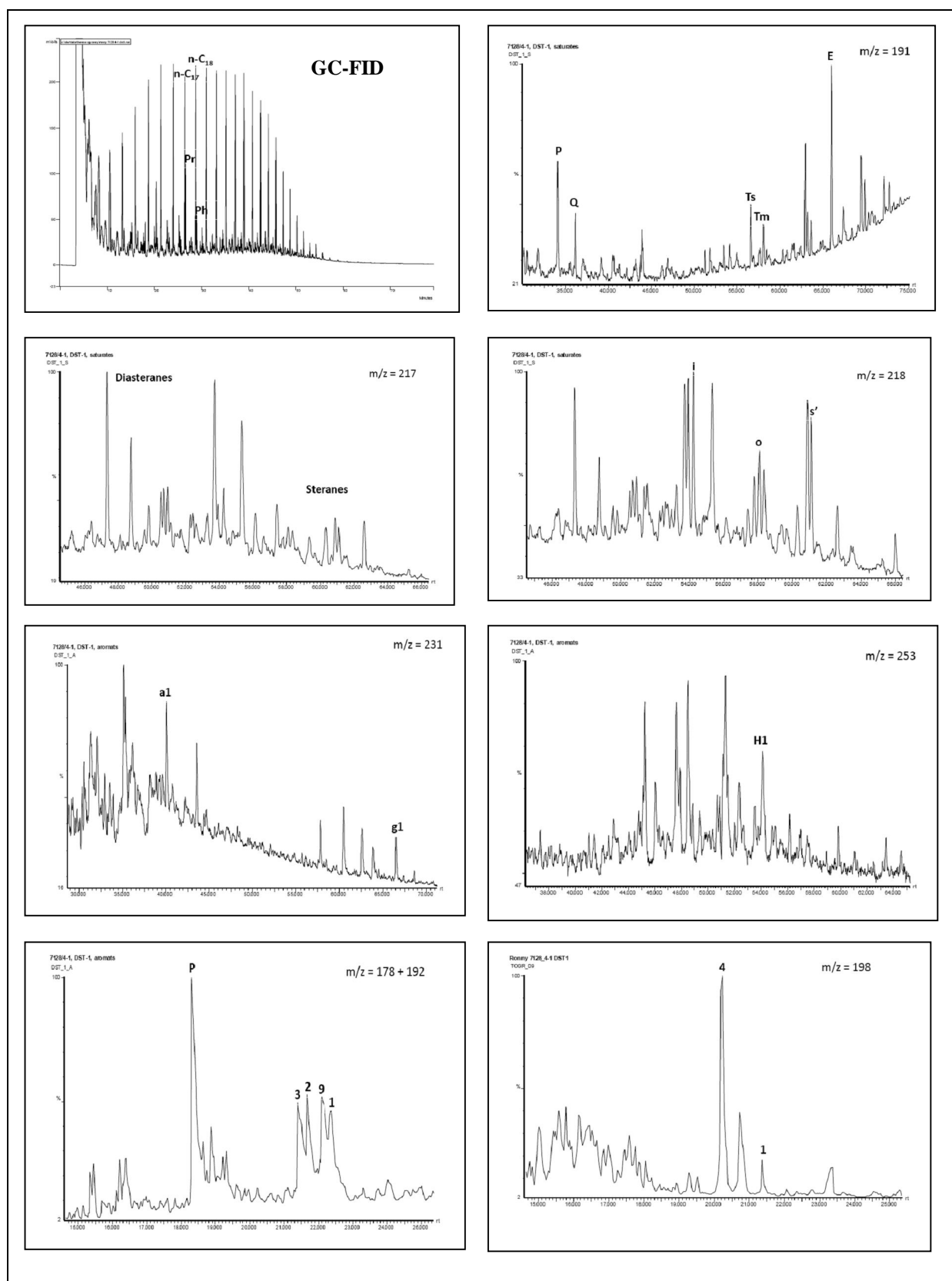


Figure 5.5. The chromatogram of 7128/4-1 DST-1 oil, taken at the core depth interval of 1592-1610 m and represents the sample 11(Weiss et al., 2000, Waples et al., 1991).

7128/4-1 DST-2 Oil, 1577-1586 m, sample 12

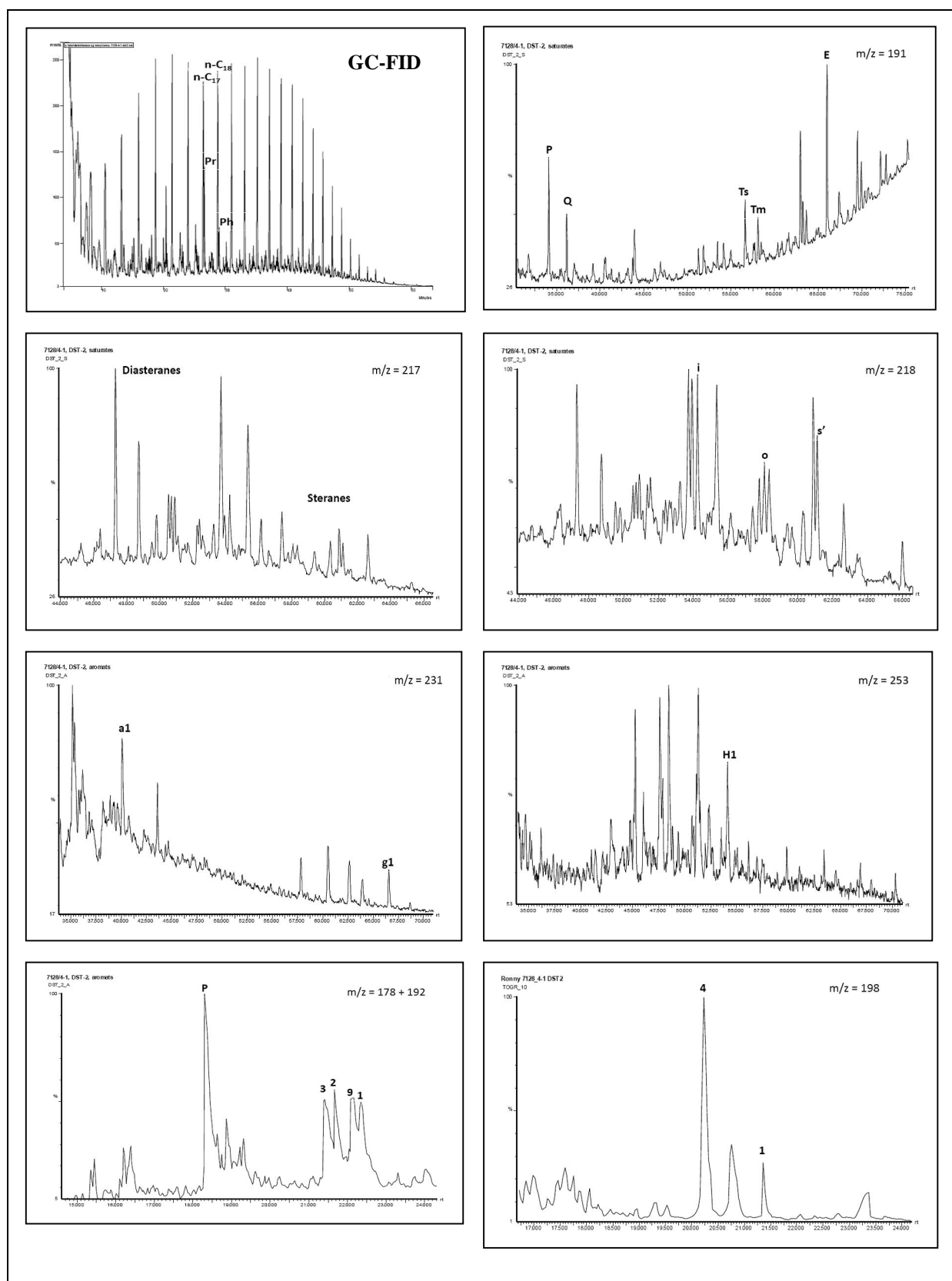


Figure 5.6. The chromatogram of 7128/4-1 DST-2 oil, taken at the core interval of 1577-1586 and represents the sample 12 (Weiss et al., 2000, Waples et al., 1991).

NSO-1 oil, sample 13

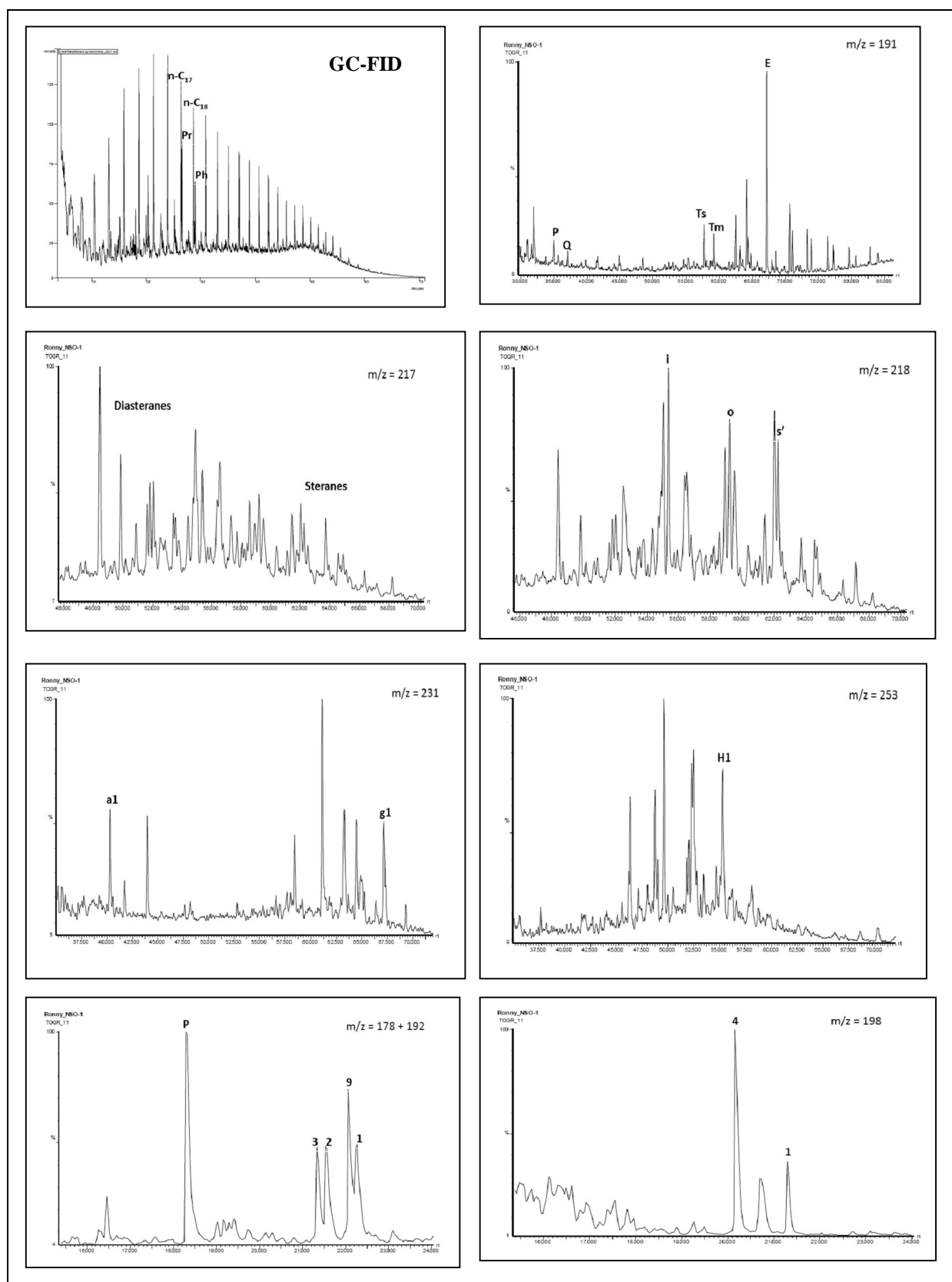


Figure 5.7. The chromatogram of NSO-1 oil represents the sample 13 (Weiss et al., 2000, Waples et al., 1991).

5.5 Rock-Eval

The analysis and results from the LECO TOC and the Rock-Eval pyrolysis for the coal samples are presented in the tables 5.5 and 5.6, respectively. The amount of total carbon, total organic carbon and total inorganic carbon are given in percentages. The S_1 signal from thermal evaporation has values listed in mg HC/ g rock, as well as the S_2 peak from pyrolysis. The S_3 top represents the late stage of pyrolysis and the values are given in mg CO_2 /g rock. The HI-index and the OI-index are listed in mg HC /g TOC, while Tmax has values given in °C. The Production Index, PI, represents the ratio of $S_1 / (S_1 + S_2)$.

The tables 5.5 and 5.6 give a detailed description of the behavior of the parameters for the LECO and Rock-Eval analysis, respectively, for a closely spaced sample interval for the wells 7128/4-1 and 7128/6-1.

					LECO	
Well	Depth	Sample	Sample nr	total carbon	total organic	total inorganic
				TC [%]	carbon TOC [%]	carbon TIC [%]
7128/4-1	2346.0	Coal	1	35.38	36.42	LD
7128/4-1	2366.5	Coal	2	82.98	85.98	LD
7128/4-1	2366.8	Coal	3	25.85	26.79	LD
7128/4-1	2376.1	Coal	4	78.29	80.68	LD
7128/4-1	2384.7	Coal	5	83.48	88.57	LD
7128/6-1	2222.7	Coal	6	59.48	58.56	0,92
7128/6-1	2226.4	Coal	7	83.57	84.15	LD
7128/6-1	2246.2	Coal	8	67.07	69.85	LD
7128/6-1	2247.7	Coal	9	79.86	83.55	LD
7128/6-1	2349.0	Coal	10	20.93	21.63	LD

Table 5.5. The parameters and values for the LECO TOC are given for the coal samples. LD means that the data is less than detectable.

Coal samples 1-5 from well 7128/4-1 (2346.0 – 2384.7 m)

LECO

The percentage of the TC varies from 25.85 % at depth 2366.80 m (7128/4-1, sample two) to 83.48 % at depth 2384.70 m (7128/4-1, sample 5).

The lowest and highest values for the TOC are also represented by the sample two (26.79%) and the sample 5 (88.57%), respectively.

Rock-Eval

The lowest values for the peaks S_1 , S_2 and S_3 belong to depth interval 2366.80 m (7128/4-1, sample three) and are 1.33 mg HC/g rock, 10.66 mg HC/g rock and 4.16 mg CO_2 /g rock, respectively. The highest values for the S_1 and S_2 signals are 15.5 mg HC/g rock and 162.33 mg HC/g rock, respectively, and is represented by the sample two (7128/4-1, 2366.50 m). The biggest amplitude for the S_3 signal with 7.75 mg CO_2 /g rock belongs to the studied sample 4 (7128/4-1, 2376.10 m).

The Tmax difference between the lowest and highest temperature is 19 °C; Tmax ranges from 447 °C in the sample 5 (7128/4-1, 2384.70 m) to 466 °C in the sample three.

The sample three has the lowest HI-index with 40 mg HC /g TOC, but contains the highest value of the OI-index with 16 mg CO_2 /g TOC. The highest HI-index with 189 mg HC /g TOC belongs to the sample two. The lowest value for the OI-index with three mg CO_2 /g TOC is represented by the sample one (7128/4-1, 2346.00 m).

The range in the PI is from 0.08 (sample three) to 0.11 (sample three).

						RockEval				
				S ₁	S ₂	S ₃	T _{max}	HI	OI	PI
Well	Depth	Sample	Sample nr	[mg HC /g rock]	[mg HC /g rock]	[mg CO ₂ /g rock]	[°C]	[mg HC /g TOC]	[mg CO ₂ /g TOC]	
7128/4-1	2346,0	Coal	1	5,81	63,18	1,04	450	173	3	0,08
7128/4-1	2366,5	Coal	2	15,5	162,33	5,66	451	189	7	0,09
7128/4-1	2366,8	Coal	3	1,33	10,66	4,16	466	40	16	0,11
7128/4-1	2376,1	Coal	4	12,5	127,5	7,75	457	158	10	0,09
7128/4-1	2384,7	Coal	5	7,75	76,25	6,75	447	86	8	0,09
7128/6-1	2222,7	Coal	6	4,2	102,4	1,2	441	175	2	0,04
7128/6-1	2226,4	Coal	7	5,2	115,4	3,2	445	137	4	0,04
7128/6-1	2246,2	Coal	8	5,8	98,85	2,42	442	142	3	0,06
7128/6-1	2247,7	Coal	9	7,44	140,44	3,05	437	168	4	0,05
7128/6-1	2349,0	Coal	10	2,61	43,42	1,19	435	201	6	0,06

Table 5.6. The parameters and values for the Rock-Eval pyrolysis given for the coal samples.

Coal samples 6-10 from well 7128/6-1 (2222.7 – 2349.0 m)

LECO

The percentage of the TC varies from 20.93 % for depth 2349.00 m (7128/6-1, sample 10) to 83.57 % for depth 2226.40 m (7128/6-1, studied sample 7).

The lowest (21.63%) and highest (84.15%) values for the TOC follow the same trend as the TC with respect to the sample depths; 2349.00 m (sample 10) and 2226.40 m (sample 7), respectively.

With respect to the TIC, the sample 6 at 2222.7 m of depth has a value of 0.92% and is representing the only sample who has reached the detection limit.

Rock-Eval

The lowest values for the peaks S_1 , S_2 and S_3 belong to depth interval 2349.00 m (sample 10) and are 2.61 mg HC/g rock, 43.42 mg HC/g rock and 1.19 mg CO_2 /g rock, respectively. The highest values for the S_1 signal is 7.44 mg HC/g rock and for the S_2 signal is 140.44 mg HC/g rock, corresponding to the depth 2247.70 m (7128/6-1, sample 9). The biggest amplitude for the S_3 signal with 3.2 mg CO_2 /g rock belongs to the studied sample 7 (7128/6-1, 2226.40 m).

The Tmax difference between the lowest and highest temperature is 10 °C; it ranges from 435 °C in the sample 10 (2349.00 m) to 445 °C in sample 7 (2226.40 m).

The sample 7 has the lowest HI-index with 137 mg HC /g TOC. The highest HI-index with 201 mg HC /g TOC belongs to the sample 10 (2349.00 m), which in addition also represents the highest OI-index with 6 mg CO_2 /g TOC. The lowest value for the OI-index with two mg CO_2 /g TOC is represented by the sample 6 (7128/6-1, 2222.70 m).

The Production Index, PI, is ranging from 0.04 (samples 6 and 7) to 0.06 for the sample 8 (7128/6-1, 2246, 20 m) and the sample 10.

6. Discussion

The results from chapter 5 will be presented and discussed in this chapter. The results are based on various plots generated for the determination of organic facies and maturity properties of the sample set. The degree of biodegradation and its effect versus maturity will be discussed. At the end, a summary of the organic facies and the maturity will be given for each sample.

6.1 Organic facies of coals and oils

6.1.1 Biomarker facies parameters

The organic facies of the sample set is discerned by the different plots in the figures 6.1–6.5. Different combinations of parameters (biomarkers) from GC-MS and GC-FID have estimated values to indicate type of facies.

Figure 6.1 shows the isoprenoid/n-alkane ratios of the sample set where maturity and biodegradation pulls in different directions. The cross plot shows that the coals and the DST oils origins from oxidizing environments. Especially the coals and the DST oils from well 7128/4-1, plot in the same zone in the figure 6.1, which means in the peat and coal environments. The coals from well 7128/6-1 have an even more terrigenous signature. The NSO-1 oil has its origin from a mixed organic source i.e. transitional environments.

The DST oils display the highest maturation according to figure 6.1. In terms of biodegradation, the NSO-1 oil seems to be more affected compared to the DST oils. This is probably the case since the DST oils contain more waxy components ($n\text{-C}_{15+}$ alkanes) which take longer time for the bacteria to eat (see also figures 5.5-5.7).

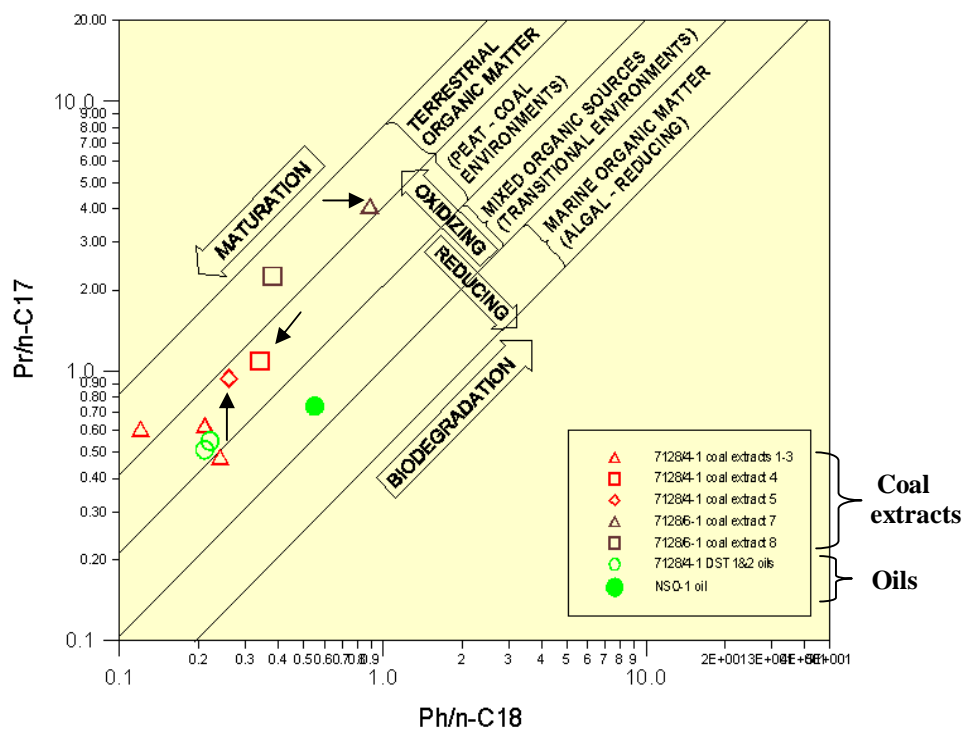


Figure 6.1. A cross-plot of the ratio $\text{Pr}/\text{n-C}_{17}$ versus the ratio $\text{Ph}/\text{n-C}_{18}$ (modified by Shanmugam, 1985). The analyzed coal extracts marked with an arrow are the samples 4 and 5 from well 7128/4-1 in addition to the sample 7 from well 7128/6-1.

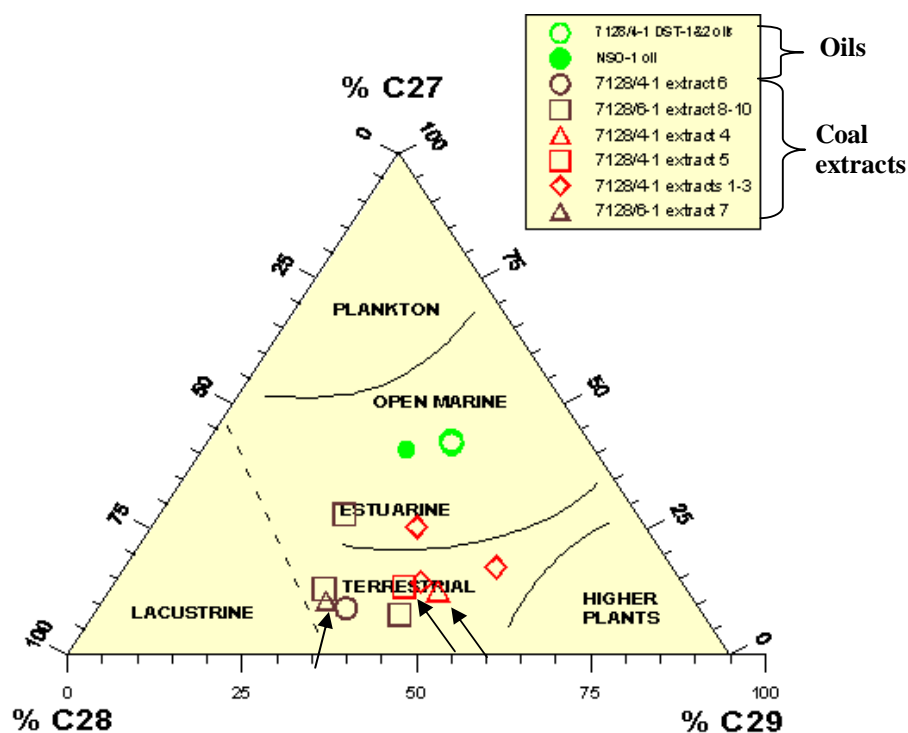


Figure 6.2. Ternary diagram showing the relationship between the C_{27} , C_{28} and C_{29} β -steranes from the sample set (Huang et al., 1979, modified by Shanmugam, 1985). The samples 4, 5 and 7 are analyzed with respect to the facies.

The ternary diagram in figure 6.2 indicates the most probable environment or facies for the samples. The majority of the coals plot near the terrigenous facies, like the samples 4 and 5. However, some of the coals indicate deposition in an estuarine environment or in the transition zone between terrigenous/lacustrine facies, like sample 7.

The DST oils together with the NSO-1 oil plot in the region between estuarine and open marine facies.

Based on figure 6.2 there is little correlation between the coals and the DST oils with respect to source facies. However, it is important to remember that interpretation of the source rocks and their facies based on sterane distribution alone can be difficult (Moldowan et al., 1985; Horstad, 1989). Most petroleum from the Norwegian Shelf plots in the central part of the diagram from Shanmugam (Karlsen, 2004). Based on this, it is likely that the NSO-1 sample placed near the open marine facies is correct.

Figure 6.3 is another plot which indicates the facies based on the ratio methyl dibenzothiophenes/methyl phenanthrenes ($\Sigma\text{MDBT}/\Sigma\text{MP}$) versus the Pr/Ph ratio. The limitations of each facies are made of Hughes et al. (1995), which classifies the plot into different zones. The zone three corresponds to marine shale and moderate sulphate-rich lacustrine facies while zone 4 belongs to terrigenous environments in the form of fluvial and deltaic facies.

The sample one from well 7128/4-1 has a Pr/Ph value indicating terrigenous facies (see tables 4.1 and 5.2). The sample one plots just within the zone 4 (fluvial/deltaic terrigenous facies) at the boundary of zone three (marine shale and moderate sulphate-rich lacustrine facies).

The samples 7 and 8 from well 7128/6-1 plot within the zone 4 and belong clearly to a more proximal terrigenous facies compared to the sample one. In comparison, the figure 6.2 shows an approach from terrigenous facies towards lacustrine facies.

Both the NSO-1 oil and the DST oils plot within the marine shale- and moderate sulphate-rich lacustrine facies in the zone three. The DST oils, though, plot closer to the boundary of

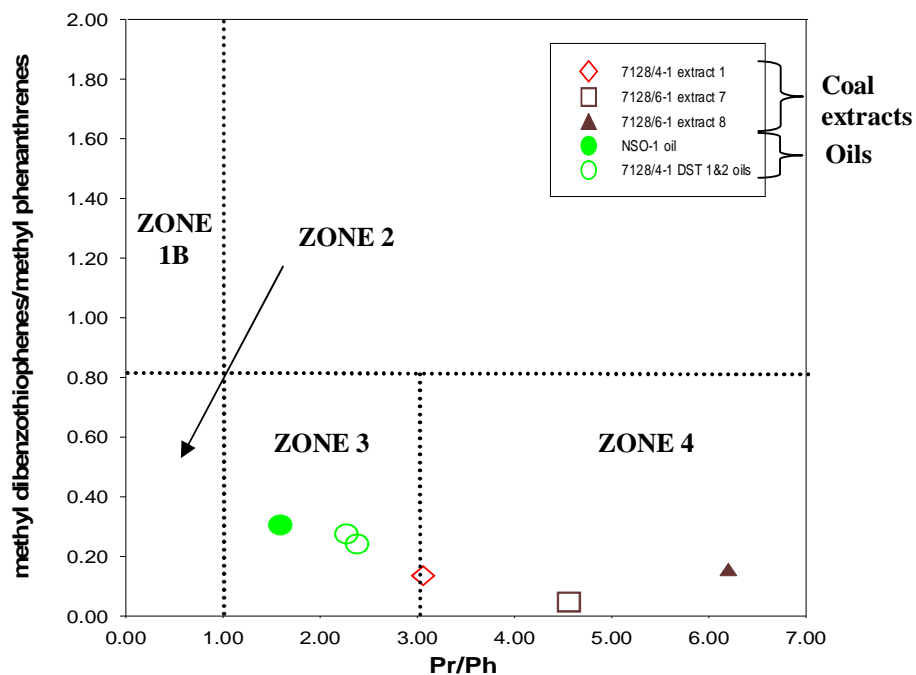


Figure 6.3. A cross-plot of parameter 27 (Radke et al., 2001); the methyl dibenzothiophenes/ methyl phenanthrenes ratio ($\Sigma\text{MDBT}/\Sigma\text{MP}$) versus the Pr/Ph ratio provides a way to infer the source rock depositional environments (from Hughes et al., 1995). The samples plot in the Zones 3 and 4, corresponding to “marine shale and moderate sulphate-rich lacustrine facies” and “terrigenous facies (fluvial and deltaic)”, respectively.

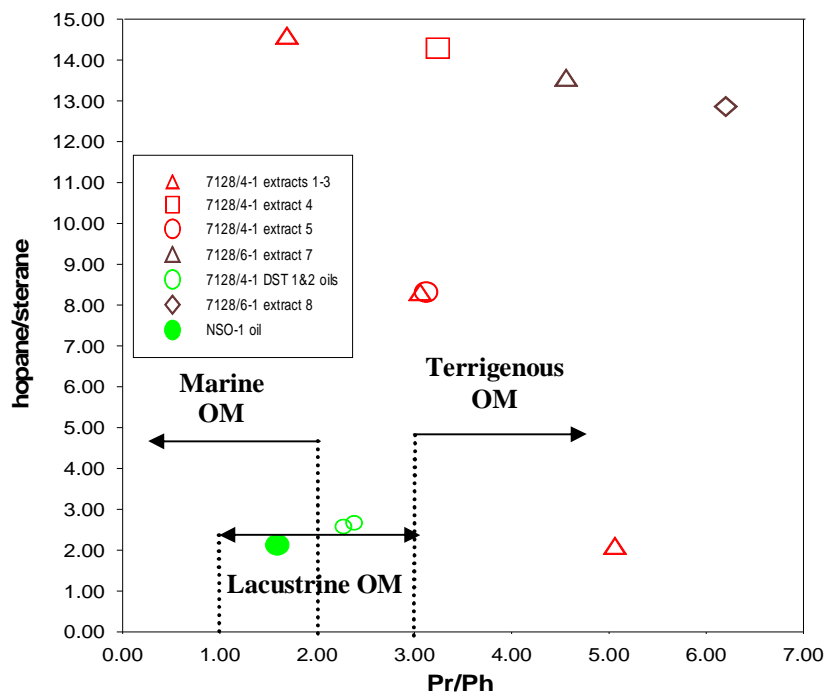


Figure 6.4. A cross-plot of the ratios Pr/Ph versus the parameter 9 hopane/sterane (Mackenzie et al., 1984) – indicating the facies of the samples. The included limitations on the facies are drawn on behalf on information from the table 4.1 from Peters and Moldowan (1993).

Zone 4 compared to the NSO-1 oil. In the figure 6.1 the sample one plots in the same region as the DST oils, which is almost the case in the figure 6.3. This could indicate a common environment of deposition in the form of a lacustrine facies. However, there is little correlation when comparing these samples with those in the figure 6.2, where none of the samples seem to origin from the lacustrine environments.

The figure 6.4 illustrates the characterization of the facies of the sample set with limitations of each facies, based on the table 4.1 from Peters and Moldowan (1993) as in the figure 6.3. Low values for the ratios Pr/Ph and hopane versus sterane indicate marine anoxic facies, while high values represent terrigenous facies (tables 4.1 and 5.2).

The plot shows that the coals from well 7128/6-1 have very high values indicating terrigenous facies, represented by samples 7 and 8. From well 7128/4-1 the analyzed samples 4 and 5 are placed just within the limit of being terrigenous and are approaching the lacustrine facies. However, among the coal samples one through three from well 7128/4-1, one sample plots in the lacustrine environment. The figures 6.1, 6.5 and 6.4 seem to correlate with respect to facies, with respect to the coals. This is in contrast to figure 6.2 which indicates that the coals from well 7128/4-1 are the most terrigenous, while the coals from well 7128/6-1 approach the lacustrine environments.

The oils have low values from the ratios Pr/Ph and hopane versus sterane. The DST oils in the figure 6.4 plot in the lacustrine region, while the NSO-1 oil plots in the transition zone of marine and lacustrine environments. The figures 6.3 and 6.4 show similar trends with respect to the facies for the oils. The figures 6.1 and 6.2 plot the NSO-1 oil in the transitional- and open marine environments, respectively, while the figures 6.3-6.4 plot within the marine shale- and moderate sulphate- rich lacustrine facies. The figures 6.3 and 6.4 plot the DST oils in the lacustrine environments, which could correlate with the peat- and coal environments plotted in the figure 6.1. On the contrary, the figure 6.2 shows facies between the open marine and estuarine for the DST oils.

The plot in the figure 6.5 indicates as in previous figures that the NSO-1 oil originates from marine facies, where algal (kerogen type I) is the main constituent. The DST oils are plotted just within the humic environment, giving humic kerogen (type III).

As the figure 6.1 illustrates, the DST oils are more mature compared to the NSO-1 oil, shown in the figure 6.5. The ratio Ph/n-C₁₈ versus Pr/n-C₁₇ for the coals represents an indicator of the facies and gives no information about the maturity. The coals from well 7128/6-1 show high

values within the area of humic kerogen while the coals from well 7128/4-1 show moderate values in the humic kerogen zone. The coals and the DST oils from well 7128/4-1 correlates with respect to kerogen type although the DST oils plot closer to the algae zone.

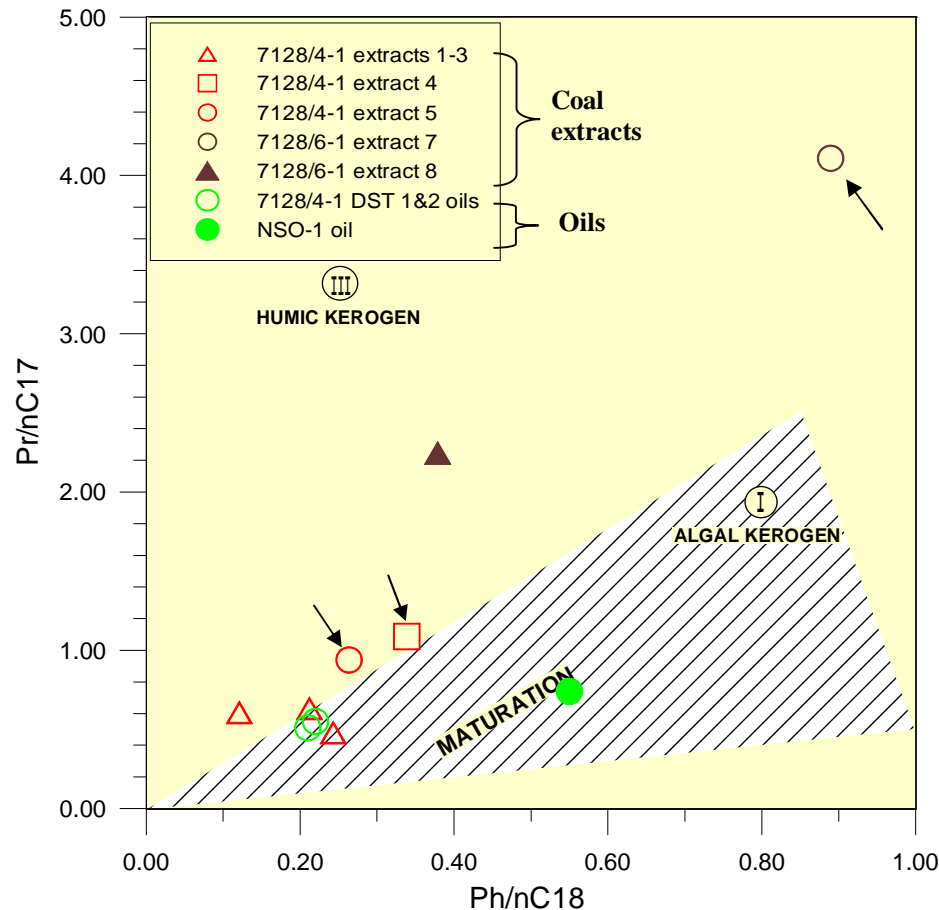


Figure 6.5. A cross-plot of the ratios Ph/n-C_{18} versus Pr/n-C_{17} (modified from Connan and Cassou, 1980) – illustrating the maturity and type of kerogen of the oils, but only indicates the type of kerogen for the coals. The analyzed coals 4, 5 and 7 are marked with arrows.

6.2 Maturity of coals and oils

Maturity of a petroleum sample means the degree of heat experienced by the source rock when the petroleum was expelled. In general, the maturity will increase with depth of burial. A source rock generating and expelling most of its oil, has reached the oil window. According to Hunt (1996), the oil window occurs within a temperature zone of 60-160 °C. On the Norwegian Shelf, the corresponding depth interval to the temperature range is typically three-5 km with a geothermal gradient around 30-35 °C.

6.2.1 Biomarker maturity parameters

The maturity of the sample set is deduced by various plots (figures 6.6-6.11). Different combinations of the parameters (biomarkers) from GC-MS and GC-FID are used to estimate values of the maturity.

The figure 6.6 shows the ratio of the 22S/ (22S+22R) isomers of the C₃₁ hopanes on the x-axis. According to Peters and Moldowan (1993) a maximum value approximating 0.6 marks the onset of oil generation and does not evolve beyond the equilibrium value. As the figure 6.6 shows, the entire sample set has reached the start of the oil window in terms of maturity.

MPDF, a methyl-phenanthrene parameter, on the y-axis shows the distribution of the maturity. This parameter in the figure 6.6 illustrates a range within the early to late stage of oil generation.

The figure 6.7 is another cross-plot showing the maturity, given by the parameters 10 and 11. Peters and Moldowan (1993) gave typically maximum values for the maturity parameters; 0.55 for the ratio 20S/ (20S+20R) and 0.7 for the ratio $\beta\beta/(\beta\beta+\alpha\alpha)$ of C₂₉ steranes.

The figure 6.7 shows that the majority of the samples lie close to the maximum value of parameter 11 (0.55), though a little below. The samples represent low values from 0.5 and below with respect to maximum value of the parameter 10, which is 0.7. Based on this, the sample set can be classified as moderately mature.

In terms of classifying individual coal samples, the coals from well 7128/6-1 represent the lowest maturity. The coals from well 7128/4-1 have an intermediate maturity similar to the DST oils and the NSO-1 oil.

The figure 6.8 shows the same trend as earlier regarding maturity – The DST oils are more mature than the NSO-1 oil, though only slightly in this case. The cross-plot of the parameters Ts/ (Ts+Tm) and 29Ts/ (29Ts + norhopane) apparently display a very low maturity for the coals. The parameter one strongly affects the determination of facies with respect to the coals. High Tm values represent an effect of facies, not an indication of maturity. According to Wang (2007), very high Tm/Ts (Ts is very low in abundance) are usually found in coals or coaly shales. In the figure 5.4, the m/z = 191 fragmentogram belonging to the sample 7 in well 7128/6-1, clearly illustrates the high Tm/Ts ratio.

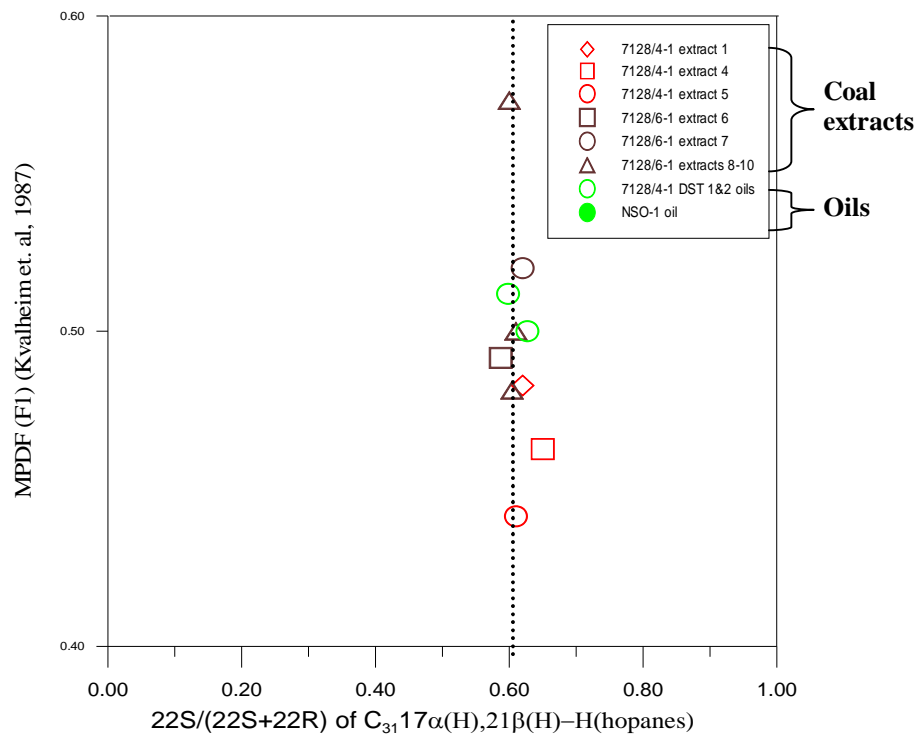


Figure 6.6. The cross-plot of the parameter three, $\frac{22S}{22S+22R}$ of $C_{31} 17\alpha(H), 21\beta(H)-H$ (hopane)], versus the parameter 20, [MPDF (F1)] from Kvalheim et al., 1987.

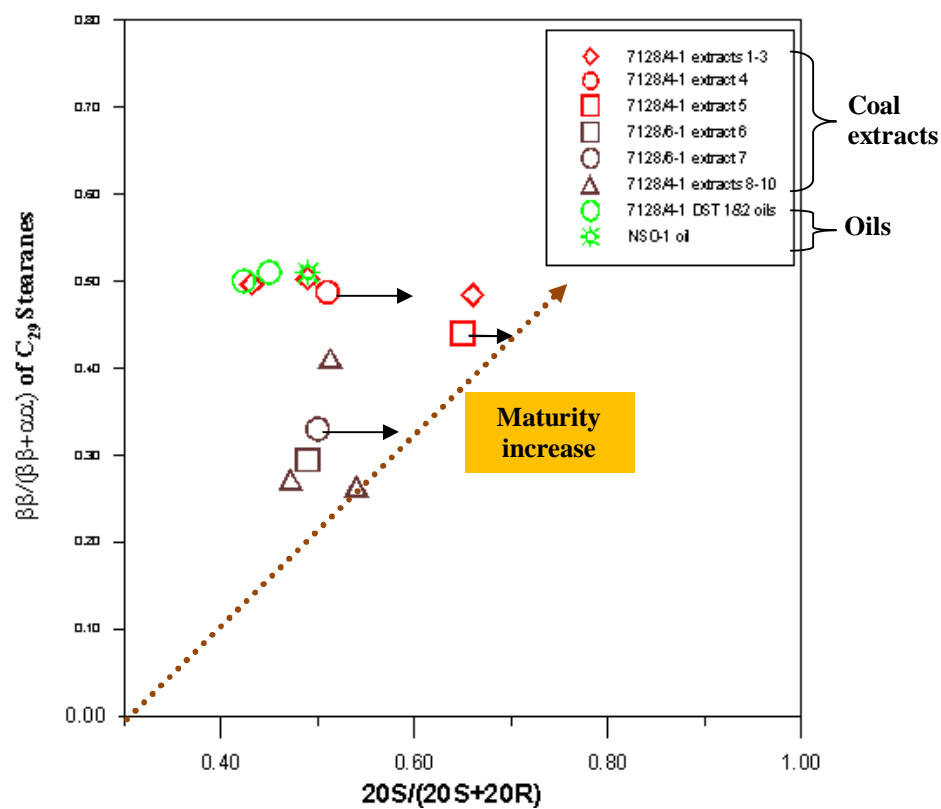


Figure 6.7. A cross-plot of the maturity parameter 11 $\frac{20S}{20S+20R}$ (Mackenzie et al., 1980) and the maturity parameter 10 $\frac{\beta\beta}{\beta\beta+\alpha\alpha}$ of C_{29} steranes (Mackenzie et al., 1980). Among the analyzed coals, indicated with arrows, the coal sample 4 plots as the most mature.

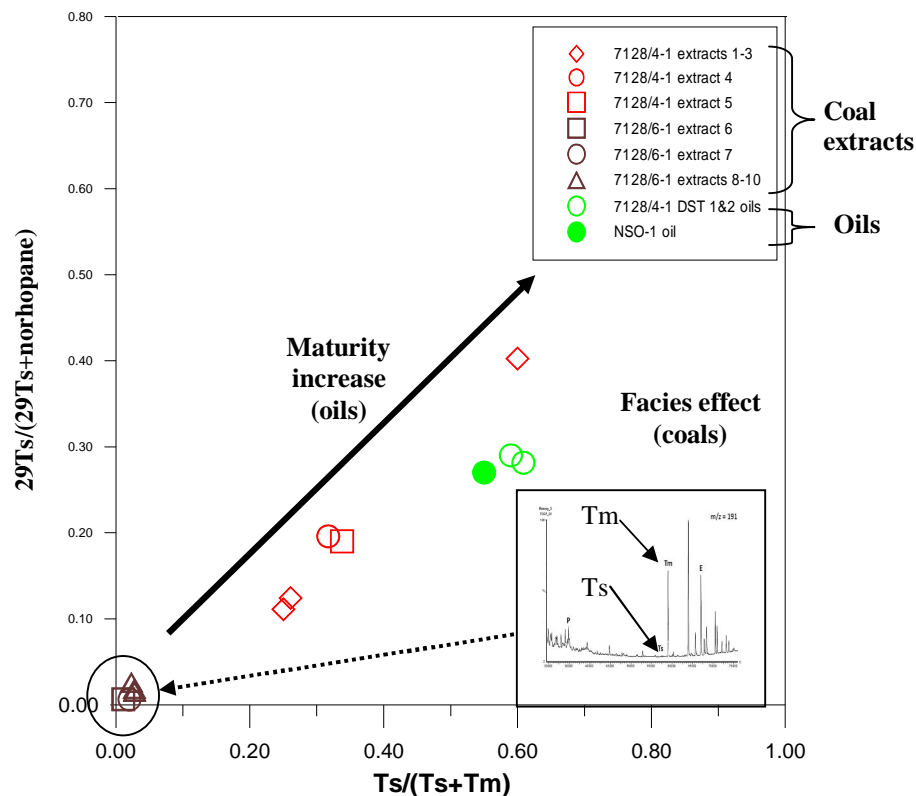


Figure 6.8. A cross-plot of the parameter one $[Ts / (Ts+Tm)]$ (Seifert and Moldowan, 1978; Mackenzie, 1984) and the parameter 5 $[29Ts / (29Ts + norhopane)]$ (Moldowan et al., 1991) - showing the maturity differences for the oils, but works as a facies indicator with respect to the coals. The inserted fragmentogram illustrates the facies effect caused by high Tm in the coals, in this case from well 7128/6-1 marked with a circle.

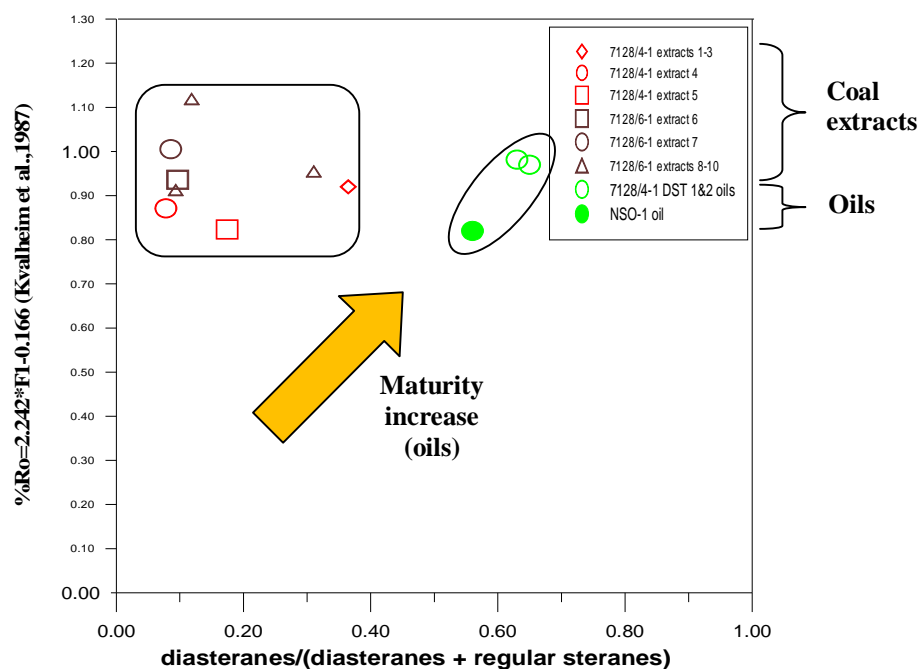


Figure 6.9. A cross-plot of the maturity parameter 12 $[diasteranes / (diasteranes + regular\ steranes)]$ (Mackenzie et al., 1985) and the maturity parameter 24 $[\%Ro = 2.242 * F1 - 0.166]$ (Kvalheim et al., 1987).

The inserted fragmentogram in the figure 6.8 illustrates the big facies effect caused by the high T_m/T_s ratio from the coal sample 7.

The cross-plot in the figure 6.9 with the parameters 12 and 24 on each axis, illustrates that the highest maturity belongs to the DST oils followed by the NSO-1 oil.

Diasteranes is considered as a clastic parameter and is created if clay minerals are found in the source rock (Peters et al., 2005). There are little clay minerals in coals in general and therefore the content of diasteranes is very small in the coals, as the figure 6.9 shows. With respect to the coals, the parameter 12 affects the facies as the parameter one, $T_s/(T_s+T_m)$, does. Therefore, the plot gives no indication on the maturity concerning the coals.

High content of steranes are typical for coals. Since the diasteranes are not that affected by biodegradation as the steranes (Ashan et al., 1997), this explains why coals are not affected by biodegradation (Peters et al., 2005). This is presented in the GC-FID chromatograms (figures 5.2-5.4).

However, biodegradation affects oils. The plot shows a higher content of diasteranes for the DST oils compared to that of the NSO-1 oil. It follows from Ashan et al. (1997) that the NSO-1 oil is more biodegraded compared to the DST oils. This fits with the GC-FID chromatograms in figures 5.5-5.7, showing that the waxy n-alkanes ($n-C_{15+}$) in the DST oils have not been biodegraded.

The figure 6.10 is a plot with $[20S/(20S+20R)]$ and $[22S/(22S+22R)]$ on the axis— displaying the stage of oil generation. According to Seifert and Moldowan (1986) the $20S/(20S+20R)$ ratio of steranes reaches equilibrium at a value of 0.55, which corresponds to 0.8 % vitrinite reflectance. The sample set is near this equilibrium value, even though the coals and the DST oils from well 7128/4-1 show some spread in the values.

The other parameter, the $22S/(22S+22R)$ ratio of hopanes, has an equilibrium value ranging from 0.57-0.62. This range corresponds to a vitrinite reflectance of 0.6 % (Seifert and Moldowan, 1986).

The figure 6.10 illustrates that the entire sample set has reached the oil generation, according to equilibrium values from Seifert and Moldowan (1986). All of the samples are found within peak oil generation zone.

The cross-plot in the figure 6.11 has the $T_s/(T_s+T_m)$ ratio on the horizontal axis and the diasteranes/ (diasteranes + regular steranes) ratio on the vertical axis. The values will in

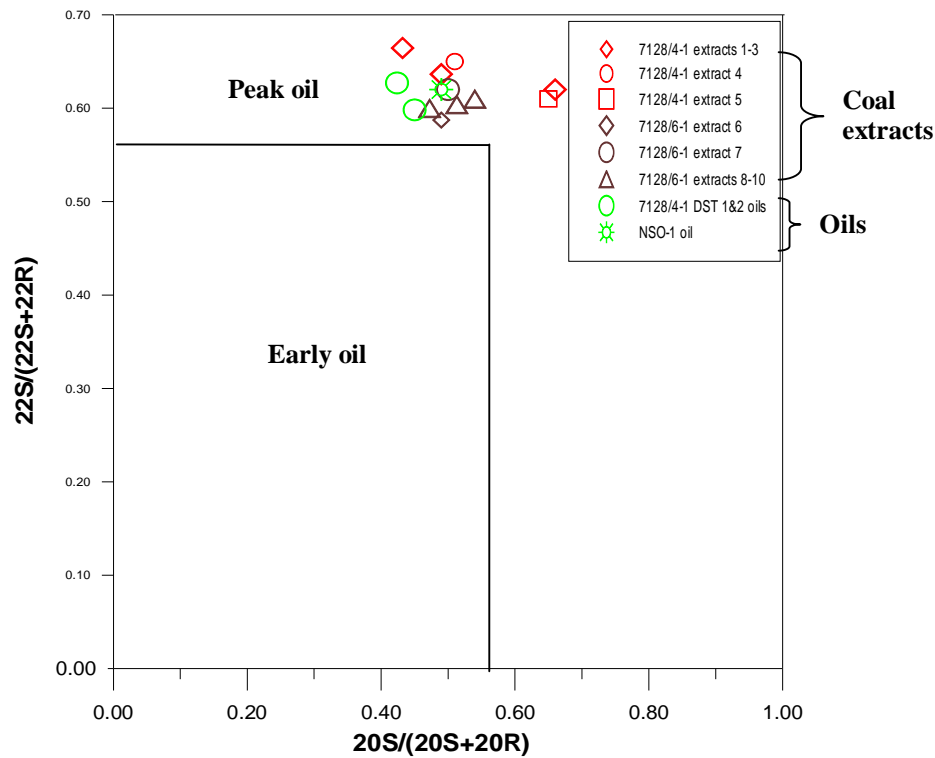


Figure 6.10. A cross-plot of the maturity parameter 11 [$20S/(20S+20R)$] (Mackenzie et al., 1980) and the maturity parameter three [$22S/(22S+22R)$] – displaying the stage of oil generation.

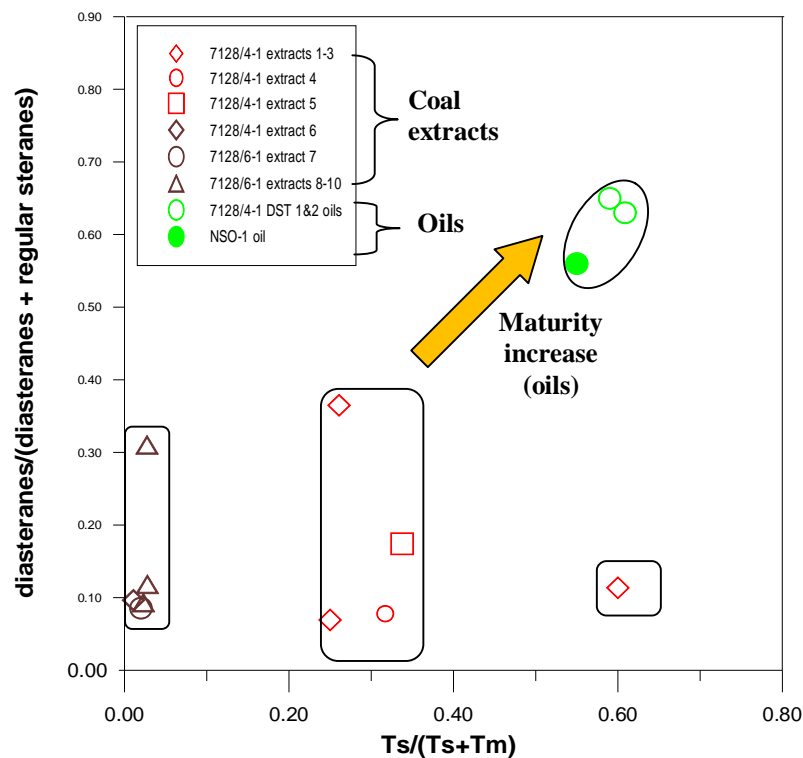


Figure 6.11. A cross-plot of the maturity parameter one, [$Ts/(Ts+Tm)$] (Seifert and Moldowan, 1978; Mackenzie, 1984), and the maturity parameter 12, [$diasteranes/(diasteranes + regular\ steranes)$] (Mackenzie et al., 1985). The parameters indicate the maturity for the oils but only affect the coals with respect to facies.

general increase by maturity for the source rocks. The DST oils from well 7128/4-1 show increased maturity when compared to the NSO-1 oil.

With respect to the coals, the parameters one and 12 have big influences on the facies rather than maturity. The facies effect of the parameters is already described in the text belonging to the figures 6.8 and 6.9. The inserted fragmentogram in the figure 6.8 shows low values of the $Ts/(Ts+Tm)$ ratio for the coals in well 7128/6-1 and illustrates the same facies effect as in the figure 6.11.

The figure 6.12 is a plot with the parameter methyl-phenanthrene MPDF (F1) on the x-axis and $[\beta\beta/(\beta\beta+\alpha\alpha)]$ of C_{29} steranes parameter on the y-axis. The MPDF (F1) shows the distribution of the maturity and illustrates a range within the early to late stage of oil generation.

Peters and Moldowan (1993) gave a typical maximum value of 0.7 for the maturity parameter $\beta\beta/(\beta\beta+\alpha\alpha)$ for the C_{29} steranes. The samples have values from 0.5 and below and can be classified as being moderately mature.

In terms of classifying individual samples, the coal sample 7 from well 7128/6-1 represents the lowest maturity of the studied coals. Nevertheless, the figure 6.12 illustrates that the samples 8-10 from the same well, have the lowest maturity among the coals. From well 7128/4-1, the sample 4 has an intermediate maturity similar to the DST oils and the NSO-1 oil, while the sample 5 is almost as mature as the sample 4.

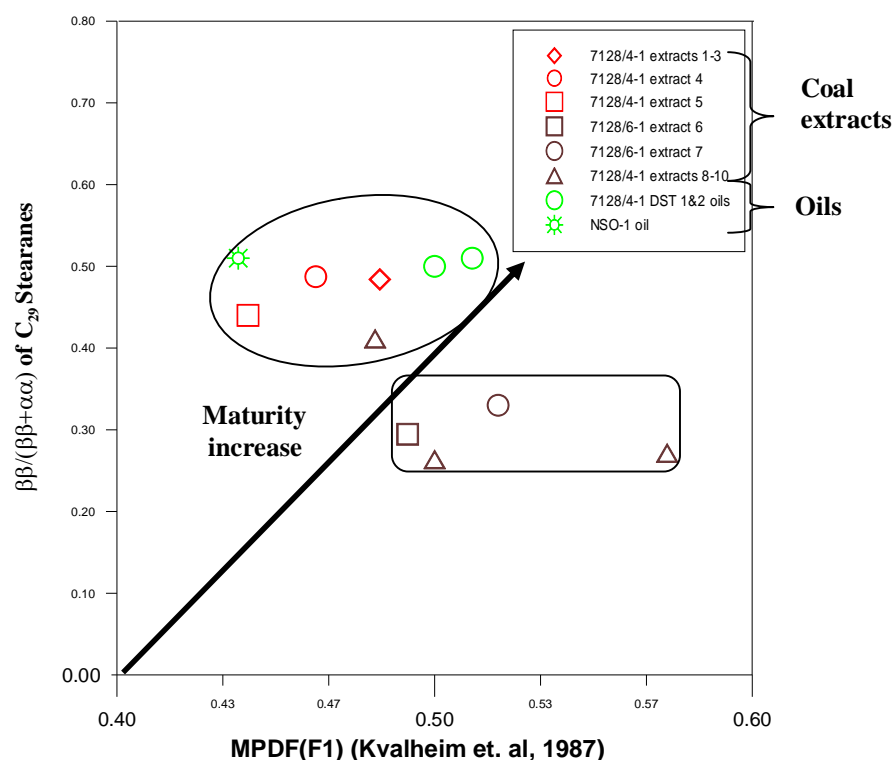


Figure 6.12. A cross-plot of the maturity parameter 20 [MPDF (F1)] (Kvalheim et al., 1987) and the maturity parameter 10 [$\beta\beta/(\beta\beta+\alpha\alpha)$ of C_{29} steranes] (Mackenzie et al., 1980).

6.3 Petroleum potential, richness and kerogen type

In chapter 6.3 all plots have a legend which classifies the coal samples as extracts, which is not correct. Therefore, these samples are termed “coal samples” outside the boxes. The geochemical properties of coals in the form of solid crushed material include the Rock-Eval pyrolysis and the LECO TOC

From the table 4.10 and the tables 5.5-5.6, the values from TOC, S_1 and S_2 are presented. The range in TOC varies from 21.63 (wt. %) to 88.57 (wt. %). The definition of coal is TOC > 50 %. According to table 2.1, not all of the samples can be classified as coals.

S_1 with the value of 1.33 mg HC/g rock for well 7128/4-1, at the sample depth of 2366.80 meters, is representing a good petroleum potential (table 5.6). Another S_1 value of 2.61 mg HC/g rock, representing very good petroleum potential, belongs to well 7128/6-1 at the sample depth of 2349.00 meters. The remaining 8 coal samples have S_1 values ranging from 4.2-15.5 mg HC/g rock, and are representing an excellent petroleum potential. Seen from the table 4.9, the excellent petroleum potential starts from >4 mg HC/g rock.

S₂ with a value of 10.66 mg HC/g rock for well 7128/4-1, at sample depth of 2366.80 meters, represents a very good petroleum potential (see table 5.6). The remaining 9 coal samples have S₂ values ranging from 43.42-162.33 mg HC/g rock and are representing an excellent petroleum potential. Seen from the table 4.9, the excellent petroleum potential starts from >20 mg HC/g rock.

By referring to the table 4.10 from Peters and Cassa (1994), it should be no surprise that all of the coal samples have excellent petroleum potential when it comes to TOC. The other parameter describing the petroleum potential is S₂ or (S₁ + S₂). By comparing table 4.10 and table 5.6, it is obvious that all samples represent an excellent petroleum potential with respect to S₂.

The figure 6.13 A) is showing a cross-plot of the total organic carbon (TOC) on the x-axis and S₂ on the y-axis. The plot gives the petroleum potential and the kerogen type of offshore California Miocene samples (Langford et al., 1990). The figure 6.13 B) shows a similar cross-plot, illustrating the petroleum potential and the kerogen type of the coal samples. The dashed lines indicate the kerogen type of the coals, and are drawn as a parallel to the original in 6.13 A) (from Langford et al., 1990).

From the figure 6.13 B) it is obvious that most of the coal samples surprisingly belong to the type II kerogen. In contrast, two samples from well 7128/4-1 are placed within the area of type III kerogen, which basically represent gas generating coals. Based on the figure 6.13 A) and B), these coal samples have the potential of generating both oil and gas since the majority of the samples belong to the type II kerogen.

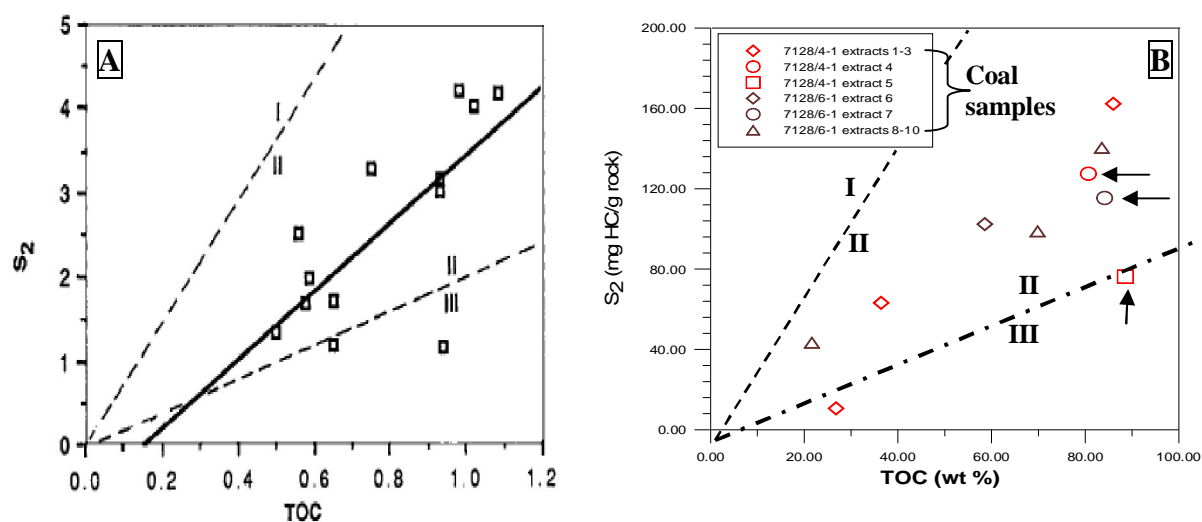


Figure 6.13 A) A cross-plot of TOC (wt %) against S₂ (mg HC/g rock) giving the petroleum potential and the kerogen type of offshore California Miocene samples from DSDP Site 467 (Langford et al., 1990). **B)** A cross-plot of TOC against S₂ using the trends from A) to indicate the kerogen type for each coal sample.

Petersen et al. (1996, 1998) found the highest average (S_1+S_2) contents and Hydrogen Index (HI) values in the Danish Central Graben coals. These are obtained from coal seams associated with a rapid sea level rise. The highest average HI values were in general observed in a palaeo-seaward direction. It is important to know the palaeo history as well as understanding the sequence stratigraphy when looking for rich and petroleum potential source rocks in the coals (Petersen et al., 1996, 1998). However, no matter how excellent the petroleum potential is, expulsion efficiency must be taken into account (Wilkins and George, 2002). Considering coals as oil-prone source rocks, Fleet and Scott (1994) state that the expulsion of petroleum from coal-bearing strata is truly the most critical factor to look at before deciding whether or not coal may expel oil.

Cooles et al. (1986) considered the HI not to be a certain parameter when measuring the petroleum potential since S_2 is very sensitive to type and amount of organic matter. In addition, the TOC measures kerogen, bitumen and oil concentration. They concluded that the variation in the HI with increased maturity depends on the oil generation and the expulsion rates. The petrographic analysis by Peters and Cassa (1994) and Baskin (1997) showed that each macerals may contribute to the HI value, each with different generation and expulsion behaviour. They considered unlike Cooles et al. (1986) that the HI is a complex parameter which cannot be related only to the petroleum potential, generation or expulsion. With this in mind, the mature coals in the figure 6.14 must be evaluated against the expulsion threshold values. The coals macrostructure with respect to expulsion and oil generation is also affected by the macerals distribution (Wilkins and George, 2002).

The figure 6.14 represents a cross-plot of Tmax (°C) against the HI (mg HC/g TOC), giving the maturity for the coal extracts. By the help of the table 4.10 from Peters (1986) it is obvious that the majority of the coal samples in my set are mature. Among the 10 coal samples, eight of them are mature. The studied samples 4, 5 and 7 are among the mature coals. One sample from well 7128/6-1 is just mature, while one sample from well 7128/4-1 is over mature. See also this plot inserted and compared to the “modified modified” (from Espitalie et al., 1984) van Krevelen diagram in figure the 6.15, which classifies the coal samples into the kerogen types I, II and III.

The figure 6.15 illustrates a cross-plot of the Oxygen Index (OI) against the HI, giving an indication of richness and potential for the coal samples. Typical for the coals are low values for the OI and low to moderate values for the HI, as seen in figure 6.15. The coals from well

7128/6-1 have a moderate HI value, but a very low OI value. The coals from well 7128/4-1 have low- moderate HI values, but in general higher OI values compared to the coals from well 7128/6-1.

In general, high values for the HI and low- moderate values for the OI represent rich source rock having excellent petroleum potential. However, HI values near the onset of hydrocarbon generation do not necessarily represent the true hydrocarbon potential, according to Killops et al. (1998). The plot in the figure 6.15 is also compared to a “modified” plot (from Espitalie et al., 1977) of a van Krevelen diagram. The aim is to classify the coals into the kerogen types I, II and III, as shown in the figure 6.17.

The “modified modified” van Krevelen diagram i.e. the figure 6.16 shows that the majority of the coals belongs to type II/ (I) kerogen, which is very unusual for coals in general. The trends for type I and type II fall together for some of the coal samples and make it difficult to classify these samples in detail. One coal sample from well 7128/4-1 indicates clearly type III kerogen, while another sample belongs to the type II/ III kerogen. The latter sample is difficult to classify since it is placed at the converging point for all types of kerogen trends.

The oil zone is found where vitrinite reflection at 0.5 % marks the onset of oil generation and 1.3 % marks the end of the oil window. Surprisingly, the figure 6.16 shows that the majority of the coal samples are found within the oil window and can be classified as oil-prone coals. The coals will in general normally generate gas as they are tremendous producers of CO₂ and water (pers. com. Dag A. Karlsen, 2008).

In terms of generating petroleum in a liquid phase, the coals must be very hydrogen-rich (Wilkins and George, 2002), which is not the case when evaluating the figures 6.15 and 6.17. The other possibility for oil-prone coals to generate oil is thin-layered coal-beds, which are interbedded with clastic sediments. The big adsorption and absorption of oil on the organic macromolecule is a barrier when it comes to expulsion of oil from coals. Isaksen et al. (1998) was claiming that these barriers exist for the migration of petroleum molecules, but to a much lesser extent if the maceral grains are dispersed in a clastic matrix. Therefore, thin coals interbedded with more permeable Lithology may act as migration conduits and expel oil more readily than thick coal seams (e.g. Moore et al., 1992; Petersen et al., 2000).

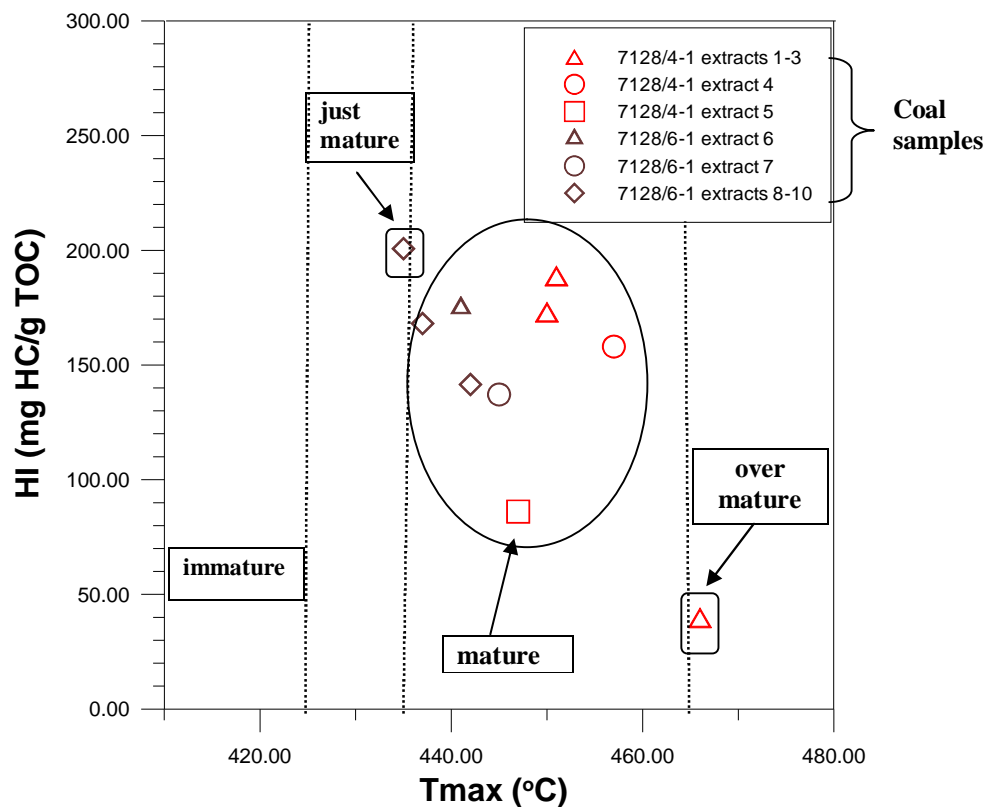


Figure 6.14. A cross-plot of the T_{max} (°C) against the HI (mg HC/g TOC), giving the degree of maturity for the coal samples. The dashed lines marks “maturity degree zones” and are drawn on behalf of the information in table 4.10 from Peters (1986).

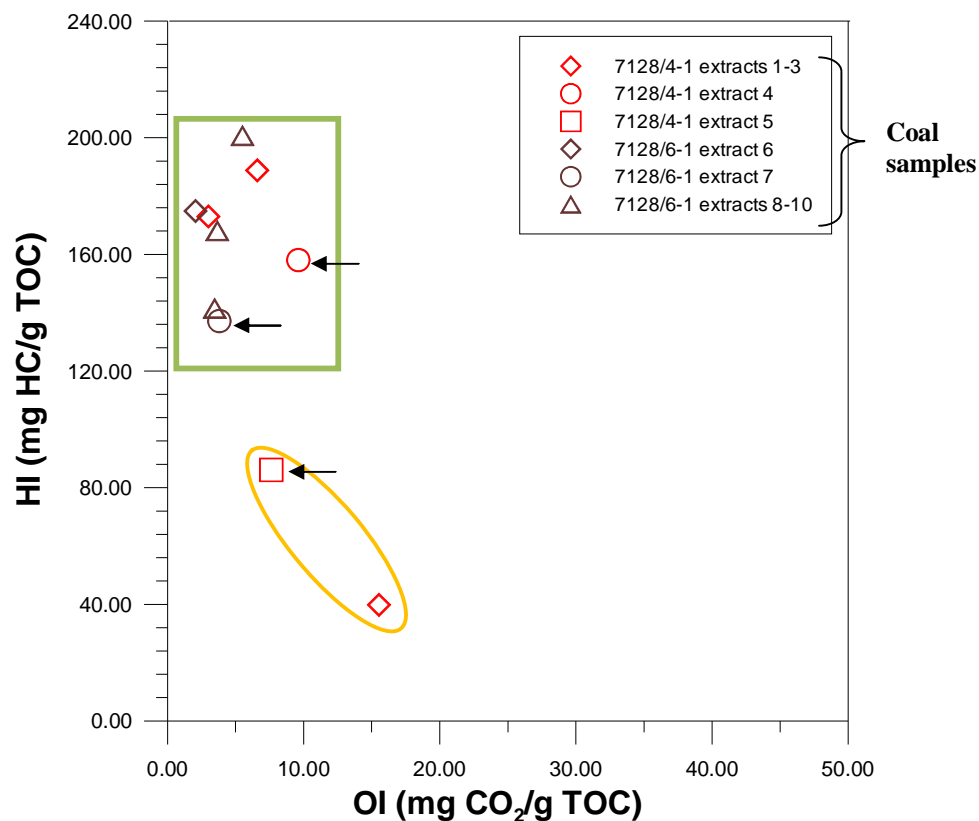
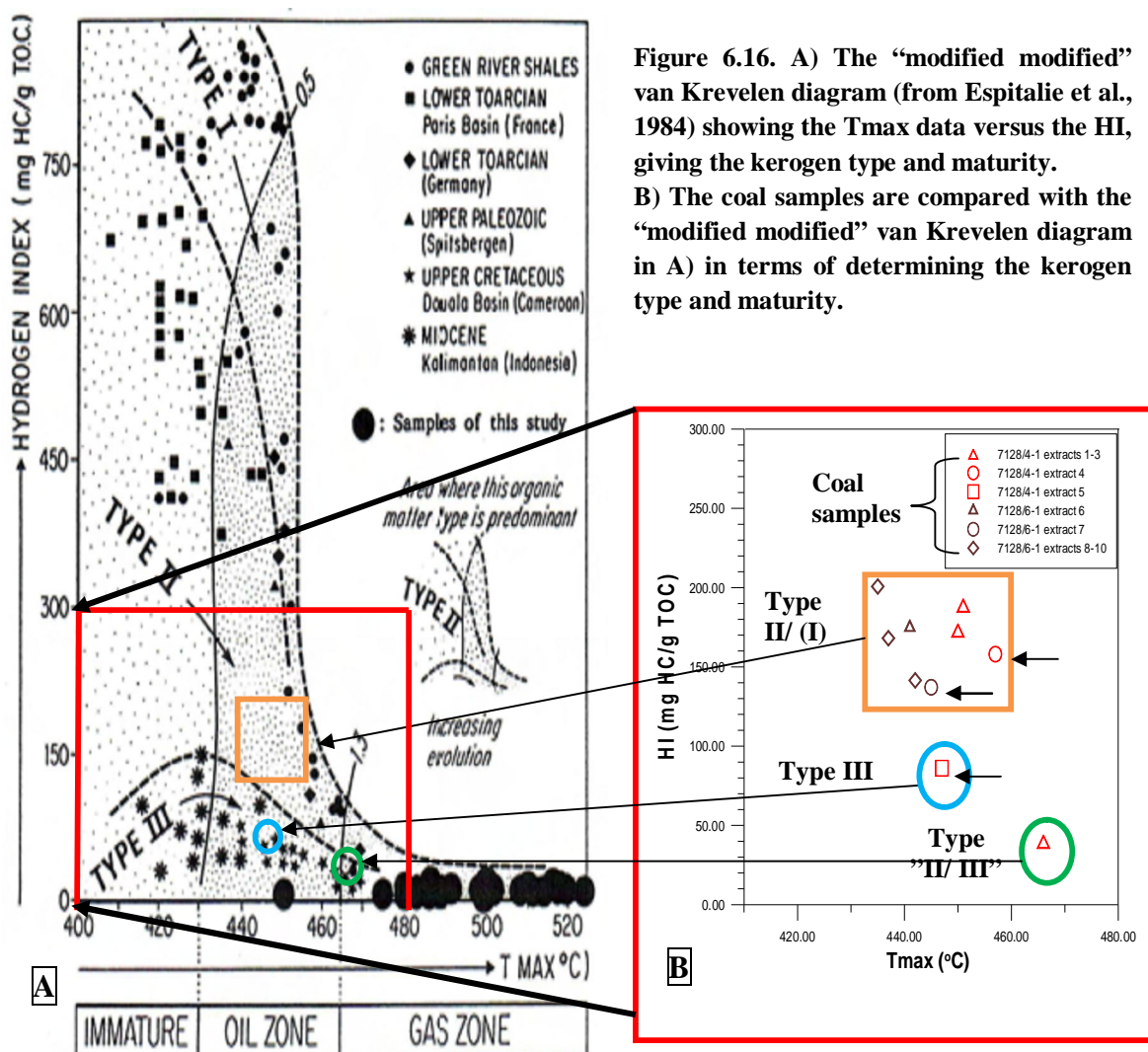


Figure 6.15. A cross-plot of the OI (mg CO₂/g TOC) against the HI (mg HC/g TOC) giving the richness and the petroleum potential of the coal samples.



One possible reason why most coals in the sample set are oil-prone could be secondary migration from oil-prone source rocks within the coals. Lie et al. (2001a) suggested that high extract/TOC ratios and hydrogen indices of Turpan Basin coals (NW China) are caused by allochthonous mature migrated oils from pre-Jurassic.

In laboratory experiments, oil under pressure was observed to migrate through core plugs from massive coals without fracturing these. This proves that oil may invade coals given the right conditions. In a follow-up study, coal samples will be emerged in oil for some time and analysed to test if the oil invades and saturates the coal (pers. com. S Ohm, 2008). If the coals become saturated by "external" derived oils, this clearly represents an alternative explanation why some coals carry a chemical signature suggesting its source to be type II kerogen (figures 6.13 B, 6.16 and 6.17).

The figure 6.17 represent the coal samples inserted into a “modified” Van Krevelen diagram by Espitalie (1977), with main emphasis on classifying the coals into kerogen-types. As the figure shows there are low-moderate values for the HI and low values for the OI, as described in the text belonging to the figure 6.15.

The “modified” van Krevelen diagram suggests that the coal samples from well 7128/6-1 and three coal samples from well 7128/4-1 approach the “type I/II” limit. It is difficult to know whether they have followed the path of type I- or type II- kerogen. Two samples from well 7128/4-1 are found in the transition zone between the type II- and the type III kerogen, in an area close to the end of coalification (figures 1.3 and 6.17 B). Since the latter samples are found close to the meta-anthracite stage, it is difficult to know if these coals have followed the path of the type II- or the type III kerogen. The potential of the type II kerogen represents generation of gas and oil, while the type III kerogen generates gas. Based on the figure 6.16, the coals have the potential to generate liquid petroleum but gaseous petroleum in form of methane is more likely.

The figure 6.19 B), illustrating the coal extracts analyzed using Iatroscan TLC-FID, indicates very low generation of saturated- and aromatic hydrocarbons as well as polar compounds (yield), especially for the coals in well 7128/6-1. The saturated- and aromatic hydrocarbons are the most important part concerning the generation of oil and gas.

Based on this, uncertainty concerning the generation of hydrocarbons from coals exists. However, if these coals occur in large quantities down- flank of the platform, and if preferentially saturated hydrocarbons migrate out of the coals leaving behind the polar compounds, the potential exists.

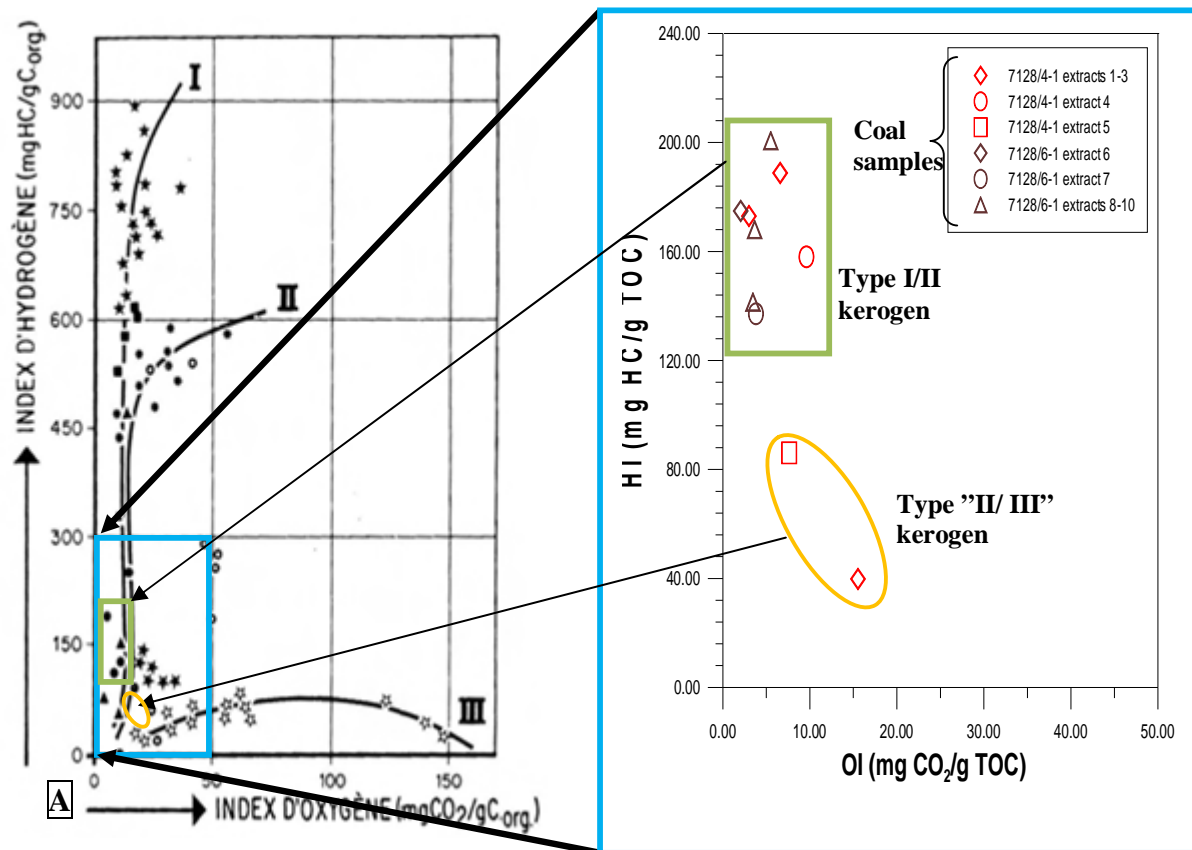
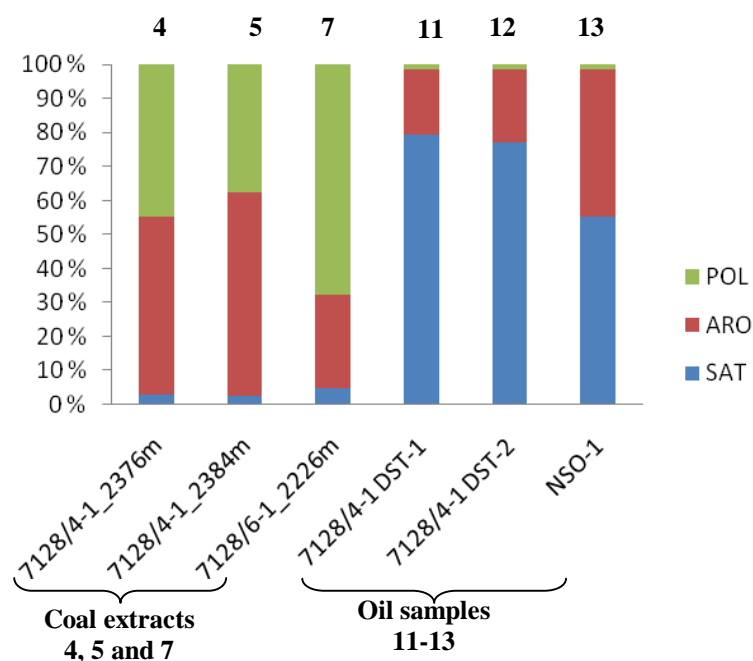


Figure 6.17. A) The “modified” van Krevelen diagram (from Espitalie et al. (1977)).
B) The coal samples are put into the “modified” van Krevelen diagram in A) in terms of classifying the kerogen type.

Figure 6.18. The percentages of the saturated and aromatic hydrocarbons and the polar compounds for the studied coals 4, 5 and 7 and the oils 11-13. Note the small amount of the saturated hydrocarbons in the coal extracts compared to the oil samples, especially when compared to the DST oils.



6.4 Volumetric contents

The percentages of the saturated- and aromatic hydrocarbons in addition to the polar compounds are presented in the figures 6.18 and 6.21. They show that the coal extracts mainly consist of aromatic hydrocarbons and polar compounds with only a few percentages of saturated hydrocarbons. In contrast, the oils mainly consist of saturated hydrocarbons followed by aromatic hydrocarbons with only a few percentages of polar compounds.

The order of absorption capacity of coals was determined by Sandvik et al. (1992) to be polar compounds > aromatic hydrocarbons > saturated hydrocarbons. The results of fractionation during expulsion and primary migration gave differences in composition between expelled oils and generated bitumen in organic matter. Later Huang et al. (1997) made migration experiments on two coals and found that the expelled oil was extensively enriched in saturated hydrocarbons. With this in mind, the figure 6.18 clearly illustrates the low amounts of aliphatic hydrocarbons in the coals but higher content in the DST oils. Since the coal samples and the DST oils are collected from the same well (7128/4-1), and are lying close to well 7128/6-1, it could be that the saturated hydrocarbons in the mature coals overcame the expulsion threshold (Wilkins and George, 2002) and migrated. If that is the case, the DST oils could be sourced entirely or partly by the coals. The migration pathway in the coals would then most likely go through cleats. Cleats are orthogonal fractures in coal with spacing in the range 0.1 – 10 cm (Speight, 1983).

The figure 6.20 b) illustrates the ratio between the saturated hydrocarbons and the total extractable organic matter (EOM) for the coals. By looking at the figures 6.18, 6.19 A) and 6.20 B) it seems likely that the coal extract 7 from well 7128/6-1 have the highest portion of aliphatic petroleum products of the coals. Nevertheless, the figure 6.19 B) shows that this extract gives the lowest yield of the saturated fraction among the coals. This is also the case for the fractions of the aromatic hydrocarbons and the polar compounds of the extract 7, respectively.

The ratio of the saturated- and the aromatic hydrocarbons for the sample set is presented in the figure 6.20 A) and follows the same trend as in the figure 6.18. This means high values for the DST oils and low values for the coal extracts. The high content of the aromatic hydro-

carbons in the NSO-1 oil compared to the DST oils (figure 6.18) explains the moderate value of the ratio SAT/ARO for the NSO-1 oil.

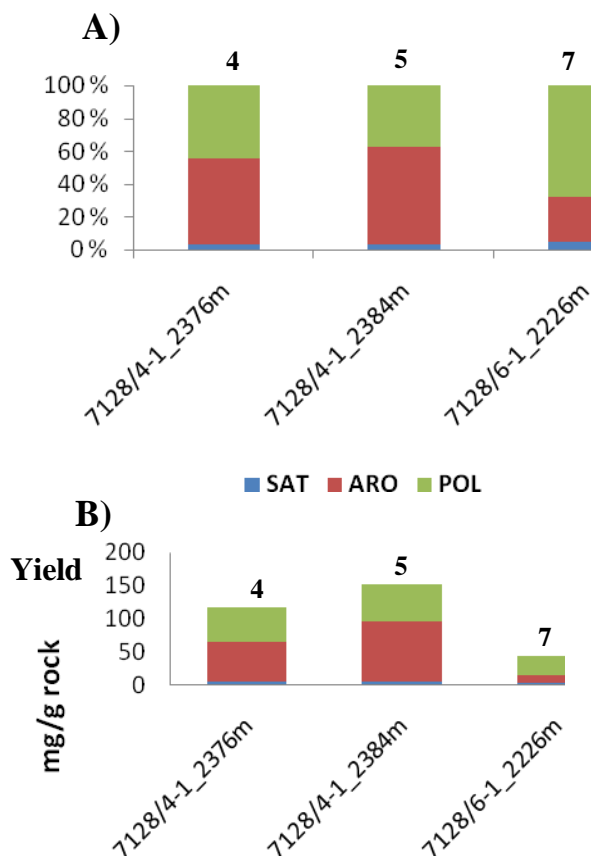


Figure 6.19. The three coal extracts 4, 5 and 7 plotted in percentages (A) and yield (B).

Note the column of the coal extract 7 from well 7128/6-1 compared to the columns of the coal extracts 4 and 5 from well 7128/4-1;

In A) the saturated hydrocarbons and the polar compounds represent the highest values for the extract 7, when measuring in percentages (%),

In B) the aliphatic and the polar fractions represent the lowest values for the extract 7, when measuring in yield (mg/g rock).

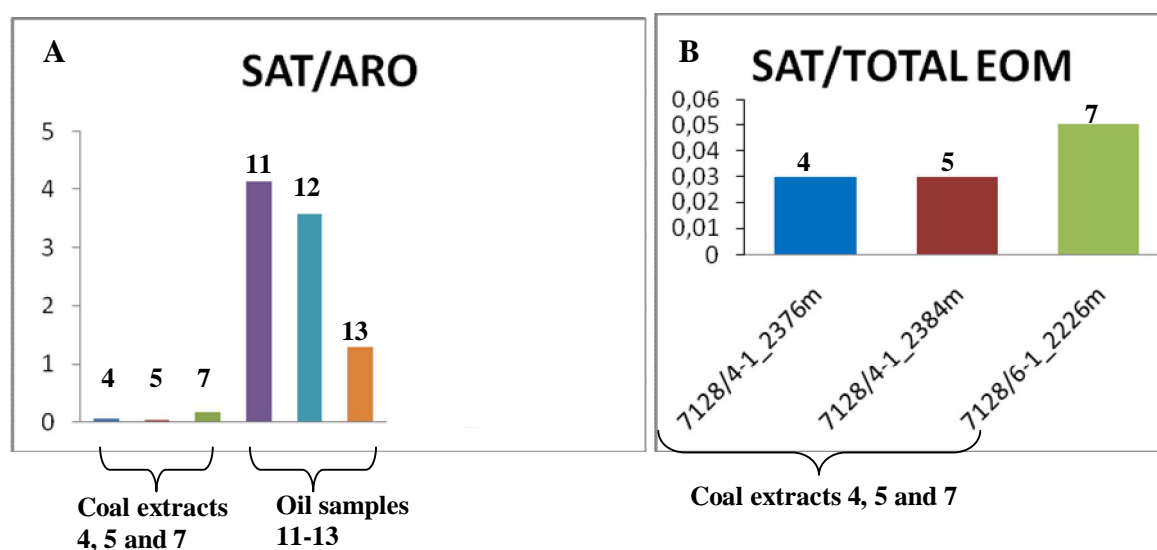


Figure 6.20. A) The ratio between the saturated- and aromatic hydrocarbons for the coal extracts and the oils. B) The ratio between the saturated hydrocarbons and the total EOM for the studied coal extracts 4, 5 and 7.

Figure 6.21 displays a high percentage of saturated hydrocarbons for the DST oils compared to the NSO-1 oil, and in particular when associated with the coal extracts. The coals have a very low content of saturated hydrocarbons, but nevertheless they have high percentages of aromatic hydrocarbons and polar compounds. By comparing this figure with the figure 6.18, it is obvious that the coal extract 7 from well 7128/6-1 contains more polar compounds and less aromatic hydrocarbons associated with the coal extracts 4 and 5.

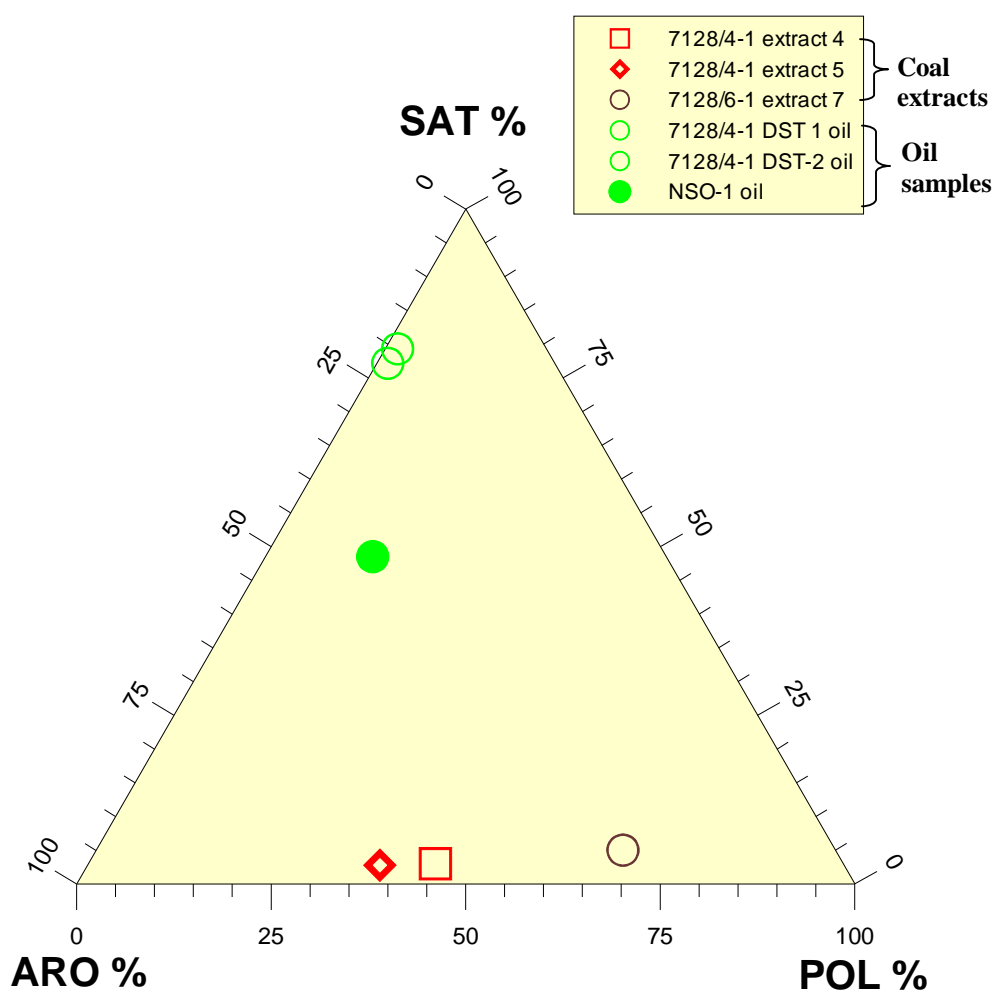


Figure 6.21. A ternary plot of the saturated (SAT) - and aromatic (ARO) hydrocarbons and polar (POL) compounds for the three coal extracts 4, 5 and 7 and the three oil samples 11-13.

6.5 Biodegradation of the samples

The microbial alteration of crude oil with access to meteoric water is called oxic biodegradation. It is necessary for biodegradation that the temperature is less than 65-80 °C. Absence of H₂S and proximity to an oil-water contact is also required (Milner et al., 1977; Connan, 1984; Ahsan, 1993). The results of biodegradation are partial or total removal of components in the following order; n-alkanes, isoparaffins, naphthenes (i.e. steranes and terpanes), aromatics and sometimes the polycyclic aromatics (Winters and Williams, 1969; Evans et al., 1971; Bailey et al., 1973; Chosson et al., 1992; Moldowan et al., 1992).

Winters and Williams (1969) have discussed how the bacteria removed the n-alkanes prior to any other compound class. The increased relative concentration of acyclic isoprenoids, like the pristane and the phytane, compared to n-C₁₇ and n-C₁₈, is the result of increased biodegradation.

The incipient biodegradation represents the loss of n-alkanes, seen to a certain extent in the figures 5.5 and 5.6, displaying the GC-FID chromatograms for the DST oils. By more pronounced biodegradation we observe removal of pristane and phytane. The NSO-1 oil is representing the heaviest biodegraded sample. This is shown in the figure 5.7 and the table 5.2, where the n-alkane peaks are more reduced compared to the DST oils. The coals are not affected by biodegradation due to its tight macrostructure.

The UCM (unresolved complex mixture) humps are observed for the three coal extracts. The highest UCM is represented by the sample 7 from well 7128/6-1 (figures 5.2-5.4). Increasing UCM probably means an increase in the vitrinite content or in woody materials, with respect to the coals. This means that the sample 7 from well 7128/6-1 represents the most terrigenous “woody” coal in the sample set, followed by the samples 4 and 5 from well 7128/4-1, taken at 2376.1 m and 2384.7 m, respectively. The sample 5, with its distinctly low UCM from the GC-FID and based on different facies plot from the GC-MS (figures 6.1, 6.2 and 6.4), seems to originate from a more distal terrigenous environment containing more of algenite and sporinite and less of vitrinite compared to the “woody” coal samples 4 and 7.

6.6 Summary of source and maturity of the samples

6.6.1 Source

Well 7128/4-1, coal extracts 4 and 5 (2376.1 m and 2384.7 m, respectively)

By comparing the tables 4.1 and 5.2, the coal extracts 4 and 5 from well 7128/4-1 have values for the ratio Pr/Ph falling just within the lacustrine organic matter, though very close to be of terrigenous origin. The figure 6.1 illustrates that these coals lie within the peat- and coal environments. The figure 6.2 shows that the majority of the coals lie within the terrigenous facies, having the highest amount of the C₂₉ ββ-steranes. The Pr/Ph ratio in the figure 6.3 indicates a terrigenous facies. The figure 6.4 shows a cross-plot indicating the coals to origin from terrigenous facies while the figure 6.5 shows that coals are humic and comes from a very oxic environment, which is true for terrigenous environments.

The GC-FID for the 7128/4-1 coals 4 and 5 (figures 5.2-5.3) show a large UCM and a high value for the Pr/Ph ratio for the sample depth 2376.1 m compared to the sample depth 2384.7 m. The sample 4 contains probably more vitrinite and thus represents a more landward facies of deposition compared to the deeper sample 5, which may contain more liptinites.

Well 7128/6-1, coal extracts 7 (2226.4 m)

The coal sample 7 from well 7128/6-1 at sample depth 2226.4 m has all ratios within the terrigenous environments, based on the tables 4.1 and 5.2. Especially the high Pr/Ph ratio of 4.56 (terrigenous environments means value three or higher), gives reason to believe this sample origins from a terrigenous facies. The figure 6.1 plots the coal sample at the terrigenous environments. The figure 6.2 plots all the coal samples from well 7128/6-1 in the terrigenous environments, though close to the lacustrine environments. This means that the coals from well 7128/6-1 contain less C₂₉ ββ-steranes and more C₂₈ ββ-steranes. The figure 6.4 illustrates a terrigenous facies based on very high values for the hopane/sterane ratio and already mentioned high Pr/Ph ratio. The plot of Ph/n-C₁₈ versus Pr/n-C₁₇ in the figure 6.5 shows that the sample 7 is found in the humic zone, far away from the algae zone. This corresponds to an oxygen-rich environment like the terrigenous facies. In comparison, the samples 4 and 5 are lying close to the algae zone.

The GC-FID chromatogram belonging to the sample 7 (figure 5.4) shows an even larger UCM in addition to a higher value for the Pr/Ph ratio compared to the coal extract 4 (figures 5.3 and 5.5). The sample 7 contains probably a lot of woody material in the form of vitrinite and represents the most typical coal in the sample set.

Well 7128/4-1, DST 1 & 2 oils (1592-1610 m and 1577-1586 m, respectively)

The two DST oils, representing the samples 11 and 12 from well 7128/4-1, have Pr/Ph ratios ranging from two-three indicating a lacustrine facies, according to the tables 4.1 and 5.2. The cross-plot in the figure 6.1 plots the oils just within the oxic peat- and coal environment. However, the figure 6.2 plots the oils between the marine facies and the estuarine facies, though closest to the marine facies. The figures 6.3 and 6.4 illustrates that the oils origins from a marine and mixed source. It is likely that some terrigenous input gives a mixed source. The figure 6.5 shows that the DST oils are of humic origin giving humic kerogen, even though the oils plot close to the algae zone.

The GC-FID chromatograms of the samples 11-12 (see figure 5.5-5.6) show moderate values for the Pr/Ph ratio compared to the coal samples 4 and 7 (already mentioned). Still, the Pr/Ph ratio gives high values when compared to the Pr/Ph ratio of the NSO-1 oil. Typical for these oils are the waxy n-alkane components, meaning that the majority of the C₁₅+ fractions of the n- alkanes have not been removed by biodegradation. The waxy n- alkanes could originate from the coals and therefore be a signature of the terrigenous input. The DST oils can be classified as waxy.

NSO-1 oil, standard North Sea oil from the Oseberg Field

The NSO-1 oil has a Pr/Ph ratio below two, which indicates a marine facies (tables 4.1 and 5.2). The figure 6.1 shows that the NSO-1 oil has its origin from mixed organic sources. This represents a transitional environment in the reducing-oxidizing zone. In the figure 6.2, the NSO-1 oil plots between the open marine and the estuarine environments, just like the DST oils. The figure 6.3, on the other hand, plots the NSO-1 oil close to the marine shale facies. Also, the figure 6.4 supports a marine facies of origin for the NSO-1 oil, since the samples are plotted close to the marine facies. As the only sample, the NSO-1 oil plots within the algae

zone, displayed in the figure 6.5. This indicates deposition under varying reducing and oxidizing conditions in a transitional setting, also indicated in the figure 6.1.

The GC-FID chromatogram for the NSO-1 oil (figure 5.7) shows a low value for the Pr/Ph ratio compared to the coals and the DST oils. The low value means that the NSO-1 oil has been deposited in reducing and anoxic environments. The NSO-1 oil does not contain much waxy n-alkane in contrast to the DST oils. The NSO-1 oil can be classified as aliphatic rich biodegraded oil.

Based on the discussion, the sample set can be classified in terms of facies:

Coal sample 7, 7128/6-1, sample depth 2226.4 m; proximal terrigenous environment.

Coal sample 4, 7128/4-1, sample depth 2376.1 m; proximal terrigenous/lacustrine environment

Coal sample 5, 7128/4-1, sample depth 2384.7 m; distal terrigenous/lacustrine environment.

Oil samples 11-12, 7128/4-1 DST 1 & 2, core depths 1577-1610 m; transitional environment.

Oil sample 13, NSO-1; marine environment.

6.6.2 Maturity

From the GC-FID-, GC-MS-, LECO TOC- and Rock-Eval analysis the increasing maturity for the sample set is characterized:

The coals can be classified in terms of maturity from the figures 6.6, 6.7, 6.10, 6.14 and 6.16. The coals have reached the start of the oil window in terms of maturity (figure 6.6), while the coals are found within peak oil generation zone, according to the figure 6.10. Based on the figure 6.14 and the table 4.10 from Peters (1986), it is clear that the majority of the coals can be classified as mature while one sample is over mature. Also, the figure 6.16 illustrates that 9 of the coal samples are found in the oil zone and one sample belongs to the gas zone. None of the coal samples are found in the immature zone.

However, only the figures 6.7 and 6.12 illustrate the maturity of the coals related to the oils. Among the coals from well 7128/6-1, the figures show that the samples 8-10 represent the lowest maturity in the sample set. The figures also show more mature coals from well 7128/4-1, in fact being as mature as the three oil samples. In the figure 6.7, the sample 4 is slightly more mature than sample 5, while the figure 6.12 illustrates that the samples 4 and 5 have the same degree of maturity.

The other figures have parameters on their axis affecting the facies rather than the maturity e.g. the diasteranes/ (diasteranes + regular steranes) ratio, the Ts/ (Ts+Tm) ratio and the Pr/Ph ratio.

The DST oils are characterized in terms of maturity from the figure 6.1 and the figures 6.5-6.11. The DST oils represent the highest maturity in the sample set (figures 6.1, 6.5, 6.8, 6.9, 6.11). The DST oils have reached the oil window in the figure 6.6, while the DST oils are closest in approaching the peak oil zone, shown in the figure 6.11. Nevertheless, the figure 6.10 shows that all of the samples have reached the peak oil zone.

Regarding the NSO-1 oil, only the figure 6.7 supports this sample to be slightly more mature than the DST oils.

Based on the discussion, the sample set can be classified in terms of increasing maturity:

Coal sample 7 (7128/6-1, 2226.4 m) → Coal sample 5 (7128/4-1, 2384.7 m) → Coal sample 4 (7128/4-1, 2376.1 m) → Sample 13 (NSO-1 oil) → Samples 11-12 (7128/4-1 DST 1&2 oils)

6.7. Kerogen type and migration

The cross-plot in the figure 6.14 is defined by the Tmax and the HI on the two axes. The illustrated plot is based on the values from the table 4.10, and shows that the majority of the coals are mature. This cross-plot is used in a “modified modified” van Krevelen diagram in the figure 6.16, visualizing that 8-9 of the coals are oil-prone and belong to the type II kerogen. The remaining one or two coal samples are gas-prone and belong to the type III kerogen. The figure 6.13 B) is a plot of the parameters TOC and S₂, showing that 8 samples belong to the type II kerogen and two samples belong to the type III kerogen. The figure 6.17 is another plot of the van Krevelen diagram with the parameters HI versus OI, indicating the same as the figures 6.13 B) and 6.14 when it comes to classifying the coals into kerogen types.

The figures 6.13 B), 6.16 and 6.17 indicates that the majority of the coals belong to type II kerogen, while one or two samples have a character more like the type III kerogen. This gives a potential for generation of oil and gas. It is possible that the DST oils are partly or entirely sourced from the coals if the “barriers” (mentioned earlier in the discussion) are overcome. It is possible that terrigenous-derived materials from the coals has affected the biomarker fingerprints related to the waxy components (C₁₅₊ fraction of the n-alkanes) in the DST oils.

7. Conclusions

The aim of the study is to evaluate if Lower Carboniferous coals on the Finnmark Platform have the capability to generate and expel oils. The geochemical characteristics of the investigated coals are vital clues to the ability of these coals at their locations, or in more distal deeper regions of the Barents Sea, to source traps in regions where the Mesozoic rocks are immature due to too shallow burial. Thus in this work is the geochemical characteristics of the coals and their organic extracts a major issue. Furthermore, it is of great importance to examine if the coals have expelled any petroleum into associated silt and sandstones and to compare such extracts with existing oils from the region, based on geochemical parameters concerning organic facies of deposition and maturity.

The coals in this study are two samples taken at different depths from well 7128/4-1 and one sample from well 7128/6-1. The oil samples, DST-1 and DST-2, are collected from well 7128/4-1. The wells 7128/4-1 and 7128/6-1 are comparatively close to each other, around 25 km in horizontal direction. The last sample, NSO-1, is a standard North Sea Oil from the Oseberg Field used as a reference sample for “North Sea Oils”.

Total organic carbon content and Rock-Eval parameters for the coals have been determined analyzed and plotted in traditional diagrams along with GC-FID and GC-MS parameters of their extracts. The latter provide detailed information on the organic facies and maturity of generated bitumen in the coals.

Different van Krevelen diagrams together with other classification diagrams indicating richness of coals, underlines that the coals in this study have an excellent petroleum potential and that they are mature. Coals from well 7128/4-1 are most mature, based on different plots from maturity facies parameters and Rock-Eval pyrolysis, followed by the coals from well 7128/6-1.

The coal samples from the wells 7128/4-1 (sample depth of 2376.1 m) and 7128/6-1 (sample depth of 2226.4 m) are both of humic origin (humic coals) deposited in terrigenous environments. These samples represent typical coal deposits, having high Pr/Ph ratios and large UCM (unresolved complex mixture), probably consisting mainly of complex

cycloalkanes and aromatic hydrocarbons derived from woody material (vitrinite). The coal sample taken at 2384.7 m from well 7128/4-1 is also of humic origin and plots within the terrigenous peat-coal environments. In contrast to the other coal samples, the Pr/Ph ratio is moderate high and the UCM is also smaller. This indicates a more distal terrigenous coal deposit, and a coal maceral composition with a more liptinite-rich composition compared to the other coals. Such coals are more oil prone than the vitrinite rich coals.

The deduced organic facies of the source rock for the DST oils in well 7128/4-1 is quite intriguing. The isoprenoid/n-alkane distributions make these oils plot, in the figure 6.1 within the peat-coal environment and in the figure 6.5 these oils fall within the region indicating them to have been sourced from a humic type of kerogen.

Other plots indicate a more mixed terrigenous/marine source type (figures 6.2-6.4). The Pr/Ph ratio is high compared to the NSO-1 oil, though lower compared to the extracts of the coals. The facies of the NSO-1 oil is indicated from the classification diagrams to be of transitional/marine origin, containing algal kerogen. It is quite clear that the DST oils are sourced from a source rock facies with a significant terrigenous component and that this source rock facies deviated drastically from the normal “North Sea Oils”.

The similarity in facies characteristics of the coals and the DST oils makes it probable that the oils, at least partly, have been sourced from the coals as the geochemical parameters of the oils are representing a mixed organic facies with a significant terrigenous component.

Different classification diagrams concerning maturity parameters indicate that the coals are in the oil window, as supported by the Rock-Eval Tmax of the coals themselves. Figure 6.6, a cross plot of MPDF versus C₃₁-hopanes, illustrates that all of the coals have reached oil-window maturity and the sample set range in maturity from the early to the late stage of oil generation. Figure 6.10 shows that the entire sample set falls within the peak oil generation zone, based on steranes and hopanes, thus the Finnmark Platform Lower Carboniferous coals are not immature, with the obvious implications this has for deeper sub-basins and grabens in the Barents Sea.

In the classification diagrams used for Rock-Eval pyrolysis and LECO TOC, the majority of the coals from the study region fall within the regions indicating a maceral composition with

type II kerogen and a few coals fall into the designated regions for more traditional terrigenous type III kerogen/coals.

Most of the investigated coals are oil prone while a few are only gas prone.

If the mentioned “internal barriers” (see discussion concerning adsorption and absorption) of expelling liquid petroleum from coals are overcome, these coals have the possibility of not only generating, but also expelling both oil and gas.

Concerning fractionation during primary migration it is clear from the work of van Koeverden (personal com.) that some sandstones in close proximity to the coals have GC-FID and GC-MS characteristics making them even more similar to the DST oils in this study than the coal extracts presented here. The implication of this would be that the investigated DST oils in this study may partly or entirely have been sourced by Lower Carboniferous coals. The similar Pr/Ph trends for coals and oils, together with waxy n-alkanes (C_{15+} fraction) derived from coals and the waxy oil signature of DST 1 & 2 support this hypothesis.

The Iatroscan plot comparing DST oils and coal extracts (see figure 6.17) also provide circumstantial evidence to suggest that some parts of the saturated hydrocarbon fraction still residing in the coals may in fact represent a residual amount from an early expulsion phase. This part may constitute part of the DST oils from the same coals formations occurring regionally. Migration of bitumen from coals will inevitably result in the escaping and migrating petroleum being enriched in non polar oil components like saturated hydrocarbons, leaving in the coals only aromatic hydrocarbons, resins and asphaltenes plus a minor proportion of saturated hydrocarbons (see also chapter 1.9- oil from coals).

In general, this study has concluded that the Lower Carboniferous coals on the Finnmark Platform has the potential for generating large amount of gas and also surprisingly oil and that the coals are oil-window mature.

Since the maturity of the coal samples as determined from Rock-Eval and GC-FID plus GC-MS methods in well 7128/4-1 is similar to that of the North Sea Oil (NSO-1) this suggests that more work should be performed concerning potential “New Play” scenario based on

Lower Carboniferous coals throughout the Finnmark Platform, the Bjarmland Platform and also other regions of the Barents Sea.

This study has proven irrefutably the oil generative potential of Lower Carboniferous coals on the Finnmark Platform and this is highly relevant for alternative exploration models in other and deeper parts of the Barents Sea.

5. References

- Ahsan, A, 1993: Petroleum biodegradation in the Tertiary Reservoirs of the North Sea. Cand. Scient. Thesis in Geology, Department of Geology, University of Oslo, Norway, 173 pp.
- Ahsan, A., Karlsen, D. A. and Patience, R. L., 1997: Petroleum biodegradation in the Tertiary reservoirs of the North Sea. *Marine and Petroleum Geology*, 14, 55-64.
- Bailey, N.J.L., Jobson, A.M. & Rogers, M.A. (1973a). Bacterial degradation of crude oil: Comparison of field and experimental data. *Chem. Geol.* 11, 203-221.
- Bailey, N.J.L., Krouse, H.R., Evans, C.R., & Rogers, M.A. (1973b). Alteration of crude oil by waters and bacteria-evidence from geochemical and isotope studies. *Amer. Assoc. Petrol. Geol. Bull.* 57, 1276-1290.
- Baskin, D.K., 1997. Atomic H/C ratio of kerogen as an estimate of thermal maturity and organic matter conversion. *American Association of Petroleum Geologists Bulletin* 81, 1437 – 1450.
- Bhullar, A. G., Karlsen, D. A., Backer-Owe, K., Le Tran, K., Skålnes, E., Berchermann, H. H. and Kittelsen, J. E., 2000: Reservoir characterization by combined micro extraction – micro thin-layer chromatography (Iatroscan) method: A calibration study with examples from the Norwegian North Sea. *Journal of Petroleum Geology*, 23, 221-244.
- Bordenave, M.L., 1993. *Applied Petroleum Geochemistry*. Éditions Technip, Paris, 1-524.
- Bray, E. E. and Evans, E. D., 1961: Distribution of n-paraffins as a clue to recognition of source beds. *Symposium on the chemical approaches to the recognition of petroleum source rocks*, Pergamon, 2-15.

Chosson, P., Connan, J., Dessort, D. and Lanau, C., 1992: In vitro biodegradation of steranes and terpanes: A clue to understanding geological situations. Biological markers in sediments and petroleum., Moldowan, J. M. et al., Eds., Prentice Hall, Englewood Cliffs, N. J., 320-349.

Clayton, J. L. and Bostick, N. H., 1986: Temperature effects on kerogen and on molecular and isotopic composition of organic matter in Pierre Shale near an igneous dike. Advances in organic geochemistry, 1985; Part I; Petroleum geochemistry., Ruehlkötter, J., Ed., Pergamon, 135-143.

Connan, J., 1984: Biodegradation of crude oils in reservoirs. Advances in petroleum geochemistry., Brooks, J. and Welte, D. H., Eds., Academic press, London, Vol. 1, 299-335.

Connan, J. and Cassou, A. M., 1980: Properties of gases and petroleum liquids derived from terrestrial kerogen at various maturation levels. *Geochimica et Cosmochimica Acta*, 44, 1-23.

Cooles, G.P., Mackenzie, A.S., Quigley, T.M., 1986. Calculation of petroleum masses generated and expelled from source rocks. *Organic Geochemistry* 10, 235 – 245.

Cornford, C., Morrow, J. A., Turrington, A., Miles, J. A. and Brooks, J., 1983: Some geological controls on oil composition in the U.K. North Sea. Petroleum geochemistry and exploration of Europe; International congress., Brooks, J., Ed., Geological Society of London, 175-194.

Cornford, C., Needham, C. E. J. and De Walque, L., 1986: Geochemical habitat of North Sea oils and gases. Habitat of hydrocarbons on the Norwegian continental shelf; proceedings of an international conference., Spencer, A. M., Ed., Graham & Trotman, 39-54.

Dow, W.G. (1977). Kerogen studies and geological interpretations. *Journal of Geochemical Exploration* 7 (2, Application of geochemistry to the search for crude oil and natural gas), 79-99.

Durand, B., 1980. Kerogen, insoluble organic matter from sedimentary rock. Editions Techniq. Paris, 1-514.

Eglinton, G. and Murphy, M. T. J., Eds., 1969: Organic geochemistry- methods and results, 781 pp.

Espitalie, J., Laporte, J.L., Madec, M., Marrquis, F., Laplat, P. and Paulet, J., 1977. Méthode rapide de caractérisation des roches mères, de leur potentiel pétrolier et de leur degré d'évolution. In: Rev. Inst. Franç. du Pétr. 32: 23-43.

Espitalie, J., F. Marquis, and I. Barsony (1984). Geochemical logging. In J. Voorhees Kent (ed.), Analytical pyrolysis techniques and applications., pp. 276-304. London, United Kingdom: Butterworth and Co.

Evans, C. R., Rogers, M. A. and Bailey, J. L., 1971: Evolution and alteration of petroleum in Western Canada. Chemical Geology, 8, 147-170.

Fleet, A., Crawley, S., 2000. Possible controls on the formation of oil-prone coals and coal-bearing strata. American Association of Petroleum Geologists Bulletin 84, 1400 (abstract).

Fleet, A.J., Scott, A.S., 1994. Coal and coal-bearing strata as oil-prone source rocks: an overview. In: Scott, A.C., Fleet, A.J. (Eds.), Coal and Coal-Bearing Strata as Oil-Prone Source Rocks? Geological Society Special Publication, vol. 77, pp.1 –8.

Grønseth, O.T., Nagy, J., Karlsen, D.A, (2004): Abstract. Organic geochemistry and foraminiferal facies of Jurassic deposits of the Mid-Norwegian shelf. Norwegian Geol. Soc. Winter Conference, Røros, January 2005.

Hedberg, H. D. 1968. Significance of high-wax oils with respect to genesis of petroleum. *AAPG Bulletin*, 52, 736 – 750.

Horstad, I., 1989: Petroleum composition and heterogeneities within the Middle Jurassic reservoir in The Gullfaks field area, Norwegian North Sea, Department of Geology, University of Oslo.

Huang, D., Qin, K., Wang, T., Zhou, X. et al., 1997. Formation and Mechanism of Oil from Coal Petroleum Industry Press, Beijing, 443 pp.

Huang, W. Y. and Meinschein, W. G., 1979: Sterols as ecological indicators. *Geochimica et Cosmochimica Acta*, 59, 739-745.

Hughes, W. B., Holba, A. G. and Dzou, L. I. P., 1995: The ratios of dibenzothiophene to phenanthrene and pristane to phytane as indicators of depositional environment and Lithology of petroleum source rocks. *Geochimica et Cosmochimica Acta*, 59.7, Elsevier Science Ltd, 3581-3598.

Hughes, W. B., Holba, A. G., Müller D.E., and Richardson, J. S. (1985): Geochemistry of greater Ekofisk crude oils. In *Petroleum Geochemistry in Exploration of the Norwegian Shelf* (ed. B.M. Thompson et al.), pp.75-92. Graham and Trotman Ltd.

Hunt, J. M. 1996. "*Petroleum Geochemistry and Geology / John M. Hunt. -2nd ed.* 620 pages. United States of America: Freeman.

Hunt, J. M. 1979. *Petroleum geochemistry and geology*. 1st ed. San Francisco: Freeman.

Isaksen, G.H., Curry, D.J., Yeakel, J.D., Jenssen, A.I., 1998. Controls on the oil and gas potential of humic coals. *Organic Geochemistry* 29, 23 – 44.

Johnston, D. J. 1990. Geochemical logs thoroughly evaluate coalbeds. *Oil & Gas Journal*, December 24, 45 – 51.

Juntgen, H., and J. Klein. 1975. Origin of natural gas from coaly sediments. *Erdol und Kohle*, 28 (2), 65 – 73.

Karlsen, D. A. and Larter, S. R., 1989: A rapid correlation method for petroleum population mapping within individual petroleum reservoirs – applications to petroleum reservoir description. *Correlation in Hydrocarbon Exploration*, Haresnape, J., Ed., 77-85

Karlsen, D. A. and Larter, S. R., 1991: Analysis of petroleum fractions by TLC-FID; applications to petroleum reservoir description. *Organic Geochemistry*, 17, 603-617.

Karlsen, D.A., Skeie, J.E., Backer-Owe, K., Bjørlykke, K., Olstad, K.B., Cecchi, M., Vik, E., Schaefer, R.G., 2004. Petroleum Migration, Faults and Overpressure-Part II-Case History, The Haltenbanken Petroleum Province, Offshore Norway. In: "Geochemistry of Reservoirs II: Linking Reservoir Engineering and Geochemical Models". Cubitt, J., England, W., Later, S. and Macleod, G. In press: 305

Karweil, J. 1969. Aktuelle Probleme der Geochemie der Kohle. In P. A. Schenk and I. Havenaar (eds.), *Advances in organic geochemistry 1968*. Oxford: Pergamon Press, pp. 59 – 84.

Killops, S.D., Funnell, R.H., Suggate, R.P., Sykes, R., Peters, K.E., Walters, C., Woolhouse, A.D., Weston, R.J., Boudou, J.-P., 1998. Predicting generation and expulsion of paraffinic oil from vitrinite-rich coals. *Organic Geochemistry* 29, 1 – 21.

Klemme, H. D., and G. F. Ulmishek. 1991. Effective petroleum source rocks of the world: Stratigraphic distribution and controlling depositional factors. *AAPG Bulletin*, 75, 1809 – 1851.

Kvalheim, O. M., Telnaes, N., Bjorseth, A. and Christy, A. A., 1987: Interpretation of multivariate data; relationship between phenanthrenes in crude oils. Multivariate statistical workshop for geologists and geochemists., Kvalheim, O. M., Ed., Elsevier, 149-153.

Langford, F.F., and M.M Blanc-Valleron (1990). Interpreting rock-eval pyrolysis data using graphs of pyrolyzable hydrocarbons vs. total organic carbon. *AAPG Bulletin* 74 (6), 799-804.

Lewan, M.D. 1993a. Identifying and understanding suppressed vitrinite reflectance through hydrous pyrolysis experiments. Abstracts and Program, 10th Annual Meeting of the Society for Organic Petrology, vol.10, pp. 1 – 3.

Lewan, M.D. 1993b. Laboratory simulation of petroleum formation: Hydrous pyrolysis. In M. H. Engel and S. A. Macko (eds.), *Organic geochemistry*. New York: Plenum Press, pp. 419 – 442.

Lewan, M.D. 1993c. Primary oil migration and expulsion as determined by hydrous pyrolysis. *Proceedings of the 13th World Petroleum Congress, Buenos Aires, 1991*. Chichester: Wiley, vol. 2, pp. 215 – 223.

Li, M., Bao, J., Lin, R., Stasiuk, L.D., Yuan, M., 2001a. Revised models for hydrocarbon generation, migration and accumulation in Jurassic coal measures of the Turpan Basin, NW China. *Organic Geochemistry* 32, 1127 –1151.

Mackenzie, A. S., Quirke, J. M. E. and Maxwell, J. R., 1980: Molecular parameters of maturation in the Toarcian shales, Paris Basin, France; II, Evolution of metalloporphyrins. *Advances in organic geochemistry 1979.*, Maxwell, J. R., Ed., Pergamon, 239-248.

Mackenzie, A. S., Maxwell, J. R., Coleman, M. L. and Deegan, C. E., 1984: Biological marker and isotope studies of North Sea crude oils and sediments. *Proceedings – World Petroleum Congress = Actes et Documents – Congres Mondial du Petrole*, 11, 45-56.

Mackenzie, A. S., Rullkoetter, J., Welte, D. H. and Mankiewicz, P., 1985: Reconstruction of oil formation and accumulation in North Slope, Alaska, using quantitative gas chromatography-mass spectrometry. *Alaska North Slope oil-rock correlation study; analysis of North Slope crude.*, Claypool, G. E., Ed., American Association of Petroleum Geologists, 319-377.

McMaster, M. and McMaster, C., 1998: *GC/MS – A Practical User's Guide*. Wiley – VCH, 189 pp.

Mello, M. R., Telnaes, N., Gaglianone, P. C., Chicarelli, M. I., Brassell, S. C. and Maxwell, J. R., 1988: Organic geochemical characterization of depositional palaeoenvironments of source rocks and oils in Brazilian marginal basins. *Advances in organic geochemistry 1987; Part I, Organic geochemistry in petroleum exploration; proceedings of the 13th international meeting on organic geochemistry.*, Novelli, L., Ed., Pergamon, 31-45.

Milner, C. W. D., Rogers, M. A. and Evans, C. R., 1977: Petroleum transformations in reservoirs. *Journal of Geochemical exploration*, 7, 101-153.

Moldowan, J. M., Seifert, W. K. and Gallegos, E. J., 1985: Relationship between petroleum composition and depositional environment of petroleum source rocks. *American Association of Petroleum Geologists Bulletin*, 69, 1255-1268.

Moldowan, J. M., Fago, F. J., Carlson, R. M. K., Young, D. C., Van, D. G., Clardy, J., Schoell, M., Pillinger, C. T. and Watt, D. S., 1991: Rearranged hopanes in sediments and petroleum. *Geochimica et Cosmochimica Acta*, 55, 3333-3353.

Moldowan, J. M., Sundararaman, P., Salvatori, T., Alajberg, A., Gjukic, B., Lee, C. Y. and Demaison, G. J., 1992: Source correlation and maturity assessment of selected oils and rocks from the Central Adriatic Basin (Italy and Yugoslavia). *Biological markers in sediments and petroleum*, Moldowan et al., Eds., Prentice Hall, Englewood Cliffs, N. J., 370-401.

Moore, P.S., Burns, B.J., Emmett, J.K., Guthrie, D.A., 1992. Integrated source, maturation and migration analysis, Gippsland Basin, Australia. *Australian Petroleum Exploration Association Journal* 32 (1), 313 – 324.

Pedersen, J. H., 2002: Atypical oils, unusual condensates and bitumens of the Norwegian Continental Shelf: an organic geochemical study, Cand. Scient. Thesis in Geology, Department of Geology, University of Oslo.

Peters, K. E., C. C. Walters, and J. M. Moldowan, 2005, *The biomarker guide*, 2d ed.: Cambridge, Cambridge University Press, 1155 p.

Peters, K. E. and Moldowan, J. M., 1993: *The biomarker guide – Interpreting molecular fossils in petroleum and ancient sediments*. Prentice Hall, Englewood Cliffs, New Jersey 07632, 363 pp.

Peters, K. E. (1986). Guidelines for evaluating petroleum source rock using programmed pyrolysis. *AAPG Bulletin* 70 (3), 318-329.

Peters, K. E., and M. R. Cassa, 1994, *Applied Source Rock Geochemistry*, in L. B. Magoon, and W. G. Dow, eds., *The Petroleum system - from source to trap: AAPG Memoir v. AAPG Memoir* 60, p. 93-120.

Petersen, H.I., Rosenberg, P., 2000. The relationship between the composition and rank of humic coals and their activation energy distributions for the generation of bulk petroleum. *Petroleum Geoscience* 6, 137 – 149

Petersen, H.I., Rosenberg, P., 1998. Reflectance retardation (suppression) and source rock properties related to hydrogen-enriched vitrinite in Middle Jurassic coals, Danish North Sea. *Journal of Petroleum Geology* 21, 247 – 263.

Petersen, H.I., Rosenberg, P., Andsbjerg, J., 1996. Organic geochemistry in relation to the depositional environments of Middle Jurassic coal seams, Danish Central Graben, and implications for hydrocarbon generative potential. *American Association of Petroleum Geologists Bulletin* 80, 47 – 62.

Potonie, H. 1908. Die rezenten Kaustobiolithe und ihre Langerstätten: Die Sapropeliten. *Abh. Kgl. Preuss. Geol. Landesanstalt*, new ser., 1 (55).

Radke, M., Welte, D. H. and Willsch, H., 1982a: Geochemical study on a well in the western Canada Basin; relation of the aromatic distribution pattern to maturity of organic matter. *Geochimica et Cosmochimica Acta*, 46, 1-10.

Radke, M., Willsch, H., Leythaeuser, D. and Teichmueller, M., 1982b: Aromatic components of coal; relation of distribution pattern to rank. *Geochimica et Cosmochimica Acta*, 46, 1831-1848.

Radke, M. and Welte, D. H., 1983: The methylphenanthrene index (MPI); a maturity parameter based on aromatic hydrocarbons. *Advances in organic geochemistry 1981.*, Speers, G., Ed., Wiley & Sons, 504-512.

Radke, M., 1988: Application of aromatic compounds as maturity indicators in source rocks and crude oils. *Marine and Petroleum Geology*, 5, 224-236.

Radke, M., Vriend, S. P. and Schaefer, R. G., 2001: Geochemical characterization of Lower

Toarcian source rock from NW Germany: Interpretation of aromatic and saturated hydrocarbons in relation to depositional environment and maturation effects. *Journal of Petroleum Geology*, 24(3), 287-307.

Rice, D. D. 1993a. Biogenic gas: Controls, habitat and resource potential. In D. G. Howell et al. (eds.), *The future of energy gases*. U. S. Geological Survey professional paper 1570. Washington, DC: U. S. Government Printing Office, pp. 583 – 606.

Rice, D. D. 1993b. Controls on coal- bed gas composition. Abstract. *AAPG Bulletin*, 77, 1658.

Sandvik, E.I., Young, W.A., Curry, D.J., 1992. Expulsion of hydrocarbon sources: the role of organic absorption. *Organic Geochemistry* 19, 77 – 87.

Saxby, J. D., A. J. R. Bennett, J. F. Corcoran, D. E. Lambert, and K. W. Riley. 1986. Petroleum generation: Simulation over six years of hydrocarbon formation from torbanite and brown coal in a subsiding basin. *Org. Geochem.*, 9 (2), 69 – 81.

Seifert, W.K. and Moldowan, J.M., 1986, Use of biological markers in petroleum exploration, in R.B. Johns, ed., *Biological Markers in the Sedimentary Record*: Amsterdam, Elsevier, p. 261-290.

Seifert, W. K. and Moldowan, J. M., 1978: Applications of steranes, terpanes and monoaromatics to the maturation, migration and source of crude oils. *Geochimica et Cosmochimica Acta*, 42, 77-95.

Shanmugam, G., 1985. Significance of coniferous rain forests and related organic matter in generating commercial quantities of oil, Gippsland Basin, Australia. *American Association of Petroleum Geologists Bulletin*, 69: 1241-1254.

Smith, J. T. 1994. Petroleum system logic as an exploration tool in a frontier setting. In L. B. Magoon and W. G. Dow (eds.), *The petroleum system- From source to trap*. AAPG Memoir 60. Tulsa. American Association of Petroleum Geologists, pp. 25 – 49.

Speight, J.G., 1983. The Chemistry and Technology of Coal. Marcel Decker, New York, 528 pp.

Stach, E., M-Th. Mackowsky, M. Teichmuller, G. H. Taylor, D. Chandra, and R. Teichmuller. 1982. *Stach's textbook of coal petrology*. 3rd ed. Berlin: Bebruder Borntraeger.

Sutton, P.A., Lewis, C. A. and Rowland, S. J., 2004: Isolation of individual hydrocarbons from the unresolved complex hydrocarbon mixture of a biodegraded crude oil using preparative capillary gas chromatography. *Organic Geochemistry*, 36 (2005), 963-970.

ten Haven, H. –L., De Leeuw, J. W., Rullkoetter, J. and Sinninghe Damste, J. S., 1987: Restricted utility of the pristane/phytane ratio as a palaeoenvironmental indicator. *Nature* (London), 330, 641-643.

Tissot, B.P., and Welte, D.H., 1984. Oil and Gas Exploration: Application of the Principles of Petroleum Generation and Migration. In: *Petroleum formation and occurrence*. Springer Verlag, 495 – 547.

Tissot, B.P., and D.H. Welte. 1978. *Petroleum Formation and Occurrence*. 1st ed. Heidelberg: Springer Verlag.

van Krevelen, D. W., 1961. *Coal: Typology- Chemistry- Physics- Constitution*. Amsterdam: Elsevier Science.

Wang, C., 2007. Anomalous hopane distributions at the Permian-Triassic boundary, Meishan, China-Evidence for the end-Permian marine ecosystem collapse. *Organic Geochemistry* 38 (2007), 52-66.

Waples, D. W. and Machihara, T., 1991: Biomarkers for geologists – A practical guide to the application of steranes and triterpanes in petroleum geology. Vol. 9, *AAPG Methods in Exploration*, AAPG, 91 pp.

Weiss, H.M., Wilhelms, A., Mills, N., Scotchmer, J., Hall, P.B., Lind, K. and Brekke, T. (2000): NIGOGA - The Norwegian Industry Guide to Organic Geochemical Analyses

[online]. Edition 4.0 Published by Norsk Hydro, Statoil, Geolab Nor, SINTEF Petroleum Research and the Norwegian Petroleum Directorate. 102 pp [cited *CITATION_DATE*]. Available from World Wide Web: <<http://www.npd.no/engelsk/nigoga/default.htm>>. where *CITATION_DATE* = date when the document was seen or downloaded, e.g. "2000-07-21" or "21 June 2000"

Wilhelms, A. and Larter, S. R., 1994: Origin of tar mats in petroleum reservoirs; Part II, Formation mechanisms for tar mats. *Marine and Petroleum Geology*, 11, 442-456.

Wilkins, R.W.T. and George, S.C., 2002. Coal as a source rock for oil: a review. *International Journal of Coal Geology* 50 (2002), 317-361.

Winters, J. C. and Williams, J. A., 1969: Microbiological alteration of crude oil in the reservoir. American Chemical Society, division of petroleum chemistry, New York Meeting Preprints, 14(4), E22-E31.

<http://www.npd.no>